Têtes de bassin versant, altérations hydrologiques et dynamique de la biodiversité. Caractérisation de l'hydrologie des assecs à partir de la base ONDE

Aurélien Beaufort, Eric Sauquet, T. Datry

Programme 2016/2018 – Thème Gestion équilibrée de la ressource - Action n° 26

Têtes de bassin versant, altérations hydrologiques et dynamique de la biodiversité

Caractérisation de l'hydrologie des assecs à partir de la base ONDE

Rapport final

Aurélien BEAUFORT (Irstea)

Eric SAUQUET (Irstea)

Thibault DATRY (Irstea, coord.)

Février 2019

- **AUTEURS**

Aurélien BEAUFORT, Post-doctorant (Irstea), aurelien.beaufort@irstea.fr

Eric SAUQUET, Directeur de Recherche (Irstea), eric.sauquet@irstea.fr

- **CORRESPONDANTS**

AFB : Claire MAGAND, DRED/DRDI, claire.magand@afbiodiversite.fr

Céline NOWAK, DRED/DSOD, celine.nowak@afbiodiversite.fr

- **AUTRES CONTRIBUTEURS**

Julie CARREAU, HydroSciences Montpellier, julie.carreau@umontpellier.fr

Thibault DATRY, Directeur de Recherche (Irstea), thibault.datry@irstea.fr

Droits d'usage : accès libre
Niveau géographique : national
Couverture géographique : France
Niveau de lecture : professionnels

- **RESUME**

Les cours d'eau en tête de bassin sont naturellement sujets à l'intermittence du débit. Ces cours d'eau intermittents ont récemment connu un regain d'intérêt marqué, en particulier pour évaluer l'impact des assecs sur la biodiversité de ces milieux dans une perspective notamment de pression accrue sur la ressource en eau et de changement climatique.

L'objectif de cette étude est de mieux comprendre le régime hydrologique des cours d'eau en tête de bassin versant en examinant plus particulièrement la dynamique des phases d'assec dans le temps et dans l'espace en France métropolitaine et la manière dont les observations recueillies par le réseau ONDE peuvent effectivement contribuer à l'amélioration des connaissances.

Des modèles empiriques ont d'abord été développés pour prédire la probabilité journalière d'intermittence à l'échelle régionale sur l'ensemble de la France métropolitaine, puis pour reconstruire la dynamique d'assèchement locale sur chaque site du réseau ONDE. Les variables explicatives utilisées comme données d'entrée sont des données journalières caractérisant le climat, l'hydrologie de surface et la piézométrie. Ces modèles ont été calés sur les observations du réseau ONDE.

La robustesse des modèles a été éprouvée à l'aide d'un ensemble de données régionales d'observations indépendantes et de même nature ou issues de débits mesurés en stations hydrométriques et des observations du réseau ONDE de l'année 2017 exclues de la phase de calage. Les résultats montrent un intérêt manifeste à utiliser les données ONDE pour caractériser le régime hydrologique des cours d'eau d'amont et deux exemples d'application des modèles développés sont proposées : une reconstitution de la probabilité régionale d'assec depuis 1989 et le calcul de métriques hydrologiques qui influencent la composition et la structure des écosystèmes aquatiques au droit de chaque site ONDE sur la période 2012-2016.

- **MOTS CLES (THEMATIQUE ET GEOGRAPHIQUE) : HYDROLOGIE, COURS D'EAU INTERMITTENT, ASSEC, FRANCE METROPOLITAINE**

- **HEADWATER STREAMS, FLOW REGIME ALTERATION AND BIODIVERSITY DYNAMICS**

- **ABSTRACT**

Headwater streams are generally naturally prone to flow intermittence. These intermittent rivers streams have recently seen a marked increase in interest, especially to assess the impact of drying on aquatic ecosystems.

The objective of this study is to better understand the river flow regime of headwater streams with a specific focus on how flow intermittence develops in both time and space in France and how discrete field observations obtained from the ONDE network may help to achieve this objective.

Empirical models have been developed first to predict the daily probability of intermittence at the regional scale across France and second to reconstruct local drying dynamics at each ONDE site. Explanatory variables used as inputs were derived from daily climate, discharge and groundwater-level data. These models were calibrated against ONDE data.

The robustness of the models was tested using an independent regional dataset of flow stees observations and of perennial and intermittent gauged streams, and ONDE observations of the year 2017 excluded from the calibration process. Results show the benefit from using ONDE data to assess the river flow regime of headwater streams and two examples of applications have been provided (reconstitution of the historical regional probability of drying since 1989, calculation of a set of hydrological indices to inform the ecosystem of intermittent rivers at each ONDE site over the period 2012-2016).

- **KEY WORDS (THEMATIC AND GEOGRAPHICAL AREA): HYDROLOGY, INTERMITTENT STREAM, DRYING, FRANCE**

- **SYNTHESE POUR L'ACTION OPERATIONNELLE**

La connaissance du fonctionnement hydrologique et écologique des petits bassins versants (ou tête de bassin versant) est assez faible malgré leur prépondérance au sein du réseau hydrographique métropolitain. En effet, seul un faible nombre de stations hydrométriques (http://www.hydro.eaufrance.fr) enregistrent en continu les débits de cours d'eau français drainant moins de 25 km². Cette répartition est liée aux enjeux (humains et économiques) concentrés en fond de vallée et à la difficulté d'instrumentation des petits cours d'eau (ex. cours d'eau en tresse à la morphologie active, accès difficile au lit…).

L'ambition première du volet « hydrologie » est de valoriser les informations issues du réseau ONDE (Observatoire National Des Etiages, onde.eaufrance.fr) pour mieux appréhender les régimes hydrologiques sur les petits cours d'eau. Les données du réseau ONDE sont des données qualitatives (hydrologie décrite par des modalités d'écoulement : « écoulement visible », « écoulement non visible », ou « assec ») et discrètes (une observation de terrain par mois au minimum), relevées sur plus de 3300 sites principalement sur les têtes de bassin versant (superficie inférieure à 50 km²).

Des développements innovants pour la reconstitution de la dynamique des assecs (passage des mesures discontinues à une chronologie décrivant de manière exhaustive les phases d'assec aux échelles régionale et locale) ont été engagés avec succès. Ils ont combiné les suivis ponctuels ONDE à des mesures des débits de la base de données HYDRO, des relevés de niveaux piézométriques de la base de données ADES et des données météorologiques issues de la base de données SAFRAN.

Des modèles empiriques à base statistique ont été mis en place pour prédire :

- les probabilités d'assec régionales sur l'ensemble de la France métropolitaine ;
- les modalités « assec »/« écoulement non visible » versus « écoulement visible » au droit des sites ONDE

au pas de temps journalier *a minima* sur la période de disponibilité des données ONDE pendant cette étude 2012-2017. Deux types de régressions ont été testés pour estimer les probabilités régionales. La dynamique journalière étant plus difficile à représenter à l'échelle locale, des structures plus complexes ont été envisagées (modèles linéaires et non linéaires). Les applications de ces modèles ont permis :

- de localiser les régions les plus affectées par les assèchements ;
- d'analyser la variabilité temporelle des assecs depuis 1989 ;
- d'identifier les drivers de l'intermittence ;
- de calculer des métriques hydrologiques descriptives des assecs (probabilité journalière d'intermittence à l'échelle régionale, durée maximale des épisodes d'assec, date du premier assec, nombre d'événements d'assec, nombre total de jours d'assec entre mai et septembre de chaque année).

La démonstration a été faite que les données ONDE sont utiles pour la connaissance des assecs en tête de bassin versant. Les analyses réalisées militent pour la poursuite de ce réseau : de par leur localisation, le réseau ONDE vient compléter l'information fournie par les réseaux conventionnels (*i.e.* les stations hydrométriques de la base de données HYDRO), les six années d'observations ne suffisent pas à assurer la robustesse des modèles et les campagnes futures devraient réduire l'incertitude sur le paramétrage et les sorties des modèles.

Les données ONDE ont été exploitées ici pour la connaissance des assecs. Elles présentent un potentiel d'utilisation plus large en hydrologie (notamment pour l'évaluation des modélisations distribuées, bien souvent limitée aux seules stations hydrométriques), même si ces données requièrent des post-traitements pour les exploiter au mieux. On peut imaginer que les hydrologues seront de plus en plus confrontés à ce type de données avec le développement des sciences participatives et donc exploiter les proxys – dont les données ONDE - devrait devenir pratique courante.

Ces travaux de recherche ont donné lieu à deux publications - une acceptée dans HESS et la seconde acceptée avec des révisions mineures dans Hydrological Processes - fournies en Annexe. Des couches SIG descriptives des statistiques d'assec sont susceptibles d'être transférés sur demande.

- **SOMMAIRE**

- **TETES DE BASSIN VERSANT, ALTERATIONS HYDROLOGIQUES ET DYNAMIQUE DE LA BIODIVERSITE**

1. Contexte

Les têtes de bassin versant représentent une proportion substantielle des réseaux hydrographiques. Du fait de leur taille et localisation, ils ne sont pas détectables par les méthodes classiques de cartographie (images satellites ou photos aériennes) et sont donc souvent absents des cartes et des réseaux hydrographiques. Il a notamment été montré que leur prise en compte peut multiplier par cinq la densité de drainage des réseaux hydrographiques (Lowe et Likens, 2005). D'un point de vue écologique, les têtes de bassin versant sont à l'interface entre les écosystèmes terrestres et aquatiques. Leur contribution au fonctionnement des hydrosystèmes est essentielle : flux de sédiments, apports de matière organique particulaire et de nutriments, refuges/sources de colonisation pour les organismes aquatiques (Meyer *et al.*, 2007 ; Finn *et al.*, 2011). Du fait de leur isolement dans les réseaux, ils présentent une forte diversité beta, liée à des communautés biologiques très différentes entre des localités même proches (Meyer *et al.*, 2007 ; Clarke *et al.*, 2008 ; Finn *et al.*, 2011 ; Datry *et al.*, 2017).

2. Objectifs

La connaissance du fonctionnement des cours d'eau en tête de bassin reste limitée notamment du fait d'une répartition hétérogène des stations hydrométriques (préférentiellement installées sur des cours d'eau pérennes). Pour pallier l'absence d'instrumentation en continu, une voie possible est l'exploitation des données qualitatives et discontinues du réseau ONDE disponibles sur plus de 3300 stations depuis 2012.

La première ambition de cette action est de combiner et donc valoriser les informations issues du réseau ONDE pour mieux appréhender les régimes hydrologiques sur les petits cours d'eau. Des développements innovants pour la reconstitution de la dynamique des assecs (passage des mesures discontinues à une chronologie exhaustive des assecs, estimation de statistiques pertinentes pour l'hydrologie et la biologie dont fréquence annuelle, nombre moyen d'épisodes par an, etc., mise en place d'une typologie) et pour la spatialisation des statistiques le long du réseau hydrographique seront envisagés dans la continuité de travaux antérieurs (Snelder *et al.*, 2013) soutenus par l'Onema (Action 13, Hydrologie des étiages : typologie des cours d'eau temporaires et cartographie nationale).

Le second volet de cette action concerne l'étude de la biodiversité de ces milieux. Il n'est pas traité ici : la caractérisation des assecs du point de vue hydrologique est l'objet de ce rapport.

3. Caractérisation de l'hydrologie des assecs à partir de la base ONDE

Cette section présente dans un premier temps la base de données ONDE (Observatoire National Des Etiages, onde.eaufrance.fr) exploitée avant de présenter deux approches, la première développée pour estimer les probabilités d'assec à l'échelle régionale et la seconde pour reconstituer la dynamique des assecs au droit des sites du réseau ONDE.

3.1. Le réseau ONDE

3.1.1. Historique et caractéristique du réseau ONDE

L'Observatoire National Des Etiages (ONDE) a été mis en place en 2012 par l'ONEMA dans le but de constituer un réseau de connaissance stable sur les étiages estivaux et d'être un outil d'aide à la gestion des périodes de crise hydrologique (Nowak et Durozoi, 2012). Cet observatoire remplace les réseaux de suivi d'étiage existants comme le Réseau d'Observation de Crise des Assecs (ROCA) (national) ou le Réseau Départemental d'Observations des Ecoulements (RDOE) (Centre ; Poitou Charentes).

Les sites ONDE sont représentatifs des contextes hydrographiques de chaque département, choisis pour être non redondants avec des systèmes d'observation déjà existants. Ils permettent le suivi des étiages estivaux en caractérisant leur occurrence et leur intensité. Le réseau ONDE constitue un jeu de données historiques permettant de comparer des informations obtenues avec des années précédentes.

La construction du réseau ONDE et le choix d'implantation des sites dans chaque département ont été réalisés en tenant compte de critères principaux et secondaires. Les critères principaux prévoient notamment de répartir les sites proportionnellement au linéaire de cours d'eau par Hydro-EcoRégions (HER, Wasson *et al*., 2002), sur des cours d'eau d'ordre de Strahler 1 à 4 subissant des assecs naturels et/ou anthropiques. L'ensemble de ces critères sont détaillés dans la note technique du réseau ONDE (Nowak et Durozoi, 2012).

Le réseau ONDE s'organise selon deux types de suivis : un suivi usuel et un suivi complémentaire. Le suivi usuel concerne l'ensemble des sites ONDE du département (minimum de 30 sites par département) et prévoit au moins une observation par mois (autour du 25 de chaque mois) entre mai et septembre. Le suivi complémentaire est déclenché par les services de l'Etat ou sur décision de l'AFB et prévoit une fréquence d'observations plus importante ou sur une période différente que celle du suivi usuel et concerne tout ou partie des sites ONDE. Les observations ONDE restent localisées aux mêmes sites que ce soit en suivi usuel ou complémentaire. Le niveau d'écoulement des cours d'eau est apprécié visuellement selon trois modalités : « écoulement visible » correspondant un écoulement continu visible à l'œil nu, « écoulement non visible » correspondant à un site sur lequel le lit mineur présente toujours de l'eau mais un débit nul, « assec » correspondant à un site à sec où l'eau est totalement évaporée ou infiltrée sur plus de 50% au droit du site. Il existe également une modalité écoulement visible faible correspondant à un site sur lequel il y a un courant d'eau visible mais le débit faible ne garantit pas un fonctionnement biologique des écosystèmes aquatiques. Cependant l'exploitation des données à l'échelle régionale, du bassin ou nationale ne se fait que sur les trois modalités d'observations précédemment décrites.

Le nombre de sites ONDE est de 3302, dont 3262 sont actives, et à chaque site a été affecté un code SANDRE pour son référencement à l'échelle nationale. Ces sites sont répartis sur l'ensemble de la France (*Figure 1*). Le nombre d'observations sur le réseau ONDE au cours d'une année varie entre 24 919 en 2017 et 17 830 en 2014 avec une moyenne de 20750 observations par an entre 2012 et 2017.

Dans le cadre de cette action, les sites ONDE ont été rattachées au réseau hydrographique RHT (Réseau Hydrographique Théorique) (Pella *et al*., 2012). Le RHT est développé à partir du modèle numérique de terrain de la BD ALTI® de l'Institut Géographique National (IGN), reconditionné par le RHE (Réseau Hydrographique Étendu) et il intègre des attributs topographiques, hydrologiques et climatiques calculés et intégrés dans un système d'information géographique.

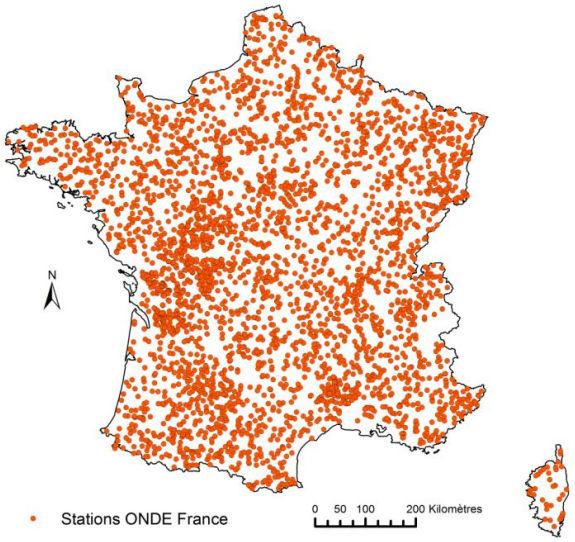

Figure 1 : Représentation des 3302 sites d'observation ONDE

Pour chaque site il est alors possible de déterminer une surface drainée ainsi que l'ordre de Strahler du cours d'eau *(Figure 2*). On constate que la majorité des sites ONDE sont situés sur des petits cours d'eau en tête de réseau comme cela était préconisé lors de la mise en place de l'observatoire. Environ 70% des sites ont une surface drainée inférieure à 50 km² et seulement quatre sites ont une surface drainée supérieure à 1000 km² (*Figure 2a*). Environ 75% des sites sont localisés sur des cours d'eau d'ordre de Strahler 1 ou 2 (*Figure 2b*). Les sites ONDE sont en majorité situés sur des cours d'eau de plaine avec des pentes inférieures à 15 m/km (75% de sites ; *Figure 2c*) et une altitude inférieure à 200 m (75% des sites ; *Figure 2d*). On retrouve peu de sites en contexte de montagne avec seulement 21 sites localisés sur un cours d'eau de pente supérieure à 150 m/km et 95 sites ayant une altitude supérieure à 1000 m. Une des raisons est la difficulté d'accès dans les secteurs de relief. De plus, les

cours d'eau de montagne sont majoritairement sujets aux étiages hivernaux, exclus du périmètre du réseau.

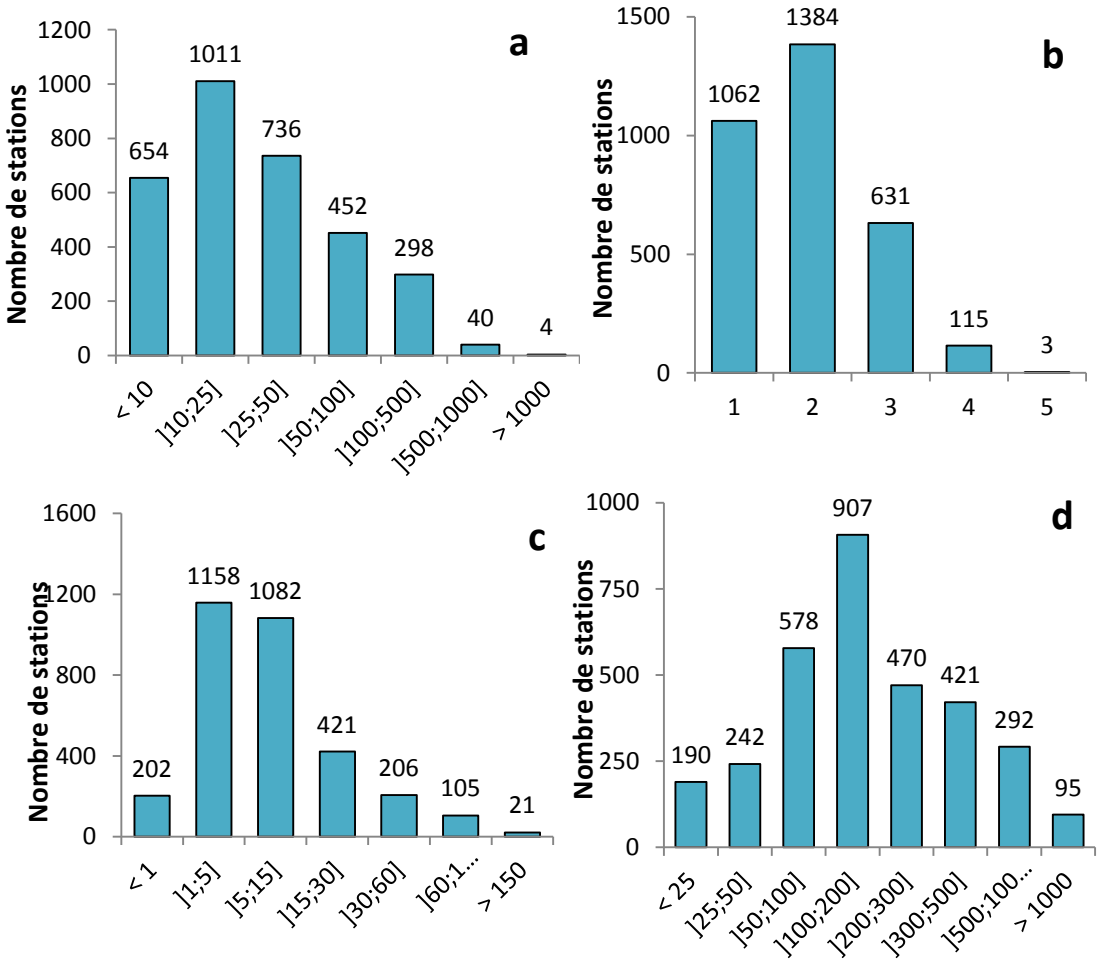

Figure 2 : Caractéristiques des 3302 sites ONDE et leur répartition par : a) surface drainée (km²) ; b) ordre de Strahler ; c) pente (m/km) ; d) altitude (m)

3.1.2. Analyse qualitative des observations

On observe 1326 sites ayant au moins une observation « assec » au cours de la période 2012-2017 et la proportion d'assecs relevés est supérieure à 50% pour 135 sites. Il n'y a que 142 sites présentant un assec tous les ans.

Nous avons recensé 1517 sites, soit environ 46% de la base de données ONDE, présentant 100% d'écoulement visible, regroupant les modalités « écoulement visible » et « écoulement visible faible ». Lorsque l'on sépare ces deux modalités, il n'y a plus que 413 sites (13%) présentant 100% de modalités « écoulement visible » ou « écoulement visible faible ». On dénombre 1520 sites présentant des « écoulements non visibles » mais cette modalité d'écoulement représente moins de 25% des observations sur 1426 sites. Les observations d'assec interviennent principalement pendant les mois de juillet, août et septembre avec plus de 75% des assecs recensés au cours de l'année. Cependant il existe quelques variations comme en juin 2014 où la proportion d'assecs dépasse 20% ou en octobre 2015 ou cette proportion atteint 15 %.

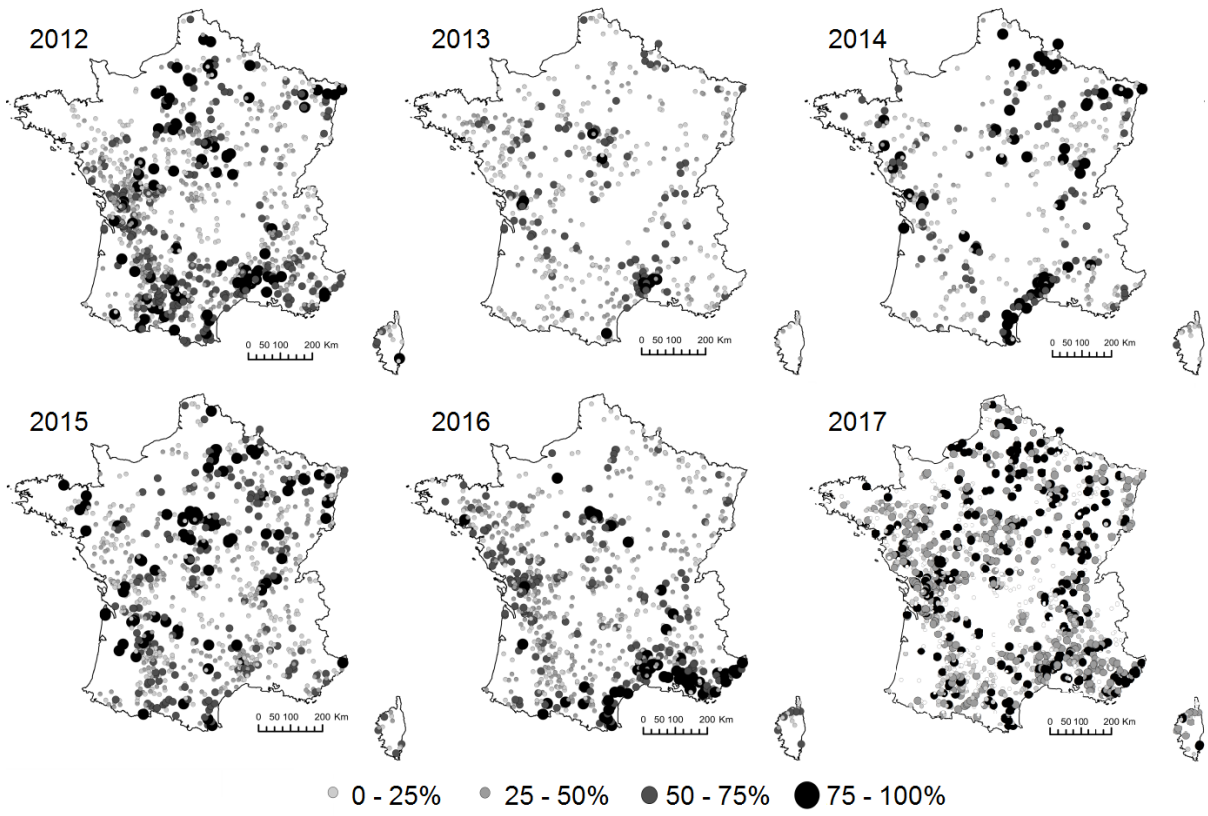

Figure 3 : Représentation des pourcentages d'observations ONDE par site par année entre 2012 et 2017.

Le nombre de sites ONDE présentant des assecs entre 2012 et 2017 peut varier fortement d'une année à une autre (*Figure 3*). Les années 2013 (310 sites) et 2014 (361 sites) sont les années où l'on observe le minimum de sites ayant au moins un assec au cours de l'année et une proportion d'assecs de 4% sur l'ensemble des observations. Les années 2015 et 2016 sont assez similaires avec respectivement 666 sites et 690 sites présentant des assecs et 9% des observations concernent des assecs. L'année 2017 est la plus sévère en termes d'assecs avec 1013 sites (soit 31% des sites examinés) présentant au moins un assec, devant 2012 avec 802 sites au moins un assec au cours de l'année. Les assecs représentent environ 9% des observations sur la période 2012-2017. Du point de vue spatiale, les sites présentant des assecs au cours des années les plus impactées sont plutôt localisés dans les régions Poitou-Charentes et Occitanie ainsi que dans le bassin versant de la Garonne. On note toutefois un nombre plus important de sites asséchés dans le Bassin Parisien en 2012 et en Bretagne en 2016. Les régions situées au Nord, Nord-Est, dans le Massif Central et dans le Sud-Est sont moins touchées par les assecs.

La proportion d'observations qualifiées d'« écoulement non visible » est peu variable d'une année à l'autre et varie de 3% en 2013 à 6.2% en 2017. Cette modalité d'écoulement reste minoritaire.

La proportion d'observations qualifiées d'« écoulement visible » dans l'année est nettement majoritaire et est supérieure à 85% entre 2012 et 2016. Elle est de 78% en 2017, l'année la plus sévère en termes d'assecs.

Cette analyse est cohérente avec les bulletins annuels du réseau ONDE publiés en fin de campagne (http://onde.eaufrance.fr/syntheses/bulletins-annuels).

3.2. Cadre général des approches développées

L'intermittence (durée, interruption, saisonnalité) est un déterminant de la richesse biologique des milieux mais peu renseignée du fait d'un positionnement « biaisé » des stations hydrométriques en France. Ainsi, peu de stations hydrométriques sont situées sur des petits cours d'eau et enregistrent des assecs en France (moins de 10% des stations hydrométriques en France métropolitaine ont présenté des débits nuls sur la totalité de leur période d'enregistrement).

La donnée ONDE permet de mieux appréhender la dynamique des assecs principalement en été ; elle est cependant qualitative et discontinue. Les recherches ont porté sur l'exploitation du potentiel de ces données pour l'appréciation des risques d'intermittence à l'échelle régionale, dans un premier temps, et

la reconstitution de la dynamique journalière au droit des sites suivis par ONDE, dans un second temps.

Les approches développées partagent les principes suivant :

- les mesures journalières de débits des stations hydrométriques présentes dans la banque de données HYDRO (http://www.hydro.eaufrance.fr) et de niveaux des nappes des piézomètres présents dans la banque de données ADES (http://www.ades.eaufrance.fr) sont réputés renseigner la dynamique entre observations ONDE. Les mesures aux stations hydrométriques choisies sont qualifiées de bonne qualité par les gestionnaires et pas ou faiblement influencées par les actions humaines. Les piézomètres sélectionnés sont ceux impliqués dans des échanges nappes-rivières (Brugeron *et al*., 2012). Nous avons toléré 5% de lacunes dans les séries ;
- les développements réalisés s'appuient sur un découpage de la France en régions hydrologiquement homogènes. Le découpage croise l'information géologique - facteur discriminant du soutien des étiages - portée par les 114 Hydro-EcoRégions (HER) de niveau 2 (Wasson *et al*., 2002) et une information sur le régime hydrologique (RH) décrit par les douze débits mensuels moyens réparti en douze classes (pluvial = classe 1 à 6 selon, transition = classe 7 et 8, nival et glaciaire = classe 8 à 12) (Sauquet *et al*., 2008) (*Figure 4*).

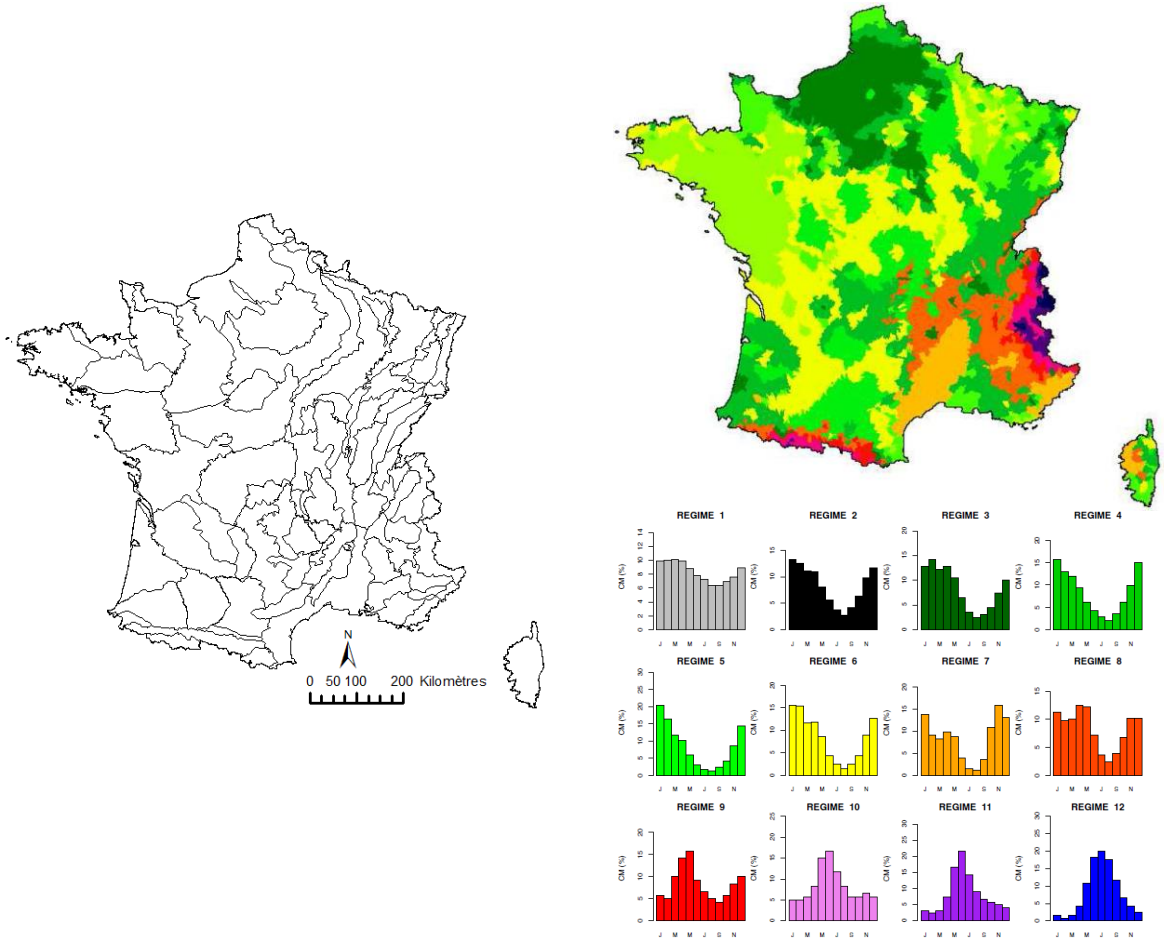

Figure 4 : Découpage en HERs de niveau 2 (gauche) et régimes hydrologiques associés à un découpage de la France en zone HYDRO (droite) utilisés pour la définition des régions hydrologiquement homogènes.

L'ensemble des sites ONDE présents dans la région HER-RH seront associés aux stations hydrométriques situés dans la même région HER-RH. Lorsque le nombre de stations hydrométriques n'atteint pas cinq, on s'autorise des regroupements (fusionner la HER-RH avec une HER de niveau 2 voisine, de même RH et située dans la même HER de niveau 1). Cela concerne 20 des 280 régions HER-RH. Ces régions présentent des tailles évoluant entre 4 et 20 000 km² (moyenne 1400 km²). Les sites ONDE au sein d'une même HER-RH seront associés à l'ensemble des piézomètres situés dans cette même HER pour l'estimation des probabilités à l'échelle régionale (cf. section 3.3, page 13) ; de la même manière, on appariera le site ONDE avec tous les piézomètres de la HER dans laquelle se situe ce site ONDE pour la reconstitution des assecs à l'échelle locale (cf. section 3.4, page 19).

Notons que deux jeux de stations/piézomètres de référence correspondant à deux périodes distinctes 2011-2017 et 1989-2017 ont été constitués avec respectivement 1600 stations hydrométriques et 750 piézomètres pour 2011-2017 et 630 stations hydrométriques et 150 piézomètres pour 1989-2017. Les données 2011-2017 seront utilisées en phase de calage, et les données 1989-2017 pour un exercice de reconstitution sur une période étendue. Peu de piézomètres présentent une proportion de lacunes inférieure à 5%. Les séquences de données absentes inférieures à 10 jours ont été comblées par interpolation linéaire pour atteindre un taux de lacune de 5%. La *Figure 5* illustre la complémentarité des réseaux en termes de taille de bassin concernés par le réseau ONDE et les stations de la banque HYDRO du jeu de référence 2011-2017.

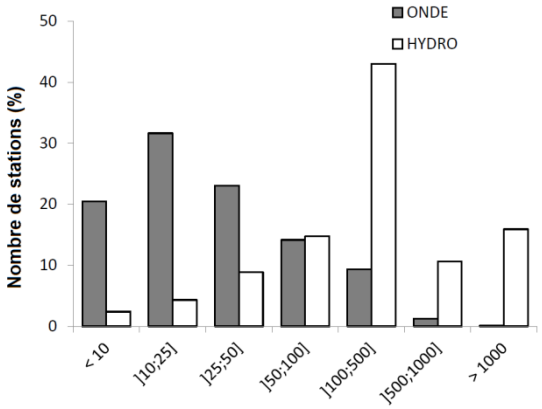

Figure 5 : Distribution des surfaces drainées déterminées à partir du RHT au niveau des 3302 sites ONDE et des 1600 stations HYDRO ayant fonctionné entre le 01/01/2011 et le 31/06/2017.

3.3. Estimation des probabilités d'assec à l'échelle régionale

La méthodologie et ses applications ont été publiées dans (Beaufort *et al*., 2018 ; Annexe 1 : Extrapolating regional probability of drying of headwater streams using discrete observations and gauging networks (Beaufort *et al.*, 2018), page 32). Cette section propose une synthèse des principaux résultats. La variable considérée est la proportion d'observations ONDE « écoulement non visible » et « assec » pour chaque jour *j* et pour chaque HER-RH. Cette statistique est supposée renseigner la probabilité régionale d'assec des cours d'eau d'ordre de Strahler inférieur à 5 (Regional Probability of Drying, $RPoDONDE_{HER\text{-}RH}$) :

$$RPoD_{HER\text{-}RH}(j) = \frac{Ndrying_{HER\text{-}RH}(j)}{Ndrying_{HER\text{-}RH}(j) + Nflowing_{HER\text{-}RH}(j)}$$

où *Ndrying* et *Nflowing* sont respectivement le nombre d'observations « écoulement non visible » et « assec » et le nombre d'observations « écoulement visible ». Des relations empiriques entre un indicateur journalier *F* issu des jeux de stations/piézomètres de référence caractérisant la situation hydrologique et piézométrique, et la variable $RPoD_{HER\text{-}RH}$ sont établies aux dates des relevés ONDE, puis appliquées en dehors de ces dates pour reconstruire la dynamique complète.

3.3.1. Méthode

La méthode considère deux étapes successives :

- *Définition de l'indicateur journalier F :* La courbe des débits classes et son équivalente pour les niveaux piézométriques sont calculées pour transformer les données brutes de débit et de niveau piézométrique en fréquence au non dépassement. On retient la moyenne des fréquences empiriques au non dépassement des débits et niveaux piézométriques sur la période [*j*-5 ; *j*] où *j* est le jour de l'observation ONDE. Cette fenêtre de six jours permet d'intégrer des réponses non concomitantes (du fait de dynamiques différentiées induites par le stockage en nappe, les temps de propagation dans les biefs, etc.). Finalement, l'indicateur *F* choisi pour décrire les conditions hydrologiques et piézométriques est :

$$F(j) = \frac{\sum_{i=1}^{i=N_Q} F_Q(i,j) + \sum_{i=1}^{i=N_{GW}} F_{GW}(i,j)}{N_Q + N_{GW}}$$

où N_Q et N_{GW} sont le nombre de stations hydrométriques et de piézomètres dans la région HER-RH et $F_Q(i,j)$ et $F_{GW}(i,j)$ sont les fréquences moyennes au non dépassement sur la période [*j*-5 ; *j*] à la station ou au piézomètre *i.*

- *Elaboration des formules empiriques reliant F et* $RPoD_{ONDE}$: Deux formules analytiques ont été calées sur les observations ONDE :
  - Une régression linéaire logarithmique (LLR) par morceau avec deux paramètres α_1 and β_1:

$$RPoD_{LLR}(j)=\begin{cases}\min(1;\alpha_1\times ln(F(j))+\beta_1) \text{ si } F< F0\\ 0 \text{ si } F\geq F0\end{cases}$$

    $F0$ est la valeur de F au-delà de laquelle aucun assec n'est observé ($RPoD_{ONDE}=0$).
  - Une régression logistiques (LR) ou modèle logit avec deux paramètres α_2 et β_2 :

$$Logit(RPoD_{LR}(j))=\ln\left(\frac{RPoD_{LR}(j)}{1-RPoD_{LR}(j)}\right)=\alpha_2\times F(j)+\beta_2$$

    et qui s'écrit encore :

$$RPoD_{LR}(j)=\frac{exp(\beta_2+\alpha_2\times F(j))}{1+exp(\beta_2+\alpha_2\times F(j))}$$

Un exemple d'application à une zone localisée dans les Cévennes est donné en *Figure 6*.

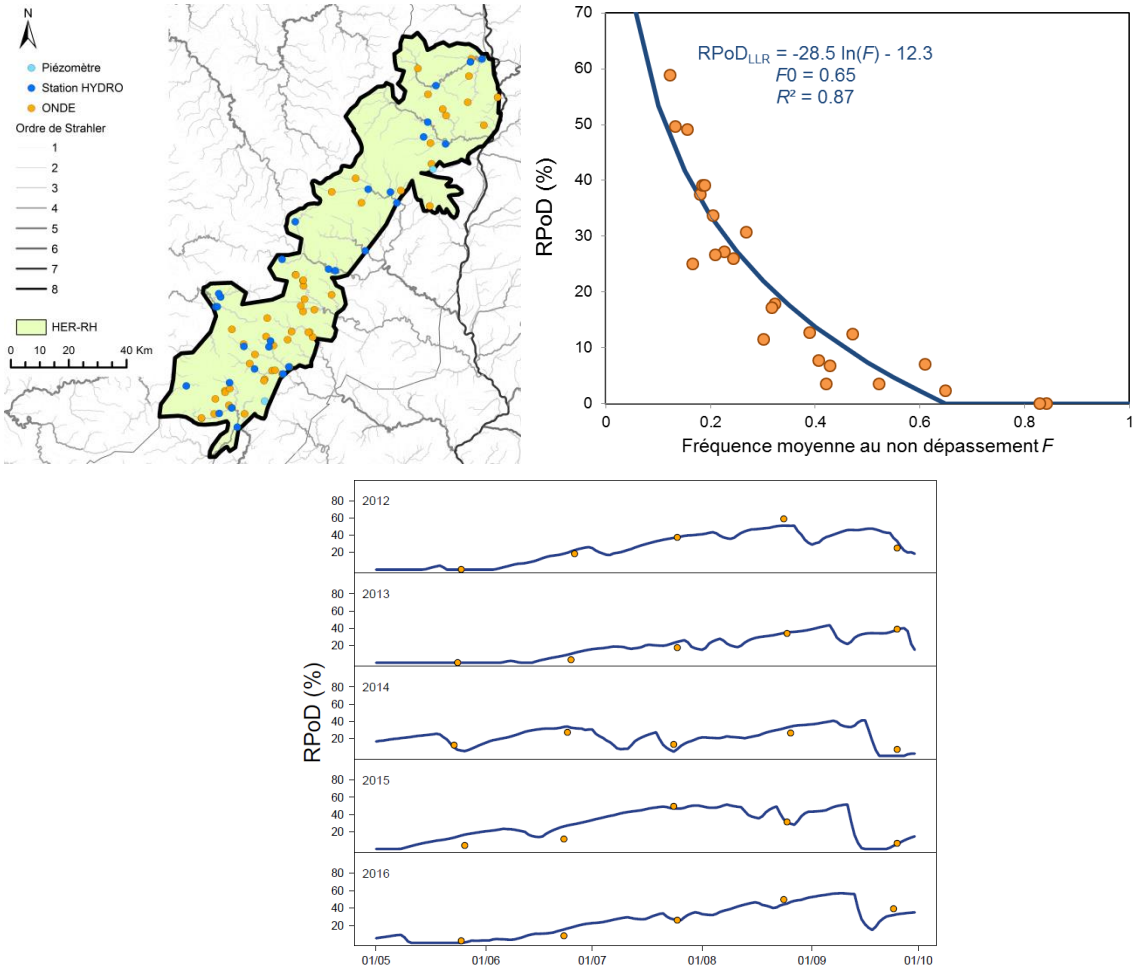

Figure 6 : Calage et application du modèle LLR sur une région HER-RH des Cévennes sur la période 2012-2016

3.3.2. Validation et incertitudes

La qualité de l'ajustement est mesurée par le critère de Nash-Sutclife (*NSE*, Nash et Sutcliffe, 1970) en comparant les valeurs de *RPoD* observées et estimées par les deux modèles LLR et LR.

Les deux modèles calés sur la période 2012-2016 avec le jeu de référence 2011-2017 sont globalement performants avec une moyenne du *NSE* de 0.8 pour LR et de 0.7 pour LLR (*Figure 7*). Avec le modèle LR, 50% des régions HER-HR (65% du territoire) présentent un *NSE* supérieur à 0.8 contre 33% des régions HER-HR (50% du territoire) avec le modèle LLR. Les scores les plus élevés s'observent dans les plaines sédimentaires, dans le sud-est de la France et dans les Pyrénées. Inversement, des performances moindres sont obtenues dans les secteurs de montagne (Alpes, Massif Central). Dans ces secteurs, les HERs de niveau 2 sont petites et le nombre de sites ONDE, de stations hydrométriques et piézomètres par combinaison HER2-HR est certainement trop faible pour

établir des relations fiables. L'estimation de *RPoD* reste impossible pour neuf combinaisons HER-HR (4.5% de la France métropolitaine) soit par absence de sites ONDE ou car le nombre total de stations hydrométriques et de sites piézométriques a été jugé insuffisant (moins de cinq) pour mettre en place une formule empirique.

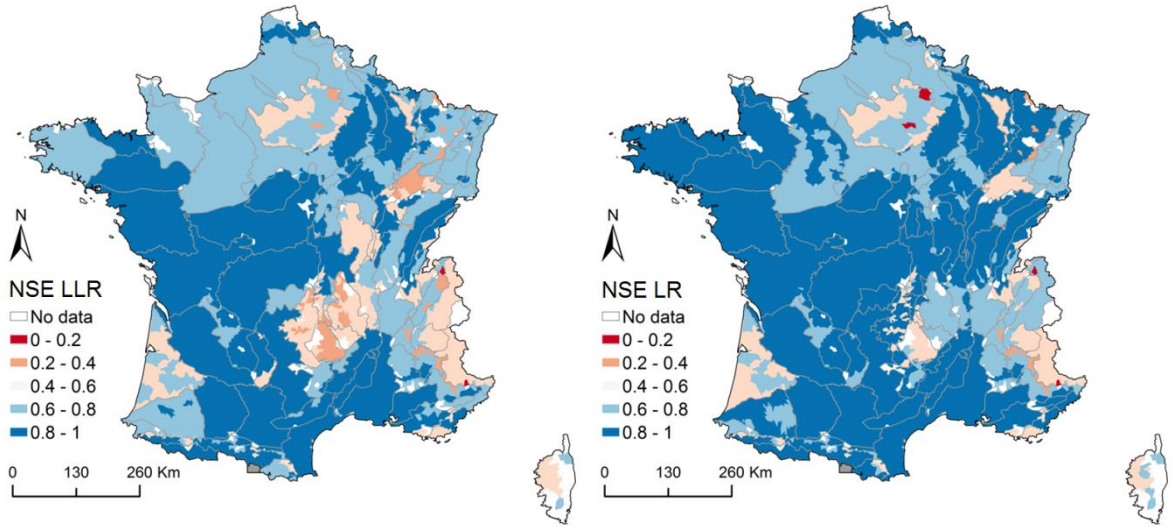

Figure 7 : Performance des modèles sur la période 2012-2016 avec le jeu de référence 2011-2017 (© Aurélien Beaufort)

Une analyse similaire a été menée avec le jeu de référence 1989-2017. Comme attendu, la performance avec ce jeu de données est moindre du fait d'une densité de stations hydrométriques et piézomètres plus faible. La différence en termes de *NSE* est inférieure à 0.1 pour 75% des régions HER-RH pour le modèle LLR et pour 64% des régions HER-RH pour le modèle LR.

Une validation a été engagée sur un réseau d'observations indépendant géré par le Groupement Régional des Fédérations de Pêche de Poitou-Charentes qui fournit un état hydraulique des cours d'eau sensibles aux assecs depuis 2006 (http://www.eau-poitou-charentes.org/Suivi-assecs-Federations-de-Peche.html). Entre juin et septembre, des observateurs parcourent le linéaire et classent ainsi l'état de l'écoulement par tronçon hydrographique deux fois par mois distinguant quatre catégories : écoulement perceptible, écoulement visible faible, rupture d'écoulement, et assec. Deux modèles régionaux LLR et LR exploitant les sites ONDE en dehors du réseau inspecté a été mis en œuvre. La *Figure 8* démontre la performance des modèles LLR et LR et par extension les capacités prédictives des modèles en extrapolation spatiale.

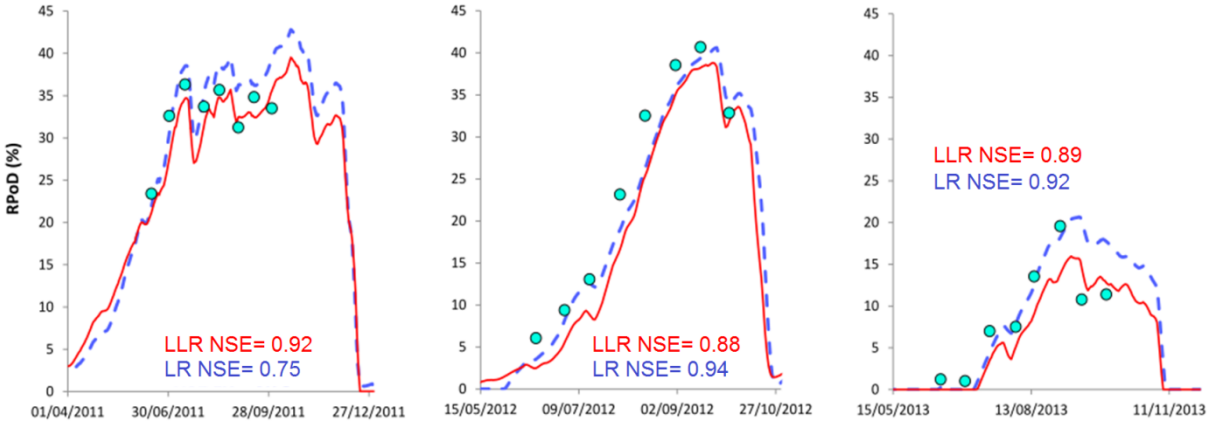

Figure 8 : Performance des modèles examinée sur les données de Poitou-Charentes avec le jeu de référence 2011-2017

A l'échelle de la France, l'analyse des performances mensuelles et annuelles sur la période de calage 2012-2016 montre que les estimations de *RPoD* sont de meilleure qualité pendant les années sèches 2012 and 2016 (*NSE*= 0.8) que pendant les années humides (p. ex. 2014 avec *NSE*< 0.7). L'efficience est moindre pendant les mois de mai et de juin lorsque les assecs sont moins fréquents, comparativement aux mois d'août et de septembre plus riches en assecs. Enfin, l'année 2017 a été réservée pour examiner la capacité en extrapolation des modèles. Les critères de Nash-Sutcliffe obtenus avec les deux jeux de référence 2011-2017 et 1989-2017 sont dans la gamme des *NSE* calculés sur les différentes années de la période de calage 2012-2016.

La *Figure 9* montre les valeurs de *RPoD* par mois observés à partir des suivis ONDE et celles obtenues par le modèle LR sur les mêmes jours. La dynamique temporelle et la répartition spatiale simulée sont conformes avec les observations : peu d'assecs en mai et des assecs généralisés en août ; des assecs principalement dans le nord de la France entre mai et septembre et sur le pourtour méditerranéen entre juillet et septembre, le Massif Central reste relativement épargné. Les écarts entre simulations et observations ne présentent pas de structure spatiale particulière.

Les deux modèles ont ainsi démontré leur capacité à prédire *RPoD* dans et en dehors de la période de calage. En revanche, il n'a pas été possible de départager objectivement les deux modèles : leurs efficiences relatives sont comparables, il n'y a pas de biais systématique manifeste (que ce soit une surestimation ou une sous-estimation d'un modèle en particulier sur les quelques années disponibles) et les conserver permet d'intégrer une partie des incertitudes lors de situations extrêmes et inédites en termes de situations hydro-climatiques passées ou futures, en dehors de la période de calage.

3.3.3. Applications

La première application est l'appréciation de la sévérité des assèchements des cours d'eau à l'échelle de la France. La *Figure 10* montre le nombre maximum de jours consécutifs avec un *RPoD* supérieur à 20% ($D_{RPoD>20\%}$) simulé par le modèle LR. Les régions les plus touchées sont situées dans le sud-est de la France et dans les plaines sédimentaires, en cohérence avec les observations de ONDE (*Figure 3*) et la hiérarchie des années en termes de sites ONDE touchées par des assecs : l'année 2012 est l'année la plus sévère, avec environ 30% de la France affichant une durée maximale $D_{RPoD>20\%}$ supérieure à 60 jours, suivie de 2015 (20% de la France avec $D_{RPoD>20\%}$> 60 jours) et 2016 (15% de la France avec $D_{RPoD>20\%}$> 60 jours). Les années 2013 et 2014 sont faiblement affectées par les assecs (moins de 6% de la France avec une durée maximale $D_{RPoD>20\%}$> 60 jours). Cette application montre la variabilité à la fois temporelle et spatiale des assecs : les régions affectées par les assecs diffèrent d'une année à une autre et il n'y a pas de « régularité » : les assecs sont dépendants du climat et chaque année propose une structure spatiale et une dynamique temporelle particulières.

La seconde application concerne une analyse de la variabilité temporelle des assecs à l'échelle nationale (*Figure 11*). Pour cette application, les modèles ont été calées avec le jeu de référence 1989-2017. Les variations de *RPoD* proposées par les deux modèles LLR et LR sont semblables et sont conformes aux observations ONDE sur la période 1989-2016. La probabilité régionale d'assec est très variable sur l'ensemble de la période de simulation, avec une alternance de phases sèches (1989 à 1991, 2003 à 2006, 2009 à 2012) et humides (1994 à 1995, 2000 à 2002, 2013 à 2014). Malgré cette variabilité interannuelle, la saisonnalité de ce processus est très marquée : les pics de *RPoD* se produisent régulièrement entre août et septembre, que ce soit en année sèche ou en année humide. Ce résultat est cohérent avec la prééminence des régimes pluviaux avec des étiages estivaux en France. Notons que ces modèles ont été utilisés en extrapolation en dehors des mois de calage (mai à septembre inclus).

Les valeurs les plus élevées de *RPoD* (supérieures à 35% sur la France) sont observées en 1989, 1990, 1991, 2003 et 2005 (courbe noire, *Figure 11*). Ainsi, il n'apparait pas une tendance à des assèchements plus marqués/étendus ces dernières années. Les valeurs de *RPoD* estimées pendant ces années sèches sont hors de la plage des valeurs observées sur la période de calage (2012-2016). Les estimations sont donc incertaines. Toutefois, les valeurs élevées de *RPoD* concordent avec les observations relevées dans des études antérieures (p. ex. Larue et Giret, 2004 ; Snelder *et al.*, 2013 ; Caillouet *et al*., 2017). Inversement, les années moins affectées par les assecs sont les années 1994, 2001 et 2014 (*RPoD* moyen inférieur à 15%). Les résultats obtenus avec le modèle LLR sont plus contrastés en termes de valeurs extrêmes que celles obtenues avec le modèle LR.

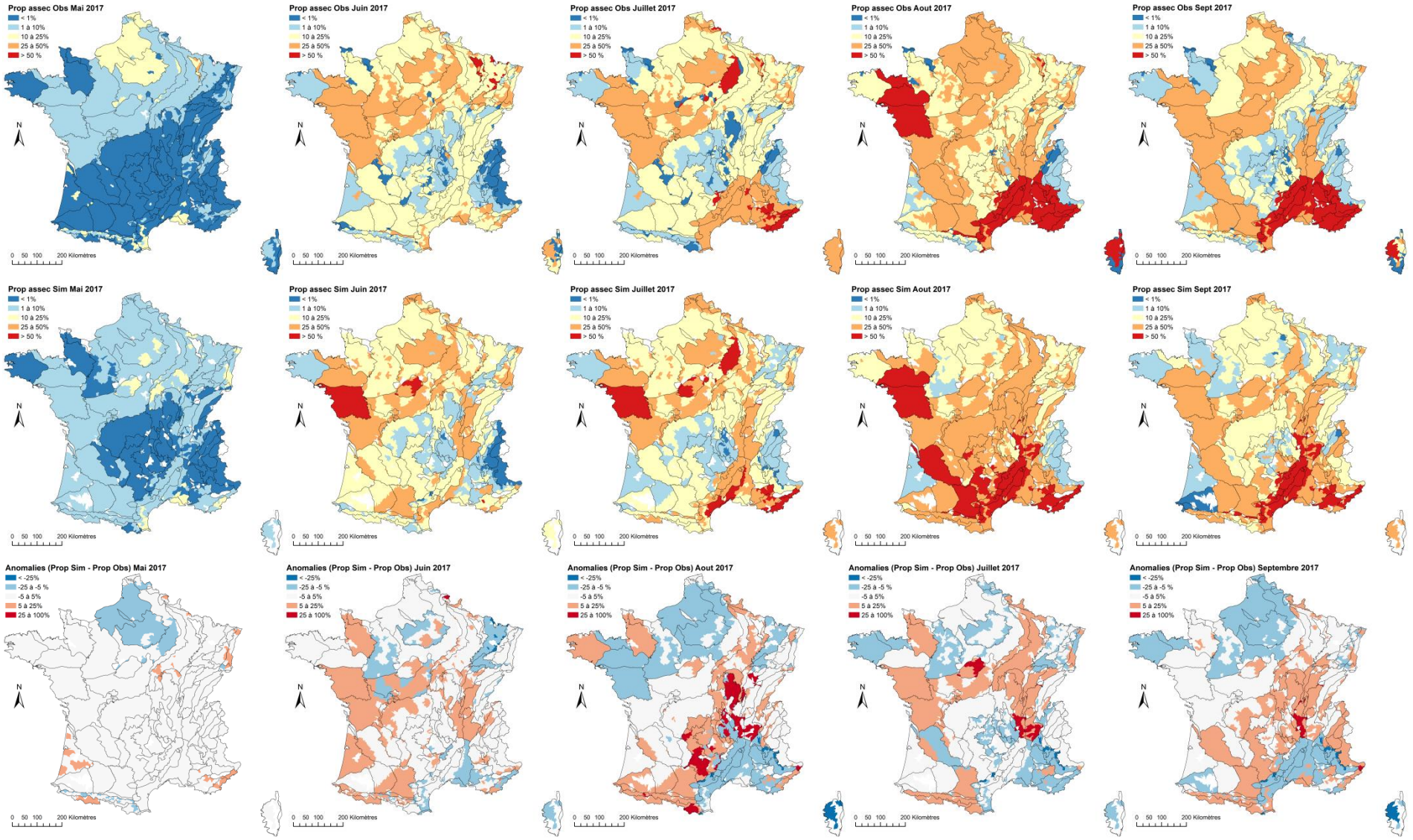

Figure 9 : Simulations et observations de RPoD aux dates d'observation ONDE en 2017 – Résultats obtenus avec le modèle LR calé sur le jeu de référence 2011-2017 et sur la période 2012-2016 (© Aurélien Beaufort)

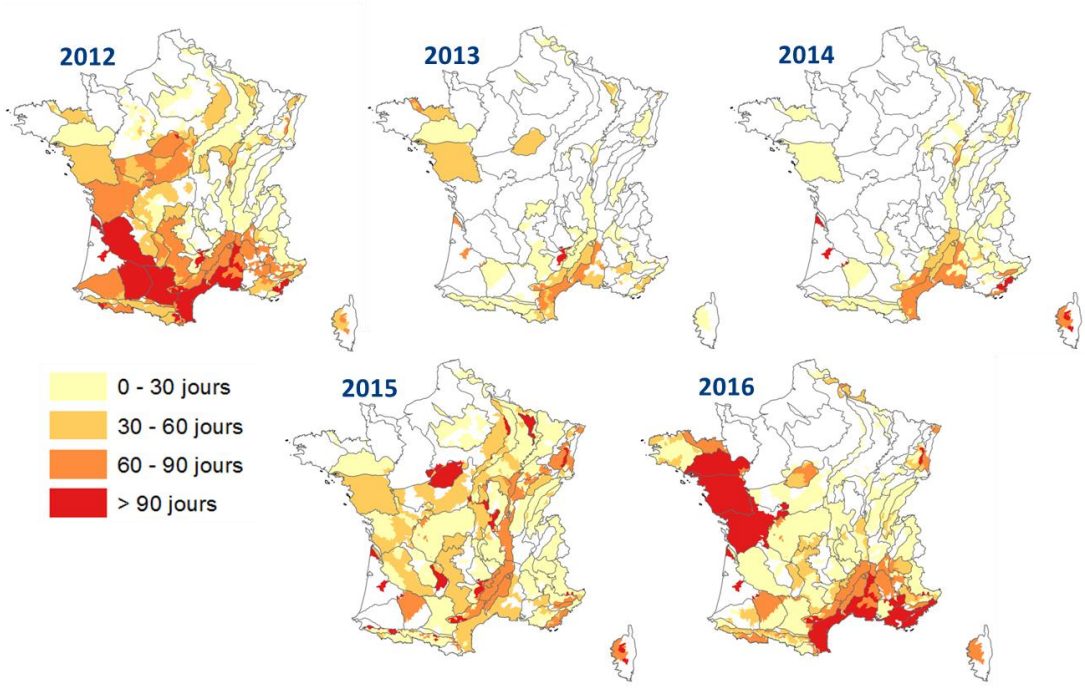

Figure 10 : Estimation de la durée avec une probabilité régionale d'assec RPoD supérieure à 20% avec le modèle LR (© Aurélien Beaufort)

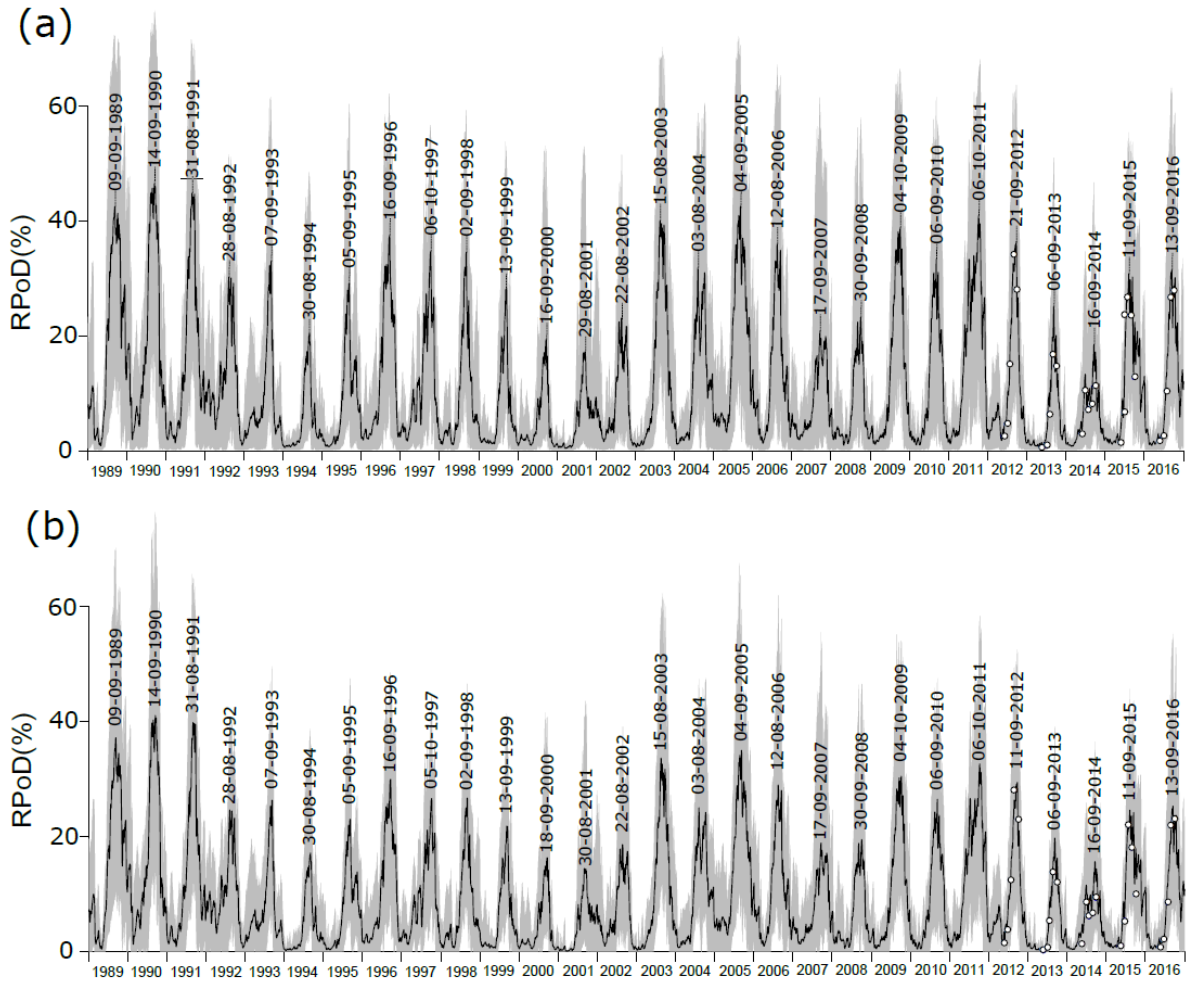

Figure 11 : RPoD simulée entre 1989 et 2016 avec le jeu de référence 1989-2017 avec (a) le modèle LR et (b) le modèle LLR. La zone grise représente le RPoD entre le 10e et le 90e percentile simulé sur l'ensemble des régions HER-RH, la courbe noire représente la RPoD moyenne simulée sur l'ensemble des régions HER-RH et les points blancs représentent les valeurs observées $RPoD_{ONDE}$ moyenne. Les dates mentionnées correspondent au jour de la valeur moyenne maximale annuelle de RPoD

3.4. Reconstitution des dynamiques d'assèchement journalières aux sites ONDE

La méthode développée a été proposée pour publication dans *Hydrological Processes* en décembre 2018 (Annexe 2 : Statistical reconstruction of local daily drying dynamics at headwater streams based on qualitative information: a case study in France (Beaufort *et al*., soumis à Hydrological Processes), page 51). L'article soumis est en cours d'évaluation et une synthèse des principaux résultats est présentée ici. La variable cible est l'état hydraulique de l'écoulement exprimé selon deux modalités : soit « écoulement non visible » et « assec », soit « écoulement visible » pour chaque jour *j* et chaque station ONDE.

3.4.1. Méthode

Pour reconstituer les phases d'assec, nous avons exclu l'usage de modèles hydrologiques. En effet,

(i) ils peinent à représenter les débits en étiage et donc encore plus les étiages extrêmes que sont les assecs. La solution usuelle pour pallier les défauts des modèles est d'appliquer un post-traitement des débits simulés pour forcer les valeurs à zéro (p. ex. Cipriani *et al.*, 2014 ; Yu *et al.*, 2018) ;

(ii) ils exploitent dans les procédures de calage et fournissent en sortie des données quantitatives de débits.

Notre choix s'est porté sur l'utilisation de modèles empiriques statistiques pour prédire l'état hydraulique à partir de variables explicatives. Il n'est pas possible d'orienter *a priori* vers un modèle particulier étant donné la complexité des processus impliqués dans les assèchements et l'effet de seuil (valeurs nulles ou strictement supérieures à zéro) qui régit l'état d'assec. De ce fait, trois structures différentes ont été testées :

- les réseaux neuronaux (Artificial Neural Network, ANN) : ce sont des outils réputés puissants pour extraire des structures beaucoup trop complexes pour un programmeur humain. Comme le nom le suggère, les algorithmes sont inspirés du fonctionnement du cerveau et destinés à reproduire la manière dont les humains apprennent ;
- les forêts d'arbres décisionnels (Random Forest, RF) : ils combinent des arbres décisionnels individuels obtenus en ré-échantillonnant l'échantillon de calage (Breiman, 2001). Chaque arbre partitionne de manière récursif les individus en groupes non-recouvrants et homogènes vis-à-vis de la variable cible. La structure de l'arbre se présente sous la forme de nœuds binaires associés à des règles de décision de type « $V \leq s$ » versus « $V > s$ » où V est l'une des variables descriptives et s une valeur numérique seuil. Lorsqu'on atteint un nœud terminal, la décision s'opère selon un vote à la majorité au sein du groupe défini par ce nœud ;
- la régression linéaire dans sa déclinaison LASSO (Least Absolute Shrinkage and Selection Operator, Tibshirani, 1996) : l'intérêt de cette variante est de fixer à zéro les poids des variables non significatives ;

pour explorer le potentiel de structures linéaires (LASSO) et non-linéaires (RF). Les réseaux de neurones émargent aux deux catégories : ils sont suffisamment souples pour être des estimateurs linéaires ou non-linéaires selon le cas d'application. Les réseaux de neurones et les forêts d'arbres décisionnels font partie des techniques devenues classiques d'apprentissage machine (« machine learning »).

Les modèles calés sur les observations ONDE fournissent l'état hydraulique du jour à partir d'un ensemble de variables prédictives (*i.e.* des données journalières climatiques, piézométriques et hydrologiques et des descripteurs « statiques » de la station ONDE) sur la période de suivi du réseau ONDE (1er mai au 30 septembre inclus).

Les observations aux sites ONDE sont insuffisantes pour garantir la robustesse des modèles avec, en moyenne, 32 observations sur la période 2012-2016. Nous avons opté pour un calage à l'échelle régionale. Au final, l'état hydraulique à la station ONDE localisée au point (x,y) au sein d'une région R est donné à la date j par :

$$FlowState(x,y,j)=f_R(y_1(x,y,j),y_2(x,y,j),\ldots,y_n(x,y,j),z_1(x,y),z_2(x,y),\ldots,z_m(x,y))$$

où $y_i(x,y,j)$, i=1, n sont les n variables explicatives au point (x,y) et à la date j et où $z_i(x,y)$, i=1, m sont les m descripteurs du site, invariants temporels, caractéristiques du point (x,y). Le modèle f_R est calé sur des regroupements de sites ONDE formant la région R. Ici, les régions choisies R pour le calage reprennent les contours des HERs. L'hypothèse retenue est celle que les sites ONDE de géologie et de

régime hydrologique similaires partage le paramétrage du modèle f_R. Le Tableau 1 présente la liste des variables potentiellement explicatives. On y retrouve les variables *FQ* et *FGw* élaborées à partir des données hydrologiques et piézométriques (cf. section 3.3.1, page 13), du fait de leur pertinence dans la reconstitution des probabilités d'assec à l'échelle régionale. Les variables climatiques sont issues de la base de données SAFRAN (Quintana-Seguí *et al.,* 2008; Vidal *et al*., 2010) et les variables morphométriques du RHT (Pella *et al*., 2012).

Type	Nom	Définition	Pas de temps de calcul
Climat	*R*0	Précipitations cumulées du jour considéré à la date *j*	Jour
	*R*1	Précipitations cumulées du jour précédent *j*	Jour
	*R*10	Précipitations cumulées 10 jours avant *j*	Jour
	*R*20	Précipitations cumulées 20 jours avant *j*	Jour
	*R*30	Précipitations cumulées 30 jours avant *j*	Jour
	*T*0	Température de l'air le jour considéré à la date *j*	Jour
	*T*1	Température de l'air du jour précédent *j*	Jour
	*T*10	Température de l'air moyenne 10 jours avant *j*	Jour
	*T*20	Température de l'air moyenne 20 jours avant *j*	Jour
	*T*30	Température de l'air moyenne 30 jours avant *j*	Jour
	*PET*0	Evapotranspiration potentielle du jour considéré à la date *j*	Jour
	*PET*1	Evapotranspiration potentielle du jour précédent *j*	Jour
	*PET*10	Evapotranspiration potentielle cumulée 10 jours avant *j*	Jour
	*PET*20	Evapotranspiration potentielle cumulée 20 jours avant *j*	Jour
	*PET*30	Evapotranspiration potentielle cumulée 30 jours avant *j*	Jour
	AI	Index d'Aridité P/ETP	Constante
	WR	Précipitations hivernales cumulées (décembre à mars)	Année
Hydrologie	F_Q0	Moyenne des fréquences au non-dépassement du débit observé à la date *j* des stations hydrométriques de la même sous-région HER-RH que le site ONDE	Jour
	F_Q 5	Moyenne des fréquences au non-dépassement des débits observés les 5 jours avant *j* des stations hydrométriques de la même sous-région HER-RH que le site ONDE	Jour
	F_Q 10	Moyenne des fréquences au non-dépassement des débits observés les 10 jours avant *j* des stations hydrométriques de la même sous-région HER-RH que le site ONDE	Jour
Piézométrie	F_{Gw}0	Moyenne des fréquences au non-dépassement du niveau piézométrique observé à la date *j* des piézomètres de la même HER que le site ONDE	Jour
	F_{Gw} 5	Moyenne des fréquences au non-dépassement des niveaux piézométriques observés les 5 jours avant *j* des piézomètres de la même HER que le site ONDE	Jour
	F_{Gw} 10	Moyenne des fréquences au non-dépassement des niveaux piézométriques observés les 10 jours avant *j* des piézomètres de la même HER que le site ONDE	Jour
Caractéristiques locales des sites ONDE	*Alti*	Altitude moyenne du bassin versant (m)	Constant
	Area	Superficie drainée (km²).	Constant
	Slope	Pente moyenne sur le bassin versant (m.km^{-1}).	Constant
	MPD	Proportion mensuelle d'observations en « assec » ou « écoulement non visible » entre 2012 et 2016 (%)	Mois

Tableau 1 : Liste des variables testées dans les modèles

3.4.2. Validation et incertitudes

Les trois modèles sont comparés à un modèle empirique naïf qui attribue à la date *j* à la station ONDE, la modalité dominante du mois considéré (« Benchmark Classifier », BC). Notons que l'année de la date *j* est exclue pour le calcul de la modalité dominante (fonctionnement en « validation croisée »).

L'analyse de performance s'est concentrée sur quatre HERs contrastées sur la période 2012-2017 (*Figure 12*). Une procédure de validation croisée incluant aléatoirement 80% des données sur la période 2012-2016 a été engagée 20 fois sur les sites ONDE pour tous les modèles. Les modèles étant calés sur 2012-2016, la capacité d'extrapolation des méthodes sur les trois mois de mai à juillet de l'année 2017 a été examinée.

L'application des modèles au droit de 65 stations hydrométriques – intermittentes ou non– (Tableau 2) présentes dans la HER a permis d'apprécier la dynamique temporelle reconstituée des assecs (en ces points, un assec ou un écoulement non visible est considéré lorsque le débit est inférieur ou égal à 1 L/s et la variable MPD (Tableau 1) est calculée à partir des débits journaliers observés au 25^{e} jour du mois, pour se conformer au calendrier du réseau ONDE) et de vérifier si les modèles ne généraient pas

des assecs sur des cours d'eau pérennes sur la période 2012-2016.

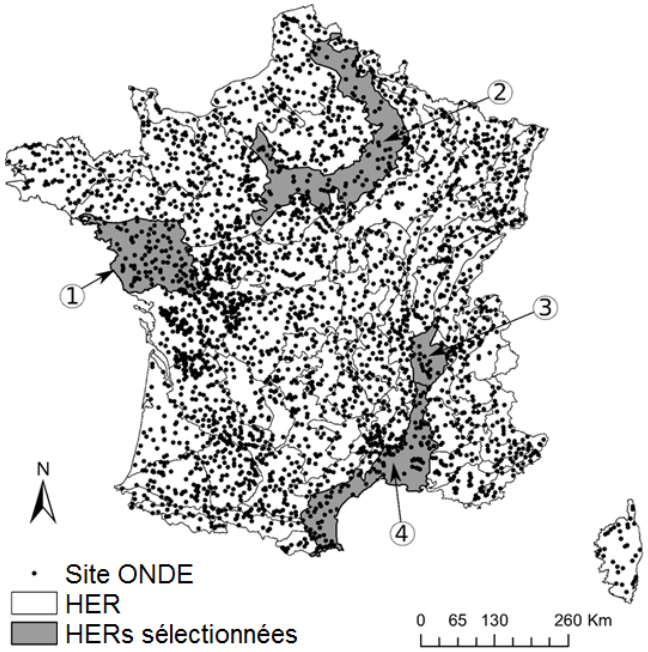

Figure 12 : Localisation des HERs retenues pour l'analyse de performance

HER	1	2	3	4
Nombre de sites ONDE (dont intermittentes)	98 (79)	93 (42)	25 (14)	111 (79)
Nombre de stations hydrométriques (dont intermittentes) *	26 (11)	13 (2)	4 (1)	22 (9)
Nombre de piézomètres	15	119	36	130
Nombre d'observations ONDE	3906	2223	785	3381
Nombre d'observations ONDE en « assec » ou « écoulement non visible »	710 (18.2%)	213 (9.6%)	113 (14.4%)	892 (26.4%)
Altitude moyenne (m)	67	105	324	132
Superficie (km²)	17800	27300	5000	17600
Précipitation annuelle moyenne (mm)	895	765	1137	676
ETP annuelle moyenne (mm)	715	616	711	1051
Indice d'aridité P/ETP (-)	1.25	1.24	1.60	0.64
Température annuelle moyenne (°C)	12.2	11.0	11.5	14.5

*Tableau 2 : Principales caractéristiques des HERs retenues pour l'analyse de performance. * : sont considérées intermittentes les stations hydrométriques ayant enregistré des débits inférieurs ou égaux à 1L/s pendant cinq jours consécutifs (Source des données : RHT, SAFRAN, HYDRO, ONDE, ADES)*

La performance des modèles a été examinée au travers des scores de vérification utilisés pour qualifier les prévisions hydrométéorologiques. Ces scores sont calculés sur les sites ONDE ici à partir de la table de contingence décrivant la distribution conjointe des modalités « écoulement visible » ou son complémentaire « assec » ou « écoulement non visible » simulées et observées aux stations ONDE. Le tableau de contingence est construit ici pour détecter les événements d'« assec » ou « écoulement non visible ».

		Observation	
		« assec » ou « écoulement non visible »	« écoulement visible »
Simulation	« assec » ou « écoulement non visible »	Détection (a)	Fausse alerte (b)
	« écoulement visible »	Non-détection (c)	Rejet correct (d)

Tableau 3 : Tableau de contingence adapté à l'identification des modalités d'écoulement aux sites ONDE

Les scores choisis issus du Tableau 3 sont :

- la sensibilité ou taux de détection (probability of detection, *POD* ou *Recall*) : $POD = a/(a+c)$; ce score mesure la proportion d'événements correctement simulés. Sa valeur se situe entre 0 et 1, 1 étant le score parfait ;
- le taux de fausses alarmes (false alarm ratio, *FAR*) : $FAR = b/(a+b)$; ce score mesure la proportion d'événements simulés alors qu'ils n'en étaient pas. Sa valeur se situe entre 0 et 1, 0 étant le score parfait ;
- la valeur prédictive positive (*Precision*) : $Precision = a/(a+b)$; ce score mesure la fraction d'événements identifiés dans les simulations. Sa valeur se situe entre 0 et 1, 1 étant le score parfait ;
- Une mesure de l'exactitude (F-Score) qui combine les deux scores *Recall* et *Precision* : $F\text{-}score = \frac{2 \times Precision \times Recall}{Precision + Recall}$; sa valeur se situe entre 0 et 1, 1 étant le score parfait.

Aux stations hydrométriques de contrôle, outre les précédents scores, la performance est mesurée en comparant les proportions d'états « assec » ou « écoulement non visible » observés P_{obs} et simulés P_{pred} (calcul du biais et de la racine de l'erreur quadratique moyenne *RMSE* à l'échelle des HERs).

Les résultats montrent que :

- (en validation croisée, *Figure 13* gauche) les trois modèles statistiques sont plus performants que le modèle naïf BC quel que soit le critère considéré. Ils fournissent des efficiences équivalentes (avec un *POD* globalement supérieur à 75%) avec un léger avantage à RF (sur la base du *F-score* et du *FAR*) ;
- (en extrapolation sur 2017, *Figure 13* droite) le meilleur modèle est le modèle naïf BC en termes de *POD* (> 60%) mais au prix d'un *FAR* élevé (> 50%) ; ce résultat sous-entend une surestimation des modalités « assec » et « écoulement non visible », en particulier dans les HER1 et HER3. Les modèles RF et LASSO conduisent à des performances modérées (*POD* < 50% sur les HER1, HER2 et HER3 et *FAR* très faibles sur les HER2, HER3 et HER4) ; ceci sous-entend une sous-estimation des modalités « assec » et « écoulement non visible ». Finalement le modèle ANN présente un *POD* > 50% et un *FAR* significativement inférieur à celui obtenu avec le modèle BC. Finalement c'est ce modèle qui détient le meilleur *F-score* pour chaque HER ;
- (sur les stations hydrométriques, *Figure 14*) les valeurs P_{pred} suggérées par les trois modèles ANN, LASSO et RF sont proches de P_{obs} plus particulièrement pour les stations avec une fréquence d'intermittence supérieure à 20%. Le modèle ANN semble le plus performant avec une valeur de *RMSE* moyenne de 3% sur les quatre HERs tests et 23 stations hydrométriques intermittentes détectées (P_{pred}> 0%) sur 2012-2016 parmi les 27 présentes dans le jeu de stations testées ; la performance est plus critiquable sur la HER4 avec un biais positif et *FAR* ≈ 40% (tendance à surestimer les occurrences d'assèchement). Le modèle RF tend à sous-estimer de manière systématique les assecs (biais négatif et une majorité de points sous la première bissectrice). Les résultats avec le modèle LASSO sont plus contrastés (pas de biais systématique et, comme RF, une majorité de points sous la première bissectrice pour les bassins faiblement intermittents). Les modèles RF et LASSO détectent moins de 20 stations intermittentes parmi les 27 considérées comme telles (c'est-à-dire les stations hydrométriques ayant enregistré des débits inférieurs ou égaux à 1L/s pendant cinq jours consécutifs).

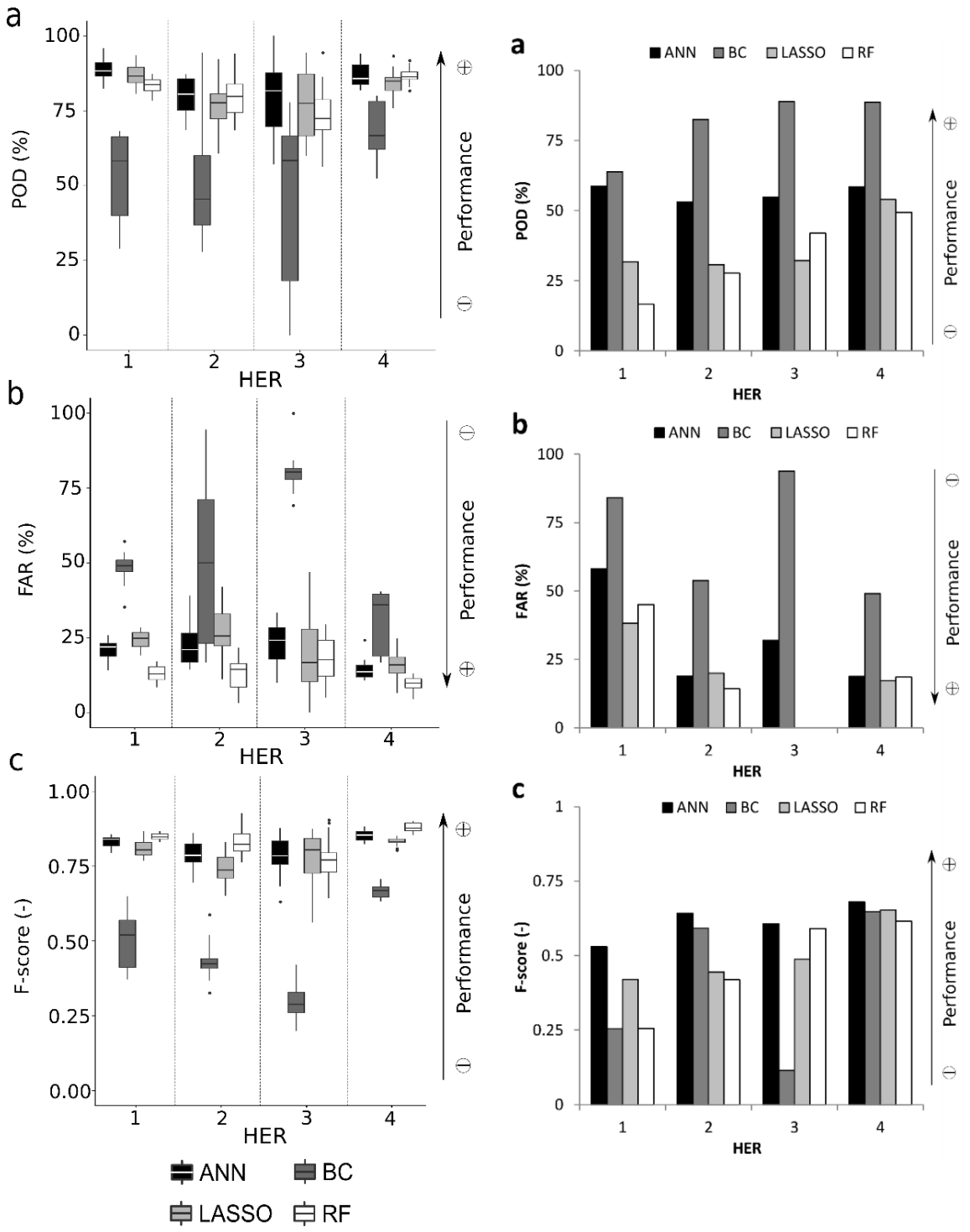

Figure 13 : Scores de performance obtenus en validation croisée sur la période 2012-2016 (à gauche) et en extrapolation sur mai-juin-juillet 2017 (à droite) pour les quatre modèles sur les sites ONDE

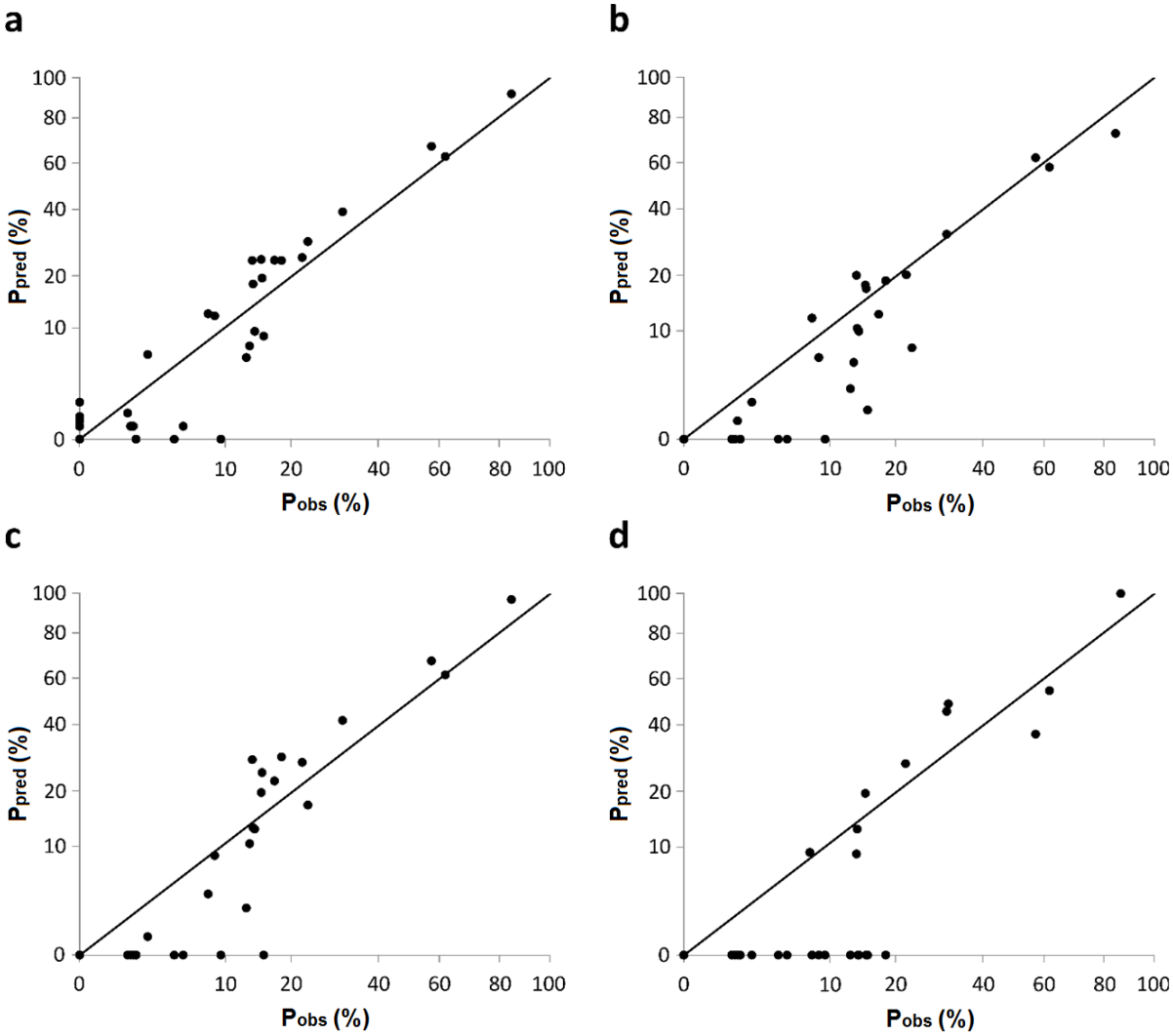

Figure 14 : Proportions d'états « assec » ou « écoulement non visible » observés P_{obs} et simulés P_{pred} aux stations hydrométriques sur la période 2012-2016 selon les quatre modèles. Chaque point est une station hydrométrique. L'échelle des ordonnées est une échelle transformée en racine. La droite tracée est la première bissectrice.

A titre d'illustration, les résultats des simulations sont présentés pour quatre stations hydrométriques intermittentes (P_{obs}> 20%) en *Figure 15*. Le modèle naïf BC propose des évaluations différentes pour chaque année, car, comme écrit plus haut, l'année du calcul est exclue des statistiques.

Pendant l'année 2012 la plus chaude, les trois modèles ANN, RF et LASSO sont cohérents et prédisent des périodes d'assec proches des observations pour trois des quatre HERs. Inversement, ils suggèrent des assecs pour la station hydrométrique de la HER4 qui n'en a pas observé. Néanmoins ces « fausses alertes » sont concomitantes avec des périodes de très faibles débits (< au quantile de fréquence au dépassement 80%).

A l'opposé, durant les années humides (2013 pour les HER2, HER3 et HER4 et 2014 pour les HER2 et HER3), les trois modèles ANN, RF et LASSO surestiment le nombre de jours d'assec ; cependant les séquences sont très courtes. La hiérarchie entre modèles évolue d'une année à une autre : les modèles RF et LASSO peuvent surpasser le modèle ANN ; cependant le modèle ANN semble plus stable et les modèles RF et LASSO peuvent fortement sous-estimer la proportion d'assecs certaines années (p. ex. 2015 et 2016 pour la HER3 avec RF et 2014 et 2015 pour la HER4 avec LASSO).

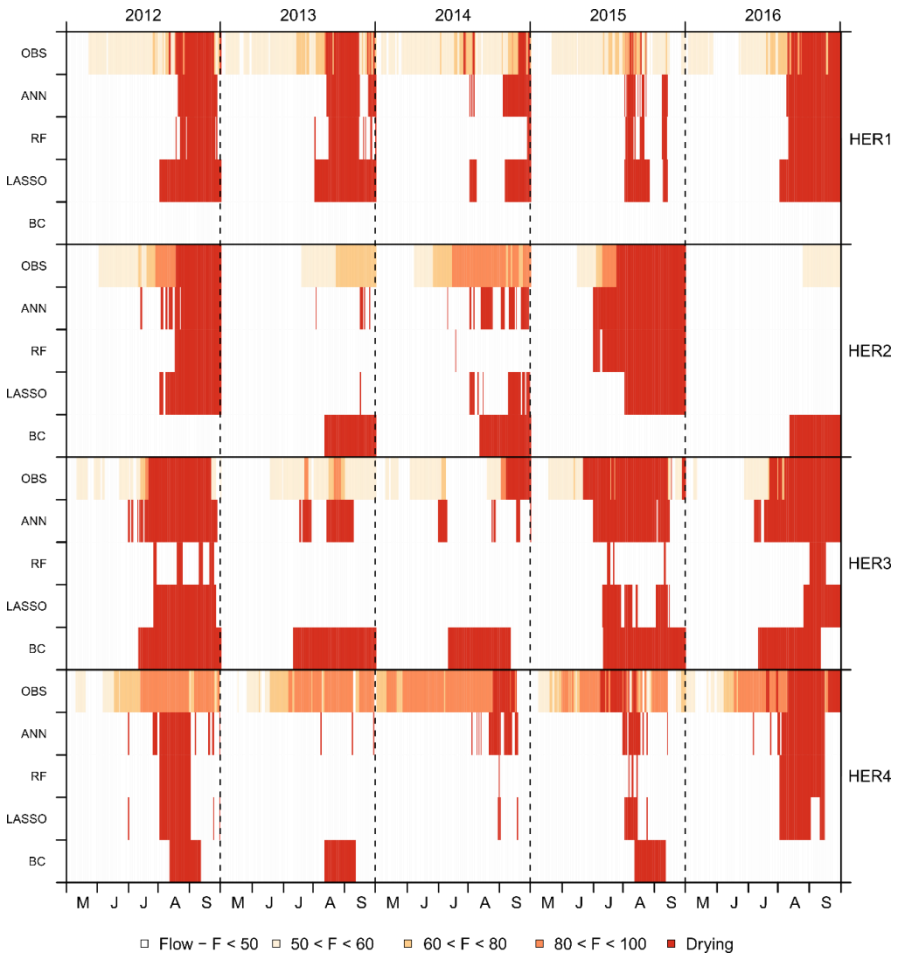

Figure 15 : Etat d'écoulement pour quatre stations hydrométriques localisées dans les quatre HERs. Les débits sont classés en quatre catégories distinctes selon leur fréquence au dépassement calculée sur l'échantillon des débits strictement positifs.

Les modèles ici développés ont montré leur plus-value par rapport à un modèle naïf qui suppose une forme de régularité dans la saisonnalité des assecs. Ils ne sont pas parfaits et leur efficience évolue d'un secteur géographique à un autre, d'une année à une autre. Ces performances différenciées sont dues à la difficulté inhérente de prédire des événements extrêmes. Un modèle, quel qu'il soit, peine à restituer une situation à laquelle il n'a jamais été confrontée pendant sa phase d'apprentissage. Le réseau ONDE est certainement encore trop jeune pour que les modèles intègrent des situations hydrométéorologiques suffisamment contrastées. A ce stade, le plus de confiance serait à attribuer aux réseaux neuronaux ANN (meilleure performance sur le *F-score* en extrapolation sur 2017 et en termes de variabilité interannuelle au droit des stations hydrométriques sur la période 2012-2016). Cette meilleure performance des réseaux neuronaux devra être confirmée ultérieurement en exploitant les futures campagnes du réseau ONDE. En outre,

- les modèles ont tendance à mieux simuler des dynamiques d'assèchement pendant les années sèches et inversement à moins bien les simuler les années humides ;
- la dispersion des performances des modèles semblent moindre dans les secteurs où les cours d'eau intermittents sont très présents (p. ex. HER1 et HER4 en validation croisée, *Figure 13* gauche, page 23).

3.4.3. *Applications*

La première application concerne l'identification et la hiérarchisation des drivers à l'origine de l'intermittence sur la base de l'examen des variables explicatives retenues en entrée des modèles.

La proportion mensuelle d'observations en « assec » ou « écoulement non visible » entre 2012 et 2016 (*MPD*) apparait comme la variable incontournable pour les modèles. Cette variable reflète le niveau moyen d'intermittence des sites ONDE et les modèles cherchent à reproduire la variabilité journalière autour des cinq moyennes mensuelles à l'aide de variables complémentaires.

Certaines études ont souligné l'importance des drivers climatiques pour l'intermittence (p. ex. Abdollahi *et al*., 2017 ; De Girolamo *et al*., 2017). Les modèles RF et LASSO semblent accorder trop d'importance à la variable *MPD*. Les prédictions s'écartent peu des valeurs moyennes, ce qui conduit à

sous-estimer les assecs lorsqu'une nouvelle situation est rencontrée, comme en 2017. ANN accorde plus d'importance aux variables climatiques que RF et LASSO. Les modèles RF et LASSO pourraient ne pas être assez flexibles pour tirer profit de variables autres que *MPD*, à l'inverse des réseaux neuronaux ANN.

Finalement, les caractéristiques locales du site ONDE (Tableau 1, page 20) ne sont pas jugées déterminantes par les trois modèles. Une des raisons possibles est que les régions HER sont suffisamment homogènes pour ne pas rendre une discrimination entre sites sur la base de ces descripteurs nécessaire. Une autre raison pourrait être que ces descripteurs ne rendent pas compte des processus structurants aux échelles (p. ex. caractérisant les échanges nappes-rivières comme la perméabilité du lit des rivières).

La seconde application est le calcul de statistiques à partir des séries reconstituées, *a priori* utiles pour interpréter la réponse biologique. Ces statistiques ont été discutées dans le cadre de l'action COST SMIRES (www.smires.eu, Science and Management of Intermittent Rivers & Ephemeral Streams). Il s'agit de statistiques établies à partir de la durée de l'épisode d'assec le plus long (*DUR*), la date du premier assec (*FreqJul*), du nombre d'événements d'assec (*NbEv*) et du nombre total de jours d'assec (*NbJ*) entre mai et septembre de chaque année. Ici nous avons retenu le modèle LASSO appliquée sur deux années contrastées 2012 et 2015 (*Figure 16*), cette dernière étant marquée par des assecs précoces et plus étendus que pour l'année 2012. Les modèles ainsi développés pourraient être appliqués sur la période 1989-2017, dans le cadre de travaux ultérieurs, pour établir des statistiques robustes et mettre à jour la carte de localisation des cours d'eau intermittents de Snelder *et al*. (2013).

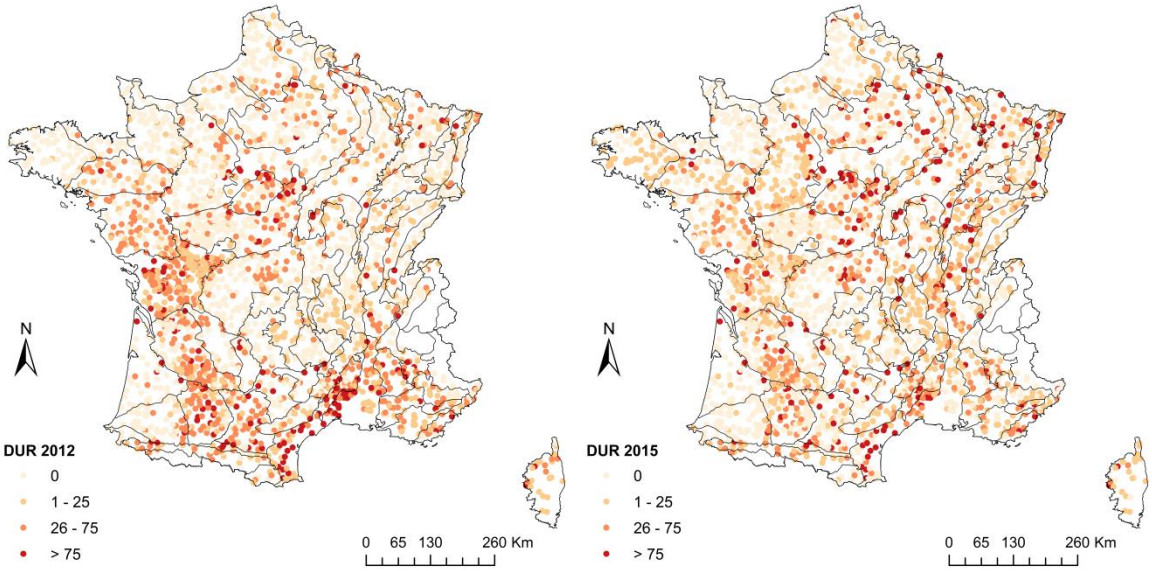

Figure 16 : Cartes de statistiques d'assec pour les années 2012 et 2015 (© Aurélien Beaufort)

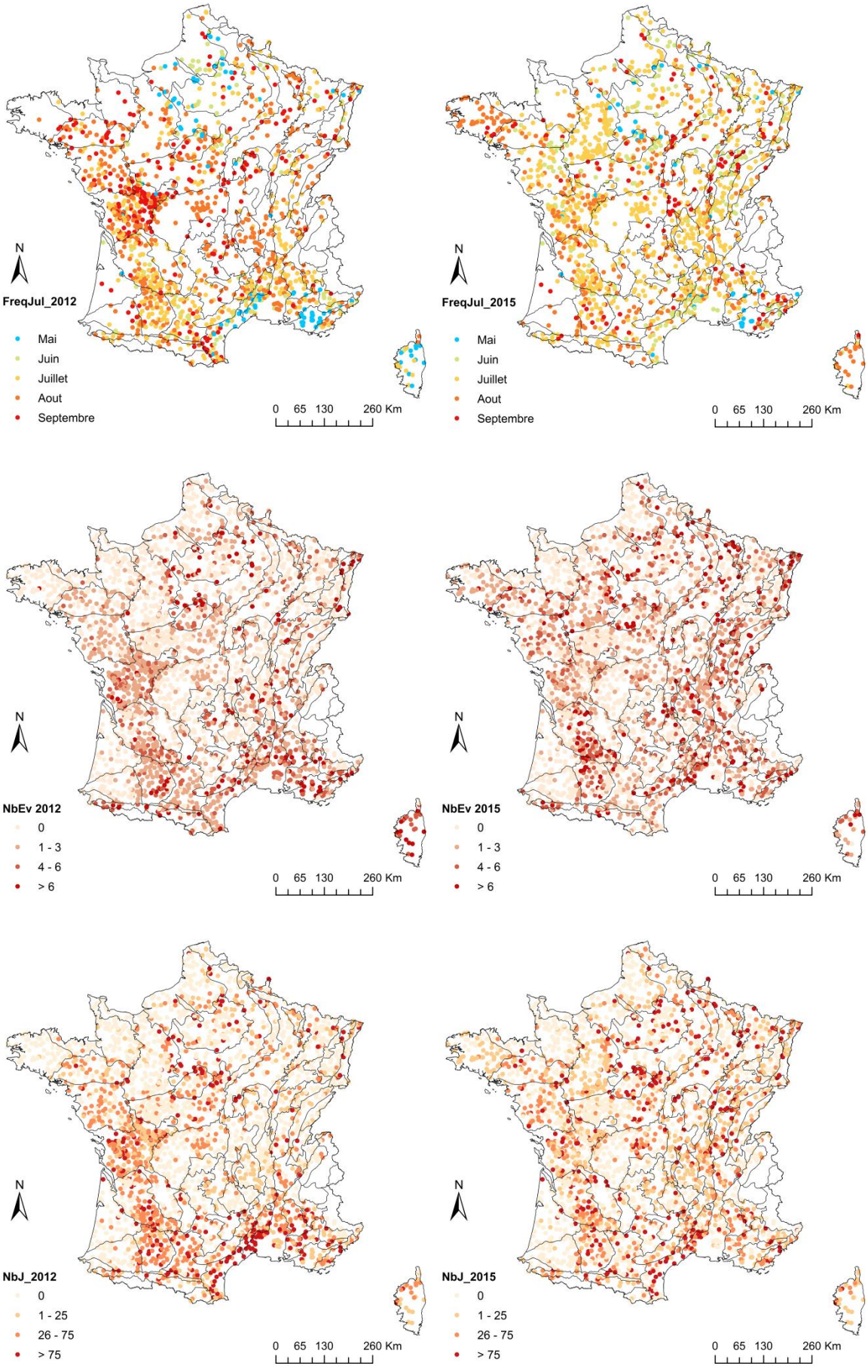

Figure 16 : Cartes de statistiques d'assec pour les années 2012 et 2015 (suite)

4. Conclusion

La connaissance du fonctionnement hydrologique et écologique des petits bassins versants (ou tête de bassin versant) est assez faible malgré leur prépondérance au sein du réseau hydrographique. En effet, seul un faible nombre de stations hydrométriques enregistrent en continu les débits de cours d'eau français drainant moins de 25 km². Les enjeux (humains et économiques) sont concentrés en fond de vallée et les cours d'eau sont parfois difficiles à instrumenter (ex. cours d'eau en tresse à la morphologie active, accès délicat au lit…).

L'ambition première du volet « hydrologie » est de valoriser les informations issues du réseau ONDE (Observatoire National Des Etiages, onde.eaufrance.fr) pour mieux appréhender les régimes hydrologiques sur les petits cours d'eau. Les données du réseau ONDE sont des données qualitatives (hydrologie décrite par des modalités d'écoulement : « écoulement visible », « écoulement non visible », ou « assec ») et discrètes (une observation de terrain par mois), relevées sur plus de 3300 sites principalement sur les têtes de bassin versant (superficie inférieure à 50 km²).

Des développements innovants pour la reconstitution de la dynamique des assecs (passage des mesures discontinues à une chronologie décrivant de manière exhaustive les phases d'assec aux échelles régionale et locale) ont été engagés avec succès. Ils ont combiné les suivis ponctuels ONDE aux mesures des débits de la base de données HYDRO et de niveaux piézométriques de la base de données ADES et à des données météorologiques issues de la base de données SAFRAN.

Des modèles empiriques à base statistique ont été mis en place pour prédire :

- les probabilités d'assec régionales sur l'ensemble de la France ;
- les modalités « assec »/« écoulement non visible » versus « écoulement visible » au droit des sites ONDE

au pas de temps journalier *a minima* sur la période de disponibilité des données ONDE pendant cette étude 2012-2017. Deux types de régressions ont été testés pour estimer les probabilités régionales. La dynamique journalière étant plus difficile à représenter à l'échelle locale, des structures plus complexes ont été envisagées (modèles linéaires et non linéaires). Les applications de ces modèles ont permis :

- de localiser les régions les plus affectées par les assèchements ;
- d'analyser la variabilité temporelle des assecs depuis 1989 ;
- d'identifier les drivers de l'intermittence ;
- de calculer différentes métriques établies sur les assecs, pertinentes *a priori* pour décrire les écosystèmes (choisies sur la base de discussions au sein du projet COST SMIRES).

En revanche, il n'a pas été possible de dresser des cartes décrivant la répartition des cours intermittents et les principales caractéristiques statistiques des assecs (durée, fréquence, saisonnalité, etc.) faute de temps. Cette ultime étape nécessitera d'actualiser les modèles avec la campagne 2018 et de les appliquer sur une période étendue (la fenêtre 1989-2018 semble pertinente car elle intègre les épisodes d'assec les plus sévères en début de période).

Démonstration a été faite que les données ONDE sont utiles pour la connaissance des assecs en tête de bassin versant. Les analyses réalisées militent pour la poursuite de ce réseau : de par leur localisation, le réseau ONDE vient compléter l'information fournie par les réseaux conventionnels (*i.e.* les stations hydrométriques de la base de données HYDRO), les six années d'observations ne suffisent pas à assurer la robustesse des modèles, les incertitudes restent fortes et les campagnes futures devraient réduire les incertitudes sur le paramétrage et les sorties des modèles en multipliant les situations hydro-climatiques.

Les données ONDE ont été exploitées ici pour la connaissance des assecs. On pressent un potentiel d'utilisation plus large en hydrologie (notamment pour l'évaluation des modélisations distribuées, bien souvent limitée aux seules stations hydrométriques), même si ces données requièrent des post-traitements pour les exploiter au mieux. On peut imaginer que les hydrologues seront de plus en plus confrontés à ce type de données avec le développement des sciences participatives et donc exploiter les proxys – dont les données ONDE - devrait devenir pratique courante.

5. Bibliographie

Abdollahi, S., Raeisi, J., Khalilianpour, M., Ahmadi,F., Kisi O. (2017). Daily Mean Streamflow Prediction in Perennial and Non-Perennial Rivers Using Four Data Driven Techniques, Water Resour Manage, 31(15), 4855-4874 https://doi.org/10.1007/s11269-017-1782-7.

Beaufort, A., Lamouroux, N., Pella, H., Datry, T., Sauquet, E. (2018). Extrapolating regional probability of drying of headwater streams using discrete observations and gauging networks, Hydrology and Earth System Sciences, 22(5), 3033–3051, doi:10.5194/hess-22-3033-2018.

Breiman, L. (2001). Random forests, Machine learning, 45(1), 5–32.

Brugeron, A., Allier, D., Klinka, T. (2012). Approche exploratoire des liens entre référentiels hydrogéologique et hydrographique : Premières identifications des piézomètres potentiellement représentatifs d'une relation nappe/rivière et contribution à leur valorisation. Rapport final BRGM/RP-61047-FR. 241 p.

Caillouet, L., Vidal, J.-P., Sauquet, E., Devers, A., Graff, B. (2017). Ensemble reconstruction of spatio-temporal extreme low-flow events in France since 1871, Hydrol. Earth Syst. Sci., 21, 2923–2951, https://doi.org/10.5194/hess-21-2923-2017.

Cipriani T., Tilmant F., Branger F., Sauquet E., Datry T. (2014). Impact of climate change on aquatic ecosystems along the Asse river network. In "Hydrology in a Changing World: Environmental and Human Dimensions" (Daniell T., Ed.), AIHS Publ. 363, 2014, 463-468.

Clarke, A., Mac Nally, R., Bond, N., Lake, P. S. (2008). Macroinvertebrate diversity in headwater streams: a review. Freshwater biology, 53(9), 1707-1721.

Datry, T, Bonada, N., Boulton, A., (2017). Intermittent Rivers and Ephemeral Streams, Academic Press, 622 pp., https://doi.org/10.1016/C2015-0-00459-2

De Girolamo, A. M., Lo Porto, A., Pappagallo, G., Gallart, F. (2015). Assessing flow regime alterations in a temporary river – the River Celone case study, Journal of Hydrology and Hydromechanics, 63(3), doi:10.1515/johh-2015-0027.

Finn, D. S., Bonada, N., Múrria, C., Hughes, J. M. (2011). Small but mighty: headwaters are vital to stream network biodiversity at two levels of organization. Journal of the North American Benthological Society, 30(4), 963-980.

Larue, J. P., Giret A. (2004). The drying up of streams in the Maine basin from 1989 to 1992, Norois, 192, 117–133, https://doi.org/10.4000/norois.944.

Lowe, W. H., Likens, G. E. (2005). Moving headwater streams to the head of the class. BioScience, 55(3), 196-197.

Meyer, J.L., Strayer, D. L., Wallace, J. B., Eggert, S. L., Helfman, G. S., Leonard, N. E. (2007). The contribution of headwater streams to biodiversity in river networks. JAWRA Journal of the American Water Resources Association 43: 86–103. doi:10.1111/j.1752-1688.2007.00008.x

Nash, J. E., Sutcliffe, J. V. (1970). River flow forecasting through conceptual models part I — A discussion of principles, Journal of Hydrology, 10(3), 282–290, doi:10.1016/0022-1694(70)90255-6, 1970.

Nowak, C., Durozoi, B., 2012. Observatoire National Des Etiages (Note technique No. 1). ONEMA.

Pella, H., Lejot, J., Lamouroux, N., Snelder, T. (2012). Le réseau hydrographique théorique (RHT) français et ses attributs environnementaux. Géomorphologie: relief, processus, environnement 18, 317–336.

Quintana-Seguí, P., Le Moigne, P., Durand, Y., Martin, E., Habets, F., Baillon, M., Canellas, C., Franchisteguy, L., Morel, S. (2008). Analysis of Near-Surface Atmospheric Variables: Validation of the SAFRAN Analysis over France, Journal of Applied Meteorology and Climatology, 47(1), 92–107, doi:10.1175/2007JAMC1636.1.

Sauquet, E., Gottschalk, L., Krasovskaia, I., 2008. Estimating mean monthly runoff at ungauged locations: an application to France. Hydrology Research 39, 403. doi:10.2166/nh.2008.331

Snelder, T. H., Datry, T., Lamouroux, N., Larned, S. T., Sauquet, E., Pella, H., Catalogne, C. (2013). Regionalization of patterns of flow intermittence from gauging station records. Hydrology and Earth System Sciences, 17(7), 2685-2699.

Tibshirani, R. (1996). Regression Shrinkage and Selection via the Lasso. Journal of the Royal Statistical Society. Series B (Methodological), 58(1), 267-288. Retrieved from http://www.jstor.org/stable/2346178.

Vidal, J.P., Martin, E., Baillon, M., Franchistéguy, L., Soubeyroux, J.M. (2010). A 50-year high-resolution atmospheric reanalysis over France with the Safran system. International Journal of Climatology 30(11): 1627–1644. DOI:10.1002/joc.2003

Wasson, J.G., Chandesris, A., Pella, H., Blanc, L. (2002). Définition des hydro-écorégions françaises métropolitaines. Rapport final MEDD, 190 pages.

Yu, S., Bond, N.R., Bunn S.E., Xu Z., Kennard M.J. (2018). Quantifying spatial and temporal patterns of flow intermittency using spatially contiguous runoff data. Journal of Hydrology, 559, 861-872, https://doi.org/10.1016/j.jhydrol.2018.03.009.

6. Table des illustrations

7. Annexe 1 : Extrapolating regional probability of drying of headwater streams using discrete observations and gauging networks (Beaufort *et al.*, 2018)

Hydrol. Earth Syst. Sci., 22, 3033–3051, 2018
https://doi.org/10.5194/hess-22-3033-2018

Hydrology and Earth System Sciences
Open Access
EGU

Extrapolating regional probability of drying of headwater streams using discrete observations and gauging networks

Aurélien Beaufort, Nicolas Lamouroux, Hervé Pella, Thibault Datry, and Eric Sauquet

Irstea, UR RiverLy, centre de Lyon-Villeurbanne, 5 rue de la Doua CS 20244, 69625 Villeurbanne, France

Correspondence: Aurélien Beaufort (aurelien.beaufort@irstea.fr)

Received: 9 November 2017 – Discussion started: 15 November 2017
Revised: 23 March 2018 – Accepted: 29 April 2018 – Published: 24 May 2018

Abstract. Headwater streams represent a substantial proportion of river systems and many of them have intermittent flows due to their upstream position in the network. These intermittent rivers and ephemeral streams have recently seen a marked increase in interest, especially to assess the impact of drying on aquatic ecosystems. The objective of this paper is to quantify how discrete (in space and time) field observations of flow intermittence help to extrapolate over time the daily probability of drying (defined at the regional scale). Two empirical models based on linear or logistic regressions have been developed to predict the daily probability of intermittence at the regional scale across France. Explanatory variables were derived from available daily discharge and groundwater-level data of a dense gauging/piezometer network, and models were calibrated using discrete series of field observations of flow intermittence. The robustness of the models was tested using an independent, dense regional dataset of intermittence observations and observations of the year 2017 excluded from the calibration. The resulting models were used to extrapolate the daily regional probability of drying in France: (i) over the period 2011–2017 to identify the regions most affected by flow intermittence; (ii) over the period 1989–2017, using a reduced input dataset, to analyse temporal variability of flow intermittence at the national level. The two empirical regression models performed equally well between 2011 and 2017. The accuracy of predictions depended on the number of continuous gauging/piezometer stations and intermittence observations available to calibrate the regressions. Regions with the highest performance were located in sedimentary plains, where the monitoring network was dense and where the regional probability of drying was the highest. Conversely, the worst performances were obtained in mountainous regions. Finally, temporal projections (1989–2016) suggested the highest probabilities of intermittence (> 35 %) in 1989–1991, 2003 and 2005. A high density of intermittence observations improved the information provided by gauging stations and piezometers to extrapolate the temporal variability of intermittent rivers and ephemeral streams.

1 Introduction

Headwater streams represent a substantial proportion of river systems (Leopold et al., 1964; Nadeau and Rains, 2007; Benstead and Leigh, 2012). From an ecological point of view, headwater catchments are at the interface between terrestrial and aquatic ecosystems and they often harbour a unique biodiversity with a very high spatial turnover (Meyer et al., 2007; Clarke et al., 2008; Finn et al., 2011). Their contribution to the functioning of hydrographic networks is essential: sediment flows, inputs of particulate organic matter and nutrients, refugia/colonisation, sources of aquatic organisms (Meyer et al., 2007; Finn et al., 2011).

Headwater streams are generally naturally prone to flow intermittence, i.e. streams which stop flowing or dry up at some point in time and space, mainly due to their upstream position in the network and their high reactivity to natural or human disturbances (Benda et al., 2005; Datry et al., 2014b). These waterways which cease flow and/or dry are referred to as intermittent rivers and ephemeral streams (IRES). The geographic extent of IRES is poorly documented due to mapping limitations (digital elevation models, satellite images, aerial photos) and because of their size and their location (Leopold et al., 1994; Nadeau and Rains, 2007; Benstead and Leigh, 2012; Fritz et al., 2013). However, the proportion of

Published by Copernicus Publications on behalf of the European Geosciences Union.

IRES in hydrological networks can be very large: for example, they represent 60 % of the length of rivers in the United States (Nadeau and Rains, 2007) and are considered to represent probably more than 50 % of the global hydrological network (Larned et al., 2010; Datry et al., 2014b). Considering only gauging stations with continuous records may lead to severe underestimation of their regional extent (Snelder et al., 2013; De Girolamo et al., 2015; Eng et al., 2016).

Recently, IRES have seen a marked increase in interest stimulated by the challenges of water management facing the global change context (water scarcity issues, climate change impact, etc.) (Acuña et al., 2014; Datry et al., 2016b). Studies have characterised the hydrological functioning of IRES (Gallart et al., 2012; Costigan et al., 2016; Sarremejane et al., 2017) to assess the effects of flow intermittence on aquatic ecosystems (Larned et al., 2010; Datry et al., 2016b; Leigh et al., 2016; Leigh and Datry, 2017). IRES have been altered due to human actions (abstraction, hill dams, low-water support, pollution, etc.) despite their high and unique biodiversity (Datry et al., 2014a; Garcia et al., 2017a). In addition, some perennial streams are becoming intermittent due to global change, water abstraction or river damming (Skoulikidis, 2009), and the extent of IRES may increase in the future (Döll and Schmied, 2012; Jaeger et al., 2014; Pumo et al., 2016; Garcia et al., 2017b; De Girolamo et al., 2017a).

A better hydrological understanding of IRES is now essential and improved management requires knowledge of both the spatial extent and arrangement of IRES within the river network (Boulton, 2014; Acuña et al., 2017). Efforts have been made to estimate the spatial distribution of IRES at the catchment scale (Skoulikidis et al., 2011; Datry et al., 2016a), at the regional scale (Gómez et al., 2005) and at the national scale (Snelder et al., 2013). In France, Snelder et al. (2013) suggested a classification of IRES regimes and spatialised their distribution. Based on an analysis of the continuous gauging network, they showed that the proportion of IRES accounted for 20 to 39 % of the hydrographic network. The accuracy of the obtained map is highly dependent on the density of the flow monitoring network. The installation of additional gauging stations is expensive and headwater systems may be difficult to monitor due to active geomorphology processes or to difficult access.

As a promising tool to advance the mapping of IRES, citizen science creates opportunities to overcome the lack of hydrological data, contributes to densifying the flow-state observation network (Turner and Richter, 2011; Buytaert et al., 2014; Datry et al., 2016b) and could be used for hydrological model calibration (van Meerveld et al., 2017). In France, Datry et al. (2016a) used such data to describe the spatio-temporal dynamics of aquatic and terrestrial habitats within five river catchments located in the western part of France. They showed that processes resulting in flow intermittence were complex at a fine scale and could vary substantially among nearby catchments. However, these data were only available in a few catchments, limiting any attempt to map large-scale patterns of flow intermittence in river networks. Since this first attempt, new sources of observational data have become available in France thanks to the ONDE network (Observatoire National des Etiages, https://onde.eaufrance.fr, last access: 22 May 2018). This unique network in Europe provides frequent discrete field observations (five inspections per year) of the flow intermittence across more than 3300 sites throughout France and located mostly in headwater areas.

However, discrete observations of intermittence do not provide any information on the persistence of dry conditions between two consecutive dates of observation. The rewetting–drying events could have significant impacts on communities whose survival is conditioned by the duration/frequency of drying. The duration of drying is of importance for ecologists, as one key driver for the composition and persistence of aquatic species (Vardakas et al., 2017; Kelso and Entrekin, 2018; Vadher et al., 2018). Temporal extrapolations of river flow regimes are thus necessary to summarise the different facets of flow intermittence at various timescales, from daily to inter-annual.

The main objective of this paper is to use discrete (in space and time) field observations of flow intermittence to extrapolate over time the daily probability of drying (averaged at the regional scale). We first carried out a quantitative analysis of the ONDE network data in order to characterise the information that they contribute in comparison with the data resulting from the conventional hydrological monitoring. Then, we developed two empirical models based on linear or logistic regressions to convert discontinuous series of flow intermittence observation from ONDE into continuous daily probability of drying, defined at the regional scale across France. Explanatory variables were derived from available continuous daily discharge and groundwater-level data of a dense gauging/piezometer network, and models were calibrated using the ONDE discrete observations. The robustness of the models was tested using (1) an independent, dense regional dataset of intermittence observations and (2) observations of the year 2017 excluded from the calibration. Finally, the resulting models were used to extrapolate the regional probability of drying in France: (i) over the period 2012–2017 to identify the regions most affected by flow intermittence; (ii) over the period 1989–2017, using a reduced input dataset, to analyse temporal variability of flow intermittence at the national level.

2 Material and methods

2.1 Study area

The study area is continental France and Corsica (550 000 km^2). France is located in a temperate zone characterised by a variety of climates due to the influences

of the Atlantic Ocean, the Mediterranean Sea and mountain areas.

We defined regions as combinations of "level-2 Hydro-EcoRegions" (HER2) and classes of hydrological regimes (HR). Hydro-EcoRegion (HER) corresponds to a typology developed for river management in accordance with the European Water Framework Directive. The Hydro-EcoRegion classification includes 22 "level-1 Hydro-EcoRegions" (HER1) based on geology, topography and climate, and considered the primary determinants of the functioning of water ecosystems (Wasson et al., 2002). HER2 correspond to a finer classification accounting for stream size. HER2 have a mean drainage area of 5000 km^2 (between 100 and 27 000 km^2). The hydrological regime classes (HR) were identified by reference to the work carried out by Sauquet et al. (2008) where it was possible to distinguish rainfall-fed regimes, transition and snowmelt-fed river flow regimes. Overall, we used 280 regions (that is, HER2–HR combinations) with a mean drainage area of 1400 km^2 (between 4 and 20 000 km^2).

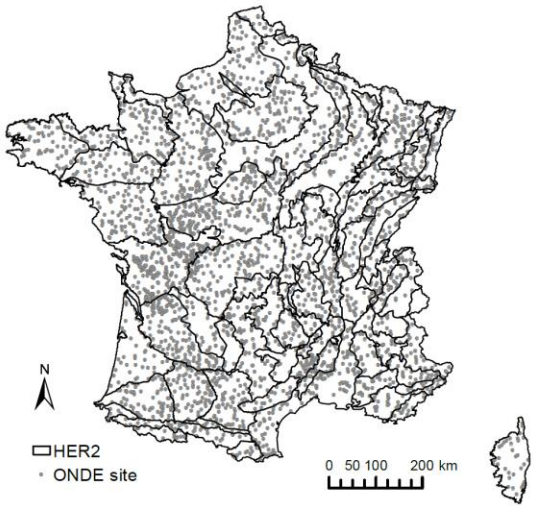

Figure 1. Location of the 3300 ONDE sites and partition into HER2.

2.2 ONDE dataset discrete national flow-state observations

The ONDE network was set up in 2012 by the French Biodiversity Agency (AFB, formerly ONEMA) with the aim of constituting a perennial network recording summer low-flow levels and used to anticipate and manage water crisis during severe drought events (Nowak and Durozoi, 2012).

There are 3300 ONDE sites distributed throughout France (Fig. 1). ONDE sites are located on headwater streams with a Strahler order of strictly less than 5 and balanced across HER2 regions to take into account the representativeness of the hydrological contexts (Nowak and Durozoi, 2012). The ONDE network is stable over time. Observations have been made monthly (around the 25th) by trained AFB staff, between April and September, every year since 2012. One of the statuses is assigned at each observation among "visible flow", "no visible flow" and "dried out". Here, we consider two intermittency statuses: "Flowing" when there is visible flow across the channel ("visible flow") and "Drying" when the channel is entirely devoid of surface water ("dried out") or when there is still water in the river bed but without visible flow (disconnected pools, lentic systems) ("no visible flow"). The proportion of drying sites determined on the basis of the ONDE network for each HER2–HR combination is considered a good estimate of the daily regional probability of drying ($RPoD_{ONDE}$) of streams with a Strahler order of less than 5. Observed values of $RPoD_{onde}$ are calculated as follows:

$$RPoD_{ONDE}(d) = \frac{(N_{drying})_{HER2-HR}}{(N_{flowing} + N_{drying})_{HER2-HR}}, \quad (1)$$

where d denotes the observation date of the ONDE network, N_{drying} and $N_{flowing}$ are the number of drying and of flowing statuses observed at ONDE sites located in the same HER2–HR combination at the observation date d, respectively.

Figure 2 illustrates the complementary nature of the ONDE network to the already existing HYDRO (http://www.hydro.eaufrance.fr, last access: 22 May 2018) French river flow monitoring network. The ONDE sites and a set of 1600 gauging stations available in the HYDRO database have been projected on the RHT (Theoretical Hydrographic Network; Pella et al., 2012) river network and the drainage area and the elevation have been estimated. A large part of ONDE sites are located on small headwater streams, with 70 % of the sites with a drainage area of less than 50 km^2, while most of the gauging stations record flows of catchments of medium size (between 100 and 500 km^2). Only four stations display a drainage area of more than 1000 km^2. The distributions of elevation of the two databases look similar. The ONDE sites are mostly located on rivers with an elevation below 200 m (75 % of sites). The ONDE sites are sparse at high elevations (95 sites located above 1000 m). This bias is likely due to access difficulties in mountainous areas.

2.3 POC dataset: a denser regional dataset used for independent validation

A spatially denser citizen science dataset of flow-state observations in western France (Poitou-Charente region) (http://atlas.observatoire-environnement.org, last access: 22 May 2018) has been used as a validation dataset to test the robustness of our models calibrated with the ONDE dataset. The POC monitoring (2011–2013) covered more than 4000 km of river length across 20 catchments. Each river was entirely surveyed every 1st and 15th of each month be-

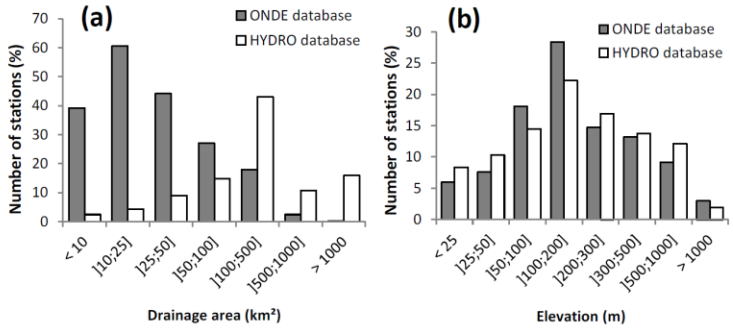

Figure 2. Distribution of the 3300 ONDE sites and of the 1600 gauging stations available in the HYDRO database against **(a)** drainage area and **(b)** elevation.

tween June and October, resulting in eight observations per year. Four intermittency statuses were available in the POC dataset (Datry et al., 2016a), but to allow comparisons with the ONDE network, we pooled the two "Flowing" and "Low Flow" POC statuses into a single "Flowing" status and the two "No flow" and "Dry" statuses into the "Drying" status. This dataset is available as maps with flow states assigned to the inspected streams. Values of RPoD at each POC observation date are calculated in the same way as $\mathrm{RPoD_{ONDE}}$. Thus $\mathrm{RPoD_{POC}}$ is given by the ratio between the number of drying statuses and the total number of observations at each inspected stream located in the same HER2–HR.

2.4 Explanatory discharge dataset

Two discharge datasets (continuous daily time series) were used as explanatory variables of discrete intermittence observations, with the objective of extrapolating the intermittence frequency over time. The two datasets included time series of daily discharge extracted from the French river flow monitoring network (HYDRO database, http://www.hydro.eaufrance.fr/, last access: 22 May 2018): (i) the 2011–2017 dataset with full records available between 1 January 2011 and 31 June 2017; (ii) the 1989–2017 dataset concerning a reduced number of gauging stations and providing daily discharges between 1 January 1989 and 31 June 2017. According to the hydrometric services in charge of the selected gauging stations, high quality of measurements was ensured and observed discharges were not or only slightly altered by human actions.

The 2011–2017 dataset was composed of 1600 gauging stations distributed across France. Each stream where a HYDRO gauging station is located has been defined as IRES or perennial. Several definitions of IRES can be found in the literature (Huxter and van Meerveld, 2012; Eng et al., 2016; Reynolds et al., 2015). In this study, we considered stations to be intermittent when five consecutive days with discharge less than $1\,\mathrm{L\,s^{-1}}$ have been observed during the period of record.

The 1989–2017 dataset consisted of 630 gauging stations selected with less than 5 % of missing data (continuous or not) during the period 1989–2017. This dataset was thereafter used to estimate the regional probability of drying before the creation of the ONDE network.

2.5 Explanatory groundwater-level dataset

Because groundwater resources influence stream intermittence, we used available time series of the daily groundwater level available in the ADES database (http://www.ades.eaufrance.fr, last access: 22 May 2018) at sites identified as involved in groundwater–surface water exchanges (Brugeron et al., 2012). Similarly to the discharge data, two sets of groundwater-level data with records available over the two periods 2011–2017 and 1989–2017 have been selected. The level of alteration of groundwater levels by water withdrawal is unknown because no information is available at this scale.

The 2011–2017 dataset was composed of 750 piezometers with daily groundwater-level data with less than 5 % of missing data (continuous or not). The selection of the 1989–2017 dataset was not easy because few groundwater-level measurements were available in the database before 2000. For example, only five piezometers met the tolerance limit on missing values considered for the 1989–2017 discharge dataset. In order to extend the dataset and because groundwater levels were less variable than stream discharges, the proportion of permitted gaps was fixed to 20 % between 1989 and 2017. This led us to select 150 piezometers. Thereafter, when the missing data period was less than 10 days, groundwater levels were reconstructed by linear interpolation in order to reduce the proportion of missing values to less than 5 % for the 150 piezometers selected.

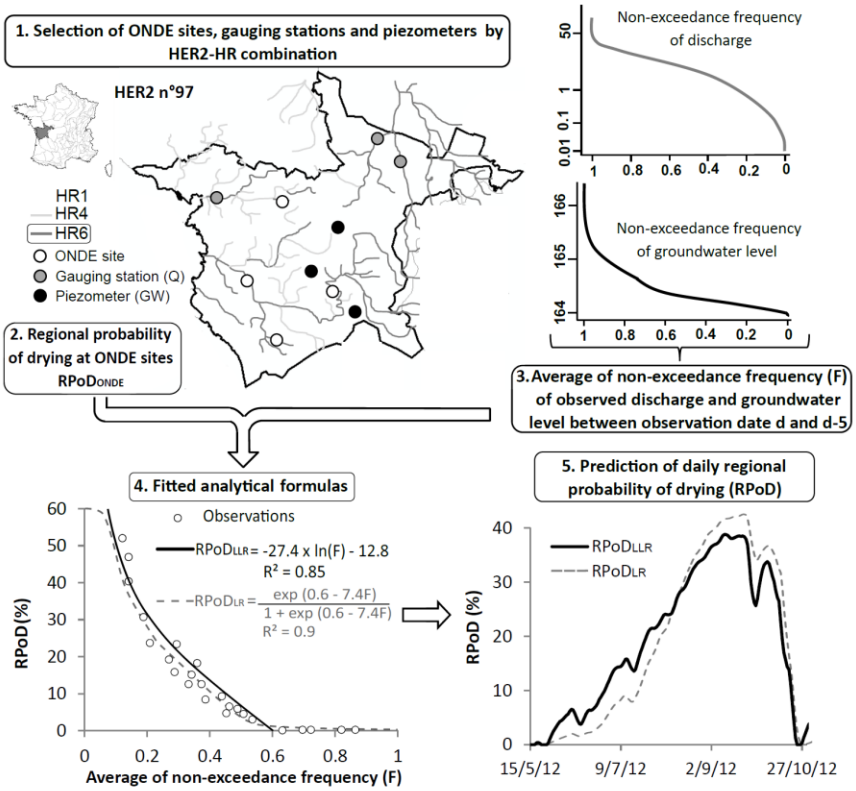

Figure 3. Strategy of parametric modelling (steps 1–4) developed to predict (step 5) the regional probability of drying (RPoD) by HER2–HR combination in France.

2.6 Statistical modelling of regional probability of drying

The parametric modelling strategy was based on five main steps (Fig. 3). The first step consisted in selecting all ONDE sites, gauging stations and piezometers located in the same HER2–HR combination. When the total number of gauging stations and piezometers was less than five for a HER2–HR combination, we merged the HER2–HR combination with a neighbouring one located in the same HER1. This was done for 20 of the 280 regions. The second step consisted in calculating the $\mathrm{RPoD}_{\mathrm{ONDE}}$ for each observation date (5 year^{-1}) and for all selected ONDE sites. In a third step, a flow duration curve was determined for each selected HYDRO gauging station. The average non-exceedance frequency of the observed discharge at gauging stations was averaged for the date of observation (d) at ONDE sites and the 5 days preceding the observation. The lag of 6 days accounted for the fact that ONDE survey dates in a region could differ by 5 days, and accounted for the inertia of physical processes (e.g. storage capacity). The same operation was carried out with selected piezometers. Finally the hydrological conditions are described by the average (across stations) F of the non-exceedance frequencies of discharge (F_q) and groundwater levels (F_{gw}) with respect to the relative proportions of gauging stations and piezometers:

$$F(d) = \frac{\sum_{i=1}^{i=N_q} F_{q_i} + \sum_{j=1}^{j=N_{\mathrm{gw}}} F_{\mathrm{gw}_j}}{(N_q + N_{\mathrm{gw}})}, \quad (2)$$

where F_{q_i} denotes the average non-exceedance frequency of discharge at the gauging station i calculated between d and $d-5$; F_{gw_j} the average non-exceedance frequency of groundwater levels at the piezometer j calculated between d and $d-5$; N_q the number of gauging stations selected in a HER2–HR combination; and Ngw the number of selected piezometers selected in the HER2–HR combination. The fourth step consisted in estimating the $\mathrm{RPoD}_{\mathrm{ONDE}}$ as a function of F. Two types of regression were fitted for each HER2–HR combination across France:

– A truncated logarithmic linear regression (LLR), with two parameters α_1 and β_1:

$$\mathrm{RPoD_{LLR}}(d) = \begin{cases} \min(1; \alpha_1 \times \ln(F(d)) + \beta_1) \text{ when } F < F0 \\ 0 \text{ when } F \geq F0. \end{cases} \quad (3)$$

$F0$ was fixed as the value of non-exceedance frequencies of discharge and groundwater levels at which no more drying status was observed across the ONDE network ($\mathrm{RPoD_{ONDE}} = 0$).

– A logistic regression (LR) with two parameters α_2 and β_2:

$$\mathrm{Logit}(\mathrm{RPoD_{LR}}(d)) = \ln\left(\frac{\mathrm{RPoD_{LR}}(d)}{1 - \mathrm{RPoD_{LR}}(d)}\right) = \alpha_2 \times F(d) + \beta_2. \quad (4)$$

LR is a multivariate analysis method well known for its relevance in binary classification issues (Lee, 2005). The $\mathrm{RPoD_{LR}}$ was then calculated as follows in Eq. (5):

$$\mathrm{RPoD_{LR}}(d) = \frac{\exp(\alpha_2 F(d) + \beta_2)}{1 + \exp(\alpha_2 F(d) + \beta_2)}. \quad (5)$$

Models were calibrated against observations available during the same period, 2012–2016, leaving out the year 2017 for an independent validation test. However, for the continuous temporal extrapolations (one over 2011–2017, the other over 1989–2017), two models were built with different piezometers and gauging stations selected as explanatory variables (see Sects. 2.4 and 2.5). Thus there are two sets of regression parameters specific to each dataset for both the LLR and LR models, leading to different prediction of RPoD.

Finally, in a fifth step, a daily regional probability of drying (RPoD) could be predicted for each HER2–HR combination with both models following analytical formulas (Eqs. 3 and 5).

2.7 Model robustness: validation using independent datasets

We used (1) the POC independent data and (2) the 2017 ONDE year to test the robustness of the LLR and LR model to predict the intermittence frequency (1) in space and (2) over time. Note that when predicting on the POC datasets, a new model was calibrated using only ONDE sites located out of POC streams.

For both datasets (POC and ONDE, 2017), the relative performance of the LLR and LR models was compared in multiple ways using both the 2011–2017 and 1989–2017 datasets. The performance of each model was evaluated by the Nash–Sutcliffe efficiency criterion (NSE) (Nash and Sutcliffe, 1970):

$$\mathrm{NSE} = 1 - \frac{\sum_{i=1}^{N} (\mathrm{RPoD_{ONDEi}} - \mathrm{RPoD_{pri}})^2}{\sum_{i=1}^{N} (\mathrm{RPoD_{ONDEi}} - \overline{\mathrm{RPoD_{ONDEi}}})^2}, \quad (6)$$

where $\mathrm{RPoD_{ONDEi}}$ is the average proportion of drying statuses over the ONDE sites located in the HER2–HR combination at the ith observation date, $\mathrm{RPoD_{pri}}$ is the predicted regional probability of drying at the ith observation date, $\overline{\mathrm{RPoD_{ONDEi}}}$ is the mean of $\mathrm{RPoD_{ONDEi}}$ over the period and N is the total number of observations in the ONDE network for each HER2–HR combination.

2.8 Model prediction

Both models have been calibrated over the period 2012–2016 and were then applied in a fifth step to predict the daily RPoD in France (Fig. 3). The RPoD was firstly predicted over the period 2012–2016 in order to identify the most affected regions by flow intermittence using the 2011–2017 datasets. The second application concerned the extrapolation of RPoD in France over a longer period using the 1989–2017 dataset to analyse the temporal variability of flow intermittence at the national level. It should be noted that model predictions only concern streams with a Strahler order of lower than 5 due to the ONDE site location.

3 Results

3.1 Quantitative analysis

3.1.1 Inter-annual intermittence according to the raw discrete ONDE network

A total of 1127 ONDE sites have recorded at least one drying event during the period 2012–2016 representing 35 % of the 3300 ONDE sites. From the ONDE database the probability of drying at the country scale was computed as the total number of drying statuses over France divided by the total number of ONDE observations available during statuses the same year (Fig. 4a). Between 2012 and 2016, the most critical year is 2012, with 15 % of drying statuses followed by 2016 (14 %) and 2015 (14 %) (Fig. 4a). The years 2013 and 2014 are less affected with only 6 % of drying statuses observed (Fig. 4a).

Drying events mainly occur between July and September, but the evolution of the month's proportion of drying can differ between years (Fig. 4b). In more detail, water levels in 2012 decrease in August when the proportion of drying is 27 %, and the situation lasts until the end of September with 25 % of drying (Fig. 4b). In 2013, the proportion of drying is

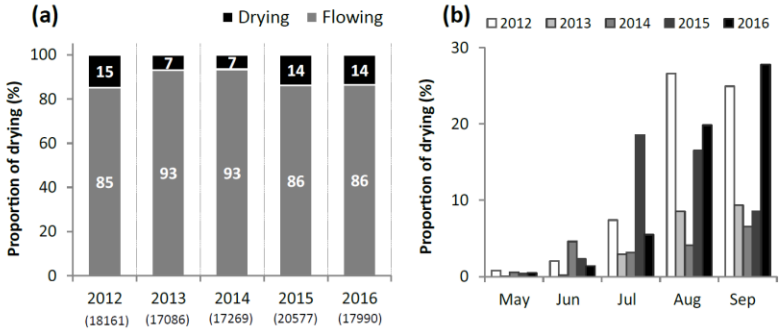

Figure 4. **(a)** Distribution of the yearly proportion of drying observed with the ONDE network with the total yearly number of ONDE observations written in brackets and **(b)** distribution of proportions of drying per year and per month.

lower than in 2012, but follows the same pattern with an increase at the end of July (3 %), reaching 9 % in August and in September. In 2014, the first peak of drying (5 %) is reached early in June. Then, the proportion of drying decreases in July (3 %) and increases slightly in August (4 %), reaching 7 % in September. In 2015, the critical period occurs at the end of July with 19 % of drying statuses, and the proportion of drying decreases slightly at the end of August (17 %) until it reaches 9 % in September. Finally, in 2016, the situation gradually deteriorates every month, reaching 20 % of drying statuses in August, and 28 % in September.

Between 2012 and 2016, a proportion of drying higher than 50 % is recorded on 93 ONDE sites and their spatial distribution is very patchy at the scale of France (black and dark grey dots, Fig. 5a). There are only 158 ONDE sites with at least one drying event every year and a variability of drying locations can be observed across years. The south-east of France is heavily affected by rivers drying, where the proportion of drying can exceed 75 % annually (black dots, Fig. 5b–f). The north-western part of France is less affected, although many ONDE sites show a proportion of drying observed above 50 % in 2014 and 2016 (Fig. 5d and f). North-eastern France is rather affected in 2012, 2014 and 2015, where several ONDE sites have more than 75 % of drying statuses (Fig. 5b, d and e). South-western France is particularly affected in 2012 and 2015 (Fig. 5b and e).

3.1.2 Comparison of flow intermittence between the raw ONDE and HYDRO datasets

The HYDRO dataset includes 90 gauging stations located on streams considered IRES, which represents only 5.6 % of the 1600 gauging stations against 35 % for ONDE sites. At the national scale, the number of IRES seems underrepresented in the south-western, central, and north-eastern parts of France and Corsica in comparison with sites experiencing drying in the ONDE network (Fig. 6).

Table 1. Annual statistics on flow intermittence calculated on HYDRO gauging stations between 1 May and 30 September.

	Stations with at least one drying event	Stations with drying > 50 %	Frequency of discharge < 1 L s^{-1}
2012	79	19	32.7
2013	47	14	37.9
2014	54	15	32.9
2015	76	21	31.1
2016	71	19	28.6

The number of gauging stations with at least one drying event (discharge < 1 L s^{-1}) observed between May and September varies between 79 in 2012 and 47 in 2014 (Table 1). The lowest numbers of gauging stations with drying events are observed in the years 2013 and 2014, while the highest numbers are related to the years 2012, 2015 and 2016. This finding is consistent with the analysis of the ONDE network (Fig. 5a, d). The frequency of drying, corresponding to the ratio between the number of dry days and the total number of days between 1 May and 30 September (153 days), in contrast, is quite constant over the years (∼ 30 %). The number of gauging stations with drying events over more than 50 % of the time varies little between wet years (14 in 2013) and dry years (21 in 2015), unlike ONDE observations, suggesting a significant temporal variability in the frequency of drying between dry and wet years (Fig. 5).

3.2 Validation of the predicted regional probability of drying

3.2.1 Regression results

The LLR and LR models, calibrated over the period 2012–2016, perform well with the 2011–2017 dataset, with a mean NSE of 0.8 with the LR model against 0.7 with the LLR

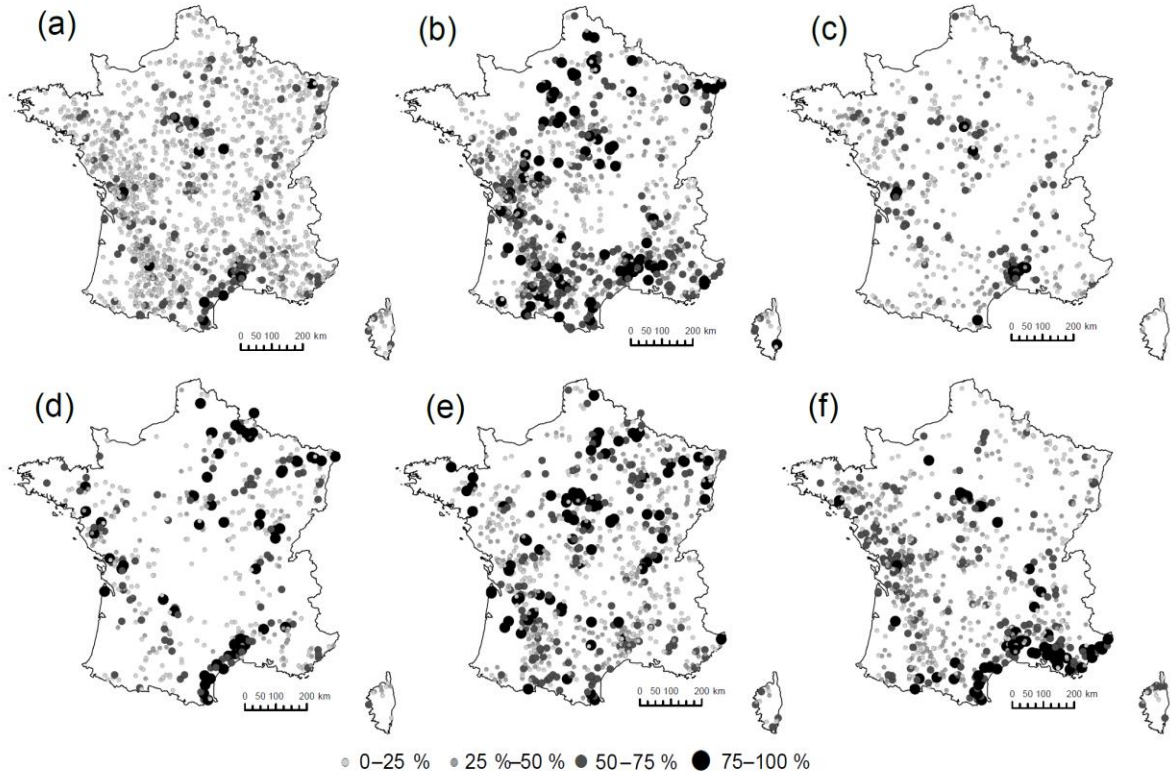

Figure 5. Distribution of the percentages of drying observed at ONDE sites for the years **(a)** 2012–2016, **(b)** 2012, **(c)** 2013, **(d)** 2014, **(e)** 2015 and **(f)** 2016.

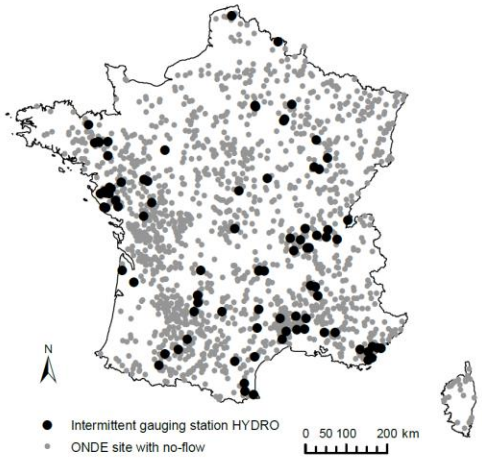

Figure 6. Map of ONDE sites and HYDRO gauging stations with at least one drying.

model (Fig. 7a and b). With the LR model, 50 % of the HER2–HR combinations obtain a NSE greater than 0.8, representing a coverage of 65 % of the French territory, while 33 % of HER2–HR combinations display a NSE higher than 0.8 (50 % of coverage of France) with the LLR model. Regions with the highest performances are located in sedimentary plains, in the south-east of France and in the Pyrenees Mountains. Conversely, the worst performances are obtained in the mountainous regions of the Alps as well as in the Massif Central. In these regions the size of the HER2 is rather small and the number of ONDE sites, gauging stations and piezometers per HER2–HR combination are certainly too few to derive reliable relations. Despite pooling, estimating RPoD remains impossible for nine HER2–HR combinations (4.5 % of coverage of France) because the number of ONDE sites, gauging stations and piezometer sites is insufficient (less than five) to perform the regression analysis.

The performance level is lower when the 1989–2017 dataset is used in models: the mean NSE with the LR and LLR models is 0.7 and 0.6, respectively (Fig. 7c and d).

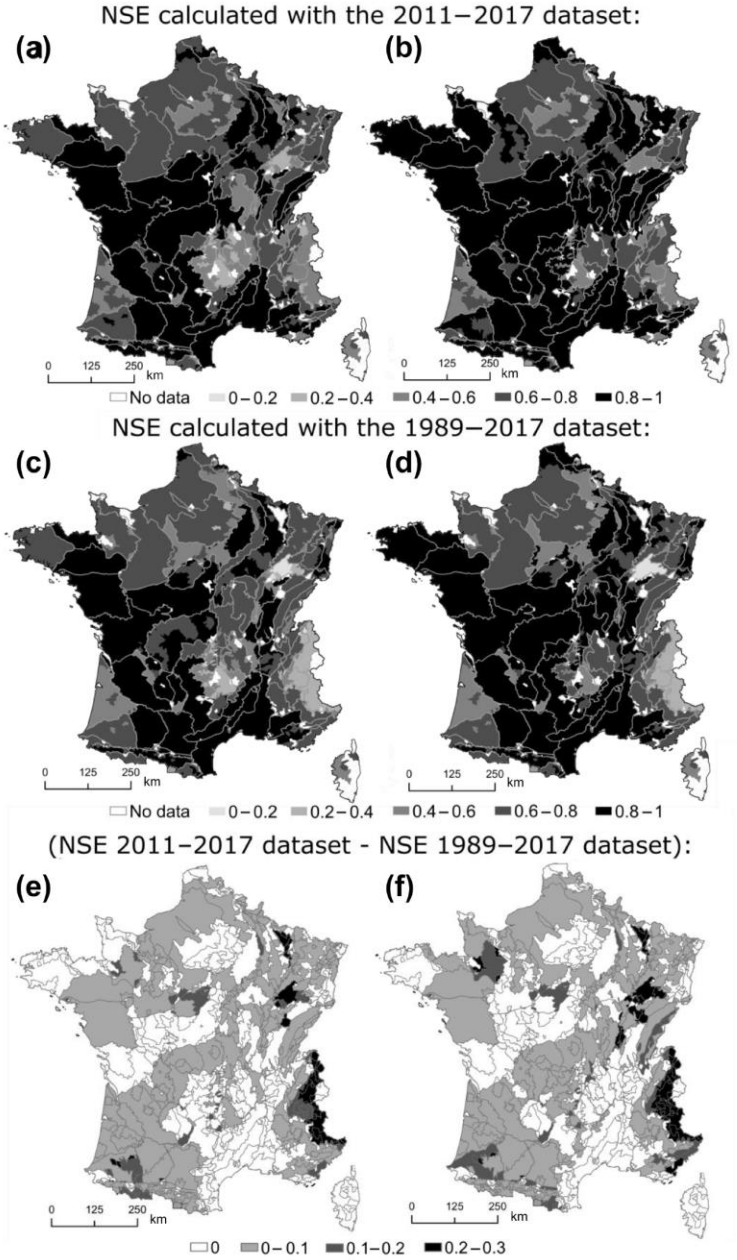

Figure 7. Map of Nash–Sutcliffe criteria (NSE) obtained for each HER2–HR combination between 2012 and 2016 with the 2011–2017 and 1989–2017 datasets according to **(a)** and **(c)** a log-linear regression (LLR) model; or **(b)** and **(d)** a logistic regression (LR) model. NSE differences between the 2011–2017 dataset and the 1989–2017 dataset are represented for **(e)** the LLR model and **(f)** the LR model.

The LR and LLR models lead to a similar performance range. However, the LR model outperforms the LLR model in terms of number of HER2–HR combinations, with NSE greater than 0.8 (Fig. 7c and d). The performance is sensitive to the dataset. As expected, the best results are obtained with the denser network. A decrease in NSE by more than 0.2 is identified for 5 % of the French territory when the 1989–2017 dataset is used (black areas; Fig. 7e and f). The regions

with the most degraded values of NSE are small HER2–HR combinations located in eastern France (Fig. 7e and f).

The decrease in performance is mainly due to the difference in the number of gauging stations and piezometers between the two datasets (Fig. 8). The most degraded NSEs correspond to HER2–HR combinations where the number of gauging stations and piezometers considered in regressions is the most reduced, i.e. with a loss higher than 50 % of the stations (black and dark grey dots; Fig. 8a and b). However, the decrease in performance remains low (the difference in NSE is below 0.1 for 75 and 64 % of HER2–HR combinations with the LLR and LR models, respectively).

3.2.2 Comparison to the POC database

The observed proportion of drying $RPoD_{POC}$ is rather well simulated by both LLR and LR models with the 2011–2017 explanatory dataset (NSE > 0.7 except for the year 2011; Fig. 9). In addition, the models are able to capture small fluctuations of $RPoD_{POC}$ during the summer period. The best results during the year 2011 are obtained with the LLR model (black curve; Fig. 9) and the LR model overestimates $RPoD_{POC}$ by 3 % (dashed grey curve; Fig. 9). In 2012, the decline in water levels is more gradual than in 2011 and a marked peak is reached in September with 40 % of $RPoD_{POC}$ (Fig. 9). This pattern is well reproduced by both models with a good fit to all observation points (Fig. 9). The year 2013 is less affected by drying occurrence and the maximum $RPoD_{POC}$ does not exceed 20 % (Fig. 9). Curves of both models fit to observations well until the end of August. Note that the LR model is slightly closer to the observations around the peak in September compared to the LLR model. However, the LR model overestimates the $RPoD_{POC}$ at the end of September and in October.

When the 1989–2017 dataset is used for explanatory variables, the simulations of RPoD are weakly degraded with both models (Fig. 9d, e, f). However, the simulated pattern is similar to the observed one. The LLR model outperforms the LR model during the 3 years of validation with the 1989–2017 dataset (black curve; Fig. 9d, e, f).

3.2.3 Temporal patterns assessment of models between 2012 and 2017

During the calibration period, the LLR and LR models tend to better simulate the RPoD during dry years 2012 and 2016 (NSE = 0.8 with the LLR and LR models; Table 2) than during wet years (e.g. 2014 with NSE < 0.7). The NSEs are lower during the months of May and June when few drying events are observed, while NSEs are much better during the driest months of August and September.

During the validation year of 2017, both models obtain a similar performance over the year independent of datasets (NSE = 0.7).

Monthly NSEs in 2017 follow the same trend as monthly NSEs of the calibration period, with lower NSEs in May (NSEs < 0.4) and June (NSEs = 0.5) and higher NSEs in July, August and September (NSEs = 0.6) with both models independent of datasets. Figure 10 shows the dispersion between predicted RPoD and drying statuses observed at ONDE sites in the scatter plot during the validation year 2017 (Fig. 10a and b) in comparison with the year 2012, which obtains the better NSE during calibration period (Fig. 10c and d). The NSEs obtained in 2017 are 0.72 with the LLR model and 0.68 with the LR model against 0.83 and 0.81 in 2012, respectively. The performance is slightly lower in 2017 but remains acceptable with NSEs close to 0.7, and both models seem able to predict RPoD from the calibration period.

3.3 Application of regional models

3.3.1 Modelling of intermittencies severity between 2012 and 2016

Both models have been applied using the 2011–2017 dataset. Figure 11 displays the maximum number of consecutive days ($D_{RPoD>20\,\%}$) with RPoD higher than 20 % simulated by both the LLR and LR models. The most affected regions are located in the south-east of France and in the sedimentary plains, which is consistent with the spatial pattern obtained from the ONDE observations (Fig. 5). The most impacted year followed the same hierarchy: the year 2012 is the most critical year, with 30 % of France displaying $D_{RPoD>20\,\%}$ higher than 60 days followed by the year 2015 (20 % of France with $D_{RPoD>20\,\%} > 60$ days) and 2016 (15 % of France with $D_{RPoD>20\,\%} > 60$ days) (Fig. 11). The years 2013 and 2014 are weakly affected, with 5 % and 6 % of France with $D_{RPoD>20\,\%}$ higher than 60 days, respectively.

The LR model tends to simulate shorter periods of drying, particularly in HER2–HR combinations located in south-eastern France in 2013 and 2014 (Fig. 11). However, there is an overall agreement between RPoD simulated by both models in terms of spatial and temporal extent of dry streams.

3.3.2 Reconstitution of historical regional probability of drying

The trend temporal patterns of RPoD predicted by the two models, considering the 1989–2017 dataset, look similar between 1989 and 2016, and the simulated RPoD fit well to $RPoD_{ONDE}$ (Fig. 12).

The proportion of drying is highly variable over the total simulation period, with alternating dry (1989 to 1991, 2003 to 2006, 2009 to 2012) and wet (1994 to 1995, 2000 to 2002, 2013 to 2014) phases. In spite of inter-annual variability, peaks of RPoD occur regularly between August and September, whether in dry years or wet years. This finding is consistent with the preeminence of rainfall-fed river flow regimes with low flows in summer, in France.

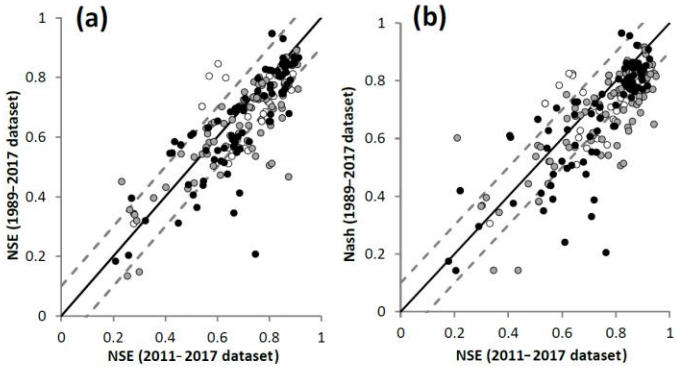

Figure 8. NSE calculated for each HER2–HR combination between 2012 and 2016 with the 1989–2017 dataset as a function of NSE calculated with the 2011–2017 dataset with, respectively, **(a)** the LLR model and **(b)** the LR model. The colours of the dots represent the proportion of gauging stations and piezometers lost between the 2011–2017 database and the 1989–2017 database: losses < 50 % (white); losses between 50 and 75 % (grey); losses > 75 % (black).

The highest values of RPoDs (above 35 % over France) are observed in 1989, 1990, 1991, 2003 and 2005 (black curve, Fig. 12a and b). The RPoDs simulated during these dry years are out of the range of the observed values over the calibration period (2012–2016). Estimations are thus uncertain. However, the high values of RPoD are consistent with observations reported in previous studies (e.g. Larue and Giret, 2004; Snelder et al., 2013; Caillouet et al., 2017). Conversely, the years less affected by drying are simulated in 1994, 2001 and 2014, with an average RPoD below 15 % throughout the year (black curve, Fig. 12a and b).

Results obtained with the LLR model are more contrasted in terms of extreme values than those obtained with the LR model (Fig. 12b).

4 Discussion

4.1 ONDE network complementarity with conventional flow monitoring network

The analysis of the ONDE observations shows that the proportion of rivers undergoing drying is significantly higher (35 %) than that observed with the conventional monitoring (HYDRO database, 8 %). This proportion, although related to a short period of records 2012 and 2016, is consistent with the percentage of 39 % of river segments classified as intermittent by Snelder et al. (2013). This analysis confirms the under-representation of IRES in the French HYDRO database, and probably others in other countries (flows are often uncontrolled in IRES). Without gauging stations located on headwaters, Snelder et al. (2013) were unable to predict IRES in eastern France (see Fig. 9, p. 2694). The high density of ONDE sites makes it possible to improve the detection of drying events and lead to better understand the spatial distribution of IRES located at the upstream extent of the hydrographic network. The ONDE network encompasses various hydrological conditions, which provides a more accurate assessment of inter-annual variability, differentiating between dry years (2012, 2015 and 2016) and wet years (2013, 2014) with clearly few drying occurrences.

The validation of the LR and LLR models against the spatially dense POC database also demonstrates the spatial representativeness of the ONDE network. Thanks to the qualitative information provided and to models such as the statistical models developed here, it is now possible to capture drying events at the regional scale.

The ONDE sites are located on small headwater streams which can be very reactive to external disturbances (rainfall deficit, change in air temperature, increase in water withdrawals, etc.) and by nature are more likely to be IRES. The gauging stations available in the HYDRO database are located on larger streams and their hydrologic response to changes in external factors (environmental or human) is slower and drying occurred with greater inertia under temperate climate. Their uneven distribution across France does not allow us to accurately characterise the inter-annual variability of drying development. Overall, the ONDE network provides very complementary information to conventional flow monitoring, leading to a better understanding of the processes of drying in upstream catchments.

4.2 Dependency on spatial gauging network density

The performance obtained with the LR and LLR models is slightly better with the 2011–2017 dataset (mean NSE = 0.75) than those obtained with the 1989–2017 dataset (mean NSE > 0.65), whose network is less dense. HER2–HR combinations are the most degraded where the number of monitoring stations is the most decreased between the two

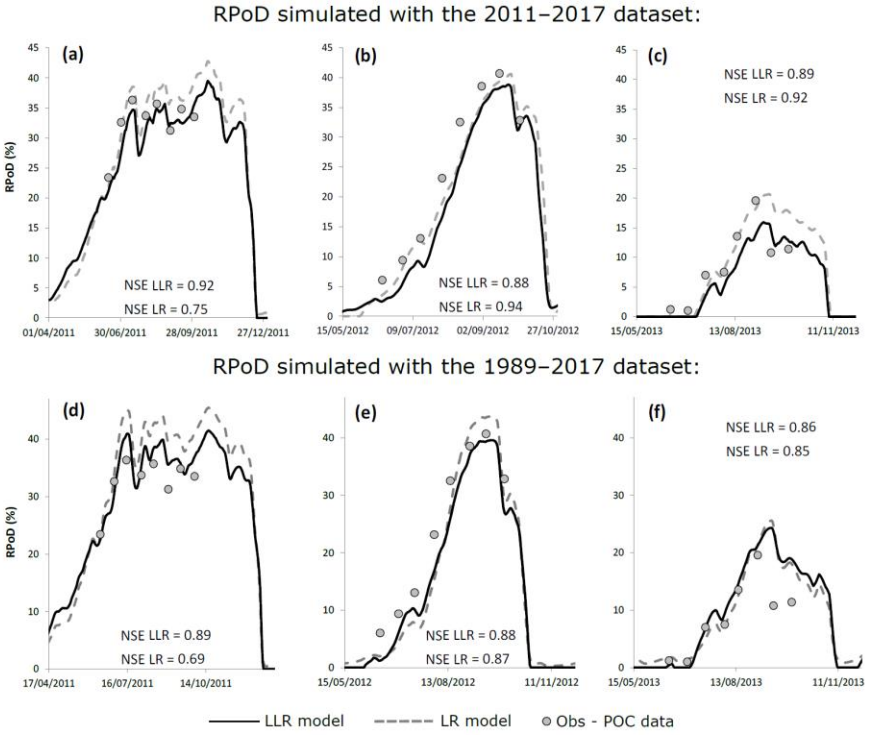

Figure 9. Comparison between observed proportion of drying $RPoD_{POC}$ and RPoD predicted by the LLR and LR models with the 2011–2017 dataset in **(a)** 2011, **(b)** 2012 and **(c)** 2013 and with the 1989–2017 dataset in **(d)** 2011, **(e)** 2012 and **(f)** 2013.

Table 2. NSE criteria obtained between 2012 and 2017 with the LLR and LR models calibrated over the period 2012–2016.

		2011–2017 dataset						1989–2017 dataset					
		Calibration					Valid.	Calibration					Valid.
		2012	2013	2014	2015	2016	2017	2012	2013	2014	2015	2016	2017
LLR model	May	0.2	0.0	0.5	0.5	0.6	0.4	0.2	0.0	0.3	0.0	0.7	0.2
	Jun	0.6	0.3	0.8	0.5	0.8	0.5	0.6	0.3	0.5	0.3	0.8	0.5
	Jul	0.7	0.5	0.6	0.6	0.8	0.7	0.7	0.5	0.5	0.4	0.8	0.6
	Aug	0.8	0.6	0.7	0.7	0.8	0.6	0.7	0.5	0.5	0.5	0.8	0.6
	Sep	0.7	0.8	0.6	0.6	0.7	0.6	0.6	0.7	0.5	0.5	0.6	0.6
	May–Sep	0.8	0.8	0.7	0.7	0.8	0.7	0.8	0.7	0.5	0.6	0.8	0.7
LR model	May	0.2	0.0	0.5	0.1	0.6	0.3	0.3	0.0	0.3	0.0	0.7	0.2
	Jun	0.6	0.5	0.8	0.5	0.8	0.4	0.6	0.4	0.5	0.3	0.7	0.4
	Jul	0.7	0.6	0.5	0.6	0.8	0.6	0.7	0.4	0.5	0.4	0.8	0.6
	Aug	0.7	0.6	0.7	0.6	0.7	0.6	0.6	0.4	0.5	0.4	0.7	0.5
	Sep	0.6	0.8	0.6	0.7	0.7	0.6	0.5	0.6	0.4	0.5	0.6	0.6
	May–Sep	0.8	0.8	0.7	0.7	0.8	0.7	0.8	0.7	0.5	0.6	0.8	0.7

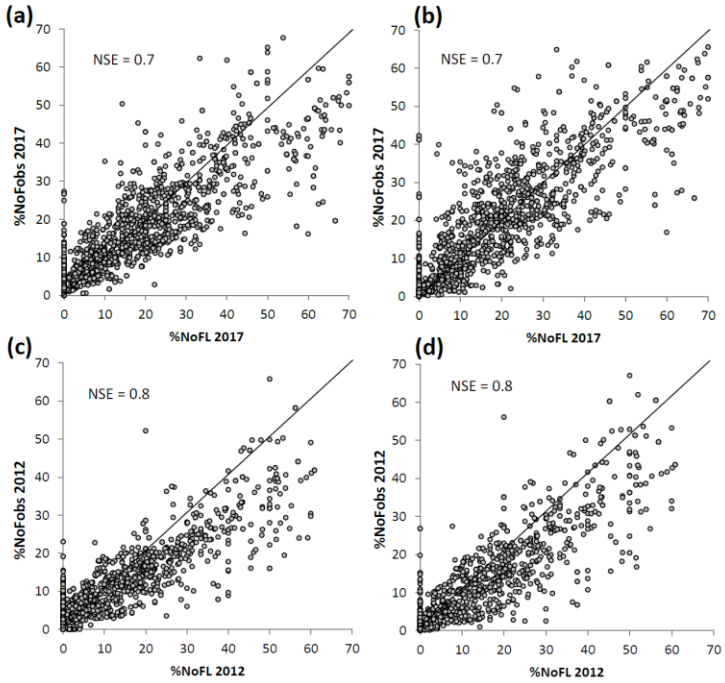

Figure 10. Scatter plot of the predicted RPoD (x axis) and drying observed at ONDE sites (y axis) in 2017 and 2012 simulated with the 2011–2017 dataset by (**a** and **c**) the LLR model and (**b** and **d**) the LR model.

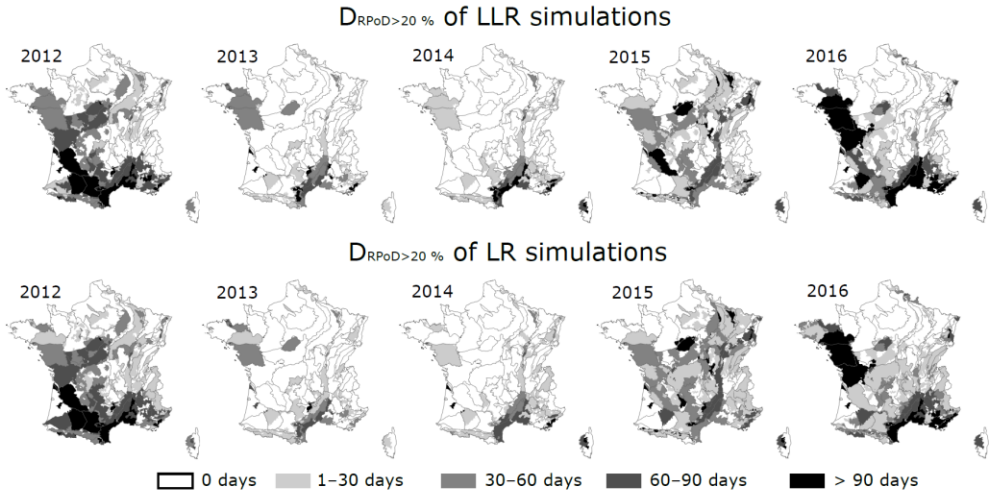

Figure 11. Maximum duration of consecutive days with RPoD higher than 20 % simulated with the LLR and LR models.

datasets. The accuracy of the predictions is dependent on the number of gauging stations, ONDE sites and piezometers available to calibrate the regressions. The highest NSEs are obtained in western sedimentary plains and south-eastern France, where a significant number of streams have dryings regardless of years (Fig. 5). The dominant river flow regime in these regions is mainly influenced by precipitation and the lowest water levels are reached in August and September,

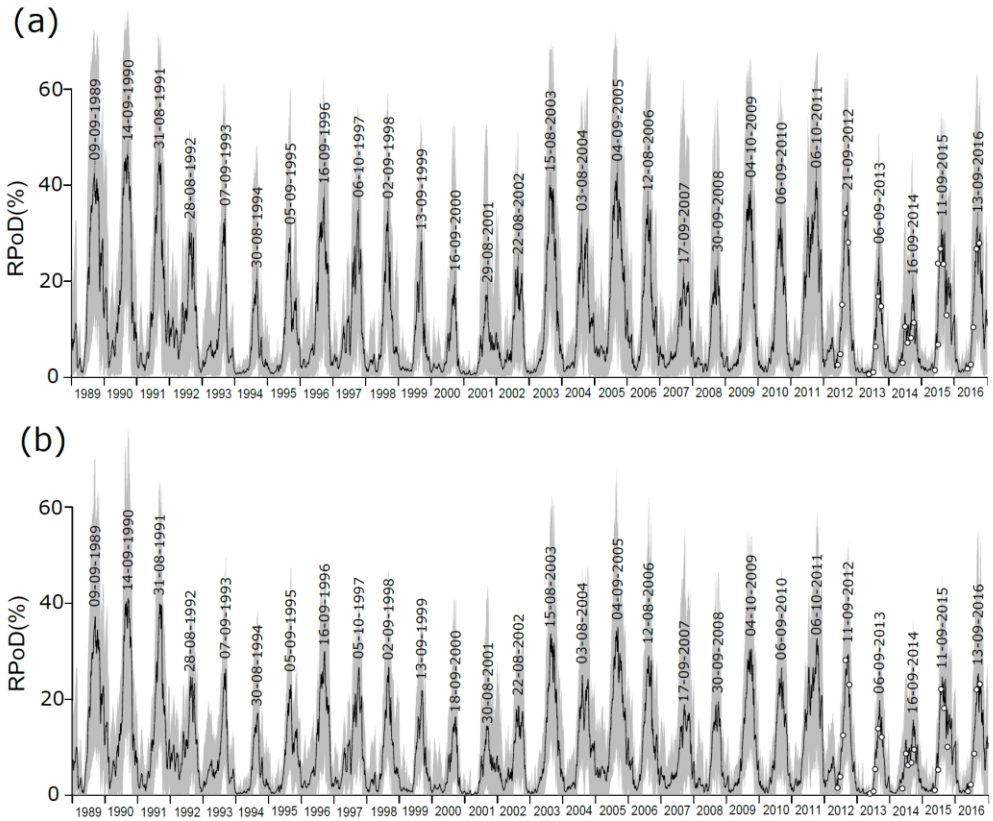

Figure 12. RPoD simulated between 1989 and 2016 with the 1989–2017 dataset with **(a)** the LR model and **(b)** the LLR model. The grey area represents the RPoD between the 90th percentile and the 10th percentile simulated on the HER2–HR combination, the black curve represents the average RPoD simulated by the HER2–HR combination and white dots represent the mean $RPoD_{ONDE}$ for each observation date. Dates mentioned correspond to the day of the maximum average RPoD simulated by the HER2–HR combination (black curve) of each year.

which corresponds to the monitoring period of the ONDE database. They benefit from a dense monitoring network (gauging stations, ONDE sites, piezometers), which allows a better representation of the hydrological functioning of streams located within the same HER2. Conversely, performance was poor in mountainous areas such as in the Alps or the Massif Central (NSE < 0.4) where river flow regimes are diversified combining rainfall and snowmelt influences. By construction, the area of HER2–HR combination in mountains is reduced, which leads to a limited number of monitoring stations, certainly not sufficient to fit the models. Moreover, the observation period for ONDE sites was limited between May and September and dryings can be missed, particularly for streams influenced by snow or ice melting with potential drying periods in winter. In regions potentially concerned with drying events from the May–September period, the actual ONDE monitoring strategy needs to be adapted to provide reliable temporal observations and extrapolations of drying frequencies.

We have chosen to average the non-exceedance frequencies of flows and groundwater levels in order to increase the monitoring network. If models had been calibrated using only gauging stations, performance will have been globally similar, or slightly better, in some HER2–HR combinations (Fig. 13). Therefore, we could not validate the real gain of using groundwater-level data in addition to discharge data. This is certainly due to the dominant proportion of the gauging stations compared to the piezometers. Indeed, in the 2011–2017 dataset, the proportion of gauging stations is greater than 75 % for more than 70 % of HER2–HR combinations, whereas the proportion of piezometers exceeds 70 % in only 5 % of HER2–HR combinations. Groundwater-level data thus have a small weight in regressions for this dataset. However, in the 1989–2017 dataset, the proportion

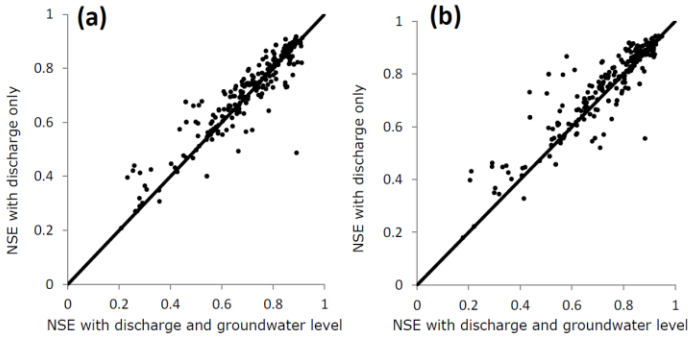

Figure 13. Comparison of NSE obtained with regression including only the discharge variable as a function of NSE obtained with discharge and groundwater-level variables in the 2011–2017 dataset with **(a)** the LLR model and **(b)** the LR model.

of piezometers is greater than 70 % in more than 30 % of HER2–HR combinations. The presence of piezometers increases the density of the monitoring network in HER2–HR combinations with few available gauging stations. Thanks to groundwater-level data, RPoD can be predicted on more HER2–HR combinations.

4.3 Interest in reconstructing the dynamic regional probability of drying

Spatio-temporal simulation of the probability of drying is crucial for advancing our understanding of IRES ecology and management. Some aquatic species can persist in a dry reach for a few days, weeks or months, while some are highly sensitive to desiccation (Datry, 2012; Storey and Quinn, 2013; Stubbington and Datry, 2013). Estimation of the total duration of days with drying at the reach scale is therefore needed to understand biological patterns in river networks (Kelso and Entrekin, 2018). To our knowledge, no study has proposed to reconstruct daily flow-state time series of headwater streams at the country scale such as France ($> 500\,000\,km^2$) using discrete observations in time and space. In the literature, studies at national scale remain focused on the detection and the mapping of IRES because these rivers are historically poorly investigated and their proportion in existing hydrographic networks remains inaccurate or misunderstood (Nadeau and Rains, 2007; Snelder et al., 2013). Recently, several studies proposed alternative methodologies in order to estimate metrics in ungauged IRES (Gallart et al., 2016) or to predict daily streamflow in river basins experiencing flow intermittence (De Girolamo et al., 2017b), but remain applicable at the local scale.

This study provides a first regional approach to use discrete data obtained from regular observations. The average non-exceedance frequency is a global hydrological statistic that only captures the hydrological conditions at the regional scale in modelling the RPoD. For rainfall-driven river flow regimes, the effect of rainfall events on flow intermittence at the HER2–HR scale is probably indirectly reflected by the daily discharge and groundwater levels used to calculate the average non-exceedance frequency. However, when more observation data are available, it is likely that including more detailed descriptors of rainfall events and local geology could improve our approach. In France, based on the 2011–2017 dataset, both models suggest the highest values of RPoD along the Mediterranean coast ($D_{RPoD > 20\,\%} > 100$ days each year). Rivers in this region are subject to a predominantly pluvial regime (Class 7; Sauquet et al., 2008), i.e. hot and dry summers followed by intense rainfall events in autumn, leading to high flows in November (Skoulikidis et al., 2017b). The catchments in this region are small and particularly reactive to environmental changes, making them highly sensitive to flow intermittence. Rivers located in the sedimentary plain in western France are also very impacted by flow intermittence. The regime is also influenced by precipitation and for the basins subject to intense agriculture significant water abstractions during summer in this region reduce water availability in rivers and in aquifers which are no longer able to support the low water levels, leading to increased flow intermittence. Regarding alteration issues in our datasets, we do not have access to the exact location and the volumes of water withdrawal for irrigation purposes. However, due to their upstream location, water availability is expected to be low, which may limit potential withdrawals and as a consequence flow alteration at ONDE sites. The alteration of groundwater levels is unknown because no information is available. However, in sedimentary plains where agricultural crops dominate the landscape, we are not sure that no human action affects low flows. It is important to note that the responses of biological communities to artificial flow intermittence are still poorly understood compared to natural IRES (Datry et al., 2014b; Skoulikidis et al., 2017a).

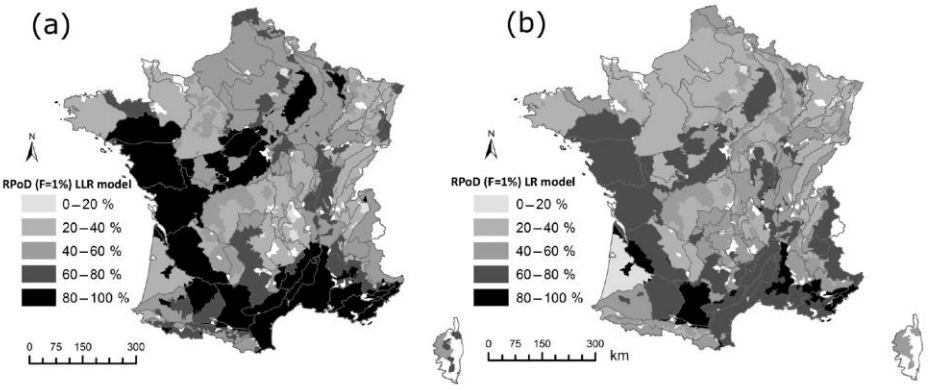

Figure 14. Regional probability of drying simulated with $F = 1\,\%$ predicted with **(a)** the LLR model and **(b)** the LR model.

4.4 Validity of historical regional probability of drying during severe low-flow period

The second application aimed at reconstructing historical RPoD over the period 1989–2016. Both models suggest the highest values of mean RPoD (> 35 %) in 1989–1991, 2003 and 2005. During these dry years, predicted values of RPoD result from extrapolation but are consistent with published studies (Mérillon and Chaperon, 1990; Moreau, 2004). For example, Mérillon (1992) estimated that for the whole of France, 11 000 km of rivers were dried at the end of the summers of 1989 and 1990. Caillouet et al. (2017) found that the low-flow event observed in 1989–1990 was particularly severe in terms of duration and affected 95 % of France. Snelder et al. (2013) showed from 628 gauging stations that the years 1989–1991, 2003 and 2005 witnessed particularly high values of duration and frequency of drying events. They found that regions with the highest probability of drying were located along the Mediterranean and Atlantic coasts, which is consistent with ONDE observations and with our results.

Both models suggest the same sequence of dry and wet years. However, the application of the LLR model leads to less contrasted RPoD than the LR model (Fig. 12).

To illustrate these differences, the RPoD has been simulated by both models with an extreme F of 1 % (Fig. 14). The $RPoD_{LLR}$ is significantly higher and exceeds 80 % in 30 % of the study area against only 5 % of the area with the $RPoD_{LR}$. On the other hand, models simulate low RPoD in HER2–HR combinations where the $RPoD_{ONDE}$ is very low between 2012 and 2016, even when F was 1 %, because this situation never occurred during the calibration period (Fig. 14). The logistic function of the LR model takes an S-shape which induced a decrease in the slope of the curve toward extreme values observed during the calibration period (2012–2016). The truncated logarithmic function of the LLR model is not bounded and RPoD can reach 100 % during extreme low-flow events by extrapolation. Since the ONDE network monitoring period does not include a period with drought as severe as in the 1990s, it is not currently possible to assess the relative performance of the two models. Refining extrapolated values requires additional information on headwater collected during more severe droughts than those observed during the last 5 years and then gives support to the pursuit of the ONDE network.

5 Conclusion

This paper investigates the spatial and temporal dynamics of the regional probability of drying (RPoD) of headwater streams by taking benefit from qualitative and discontinuous data provided by the ONDE network. Two models based on linear or logistic regressions have been developed and succeeded in reconstructing the temporal dynamics of RPoD. They are based on a strong relationship between the non-exceedance frequencies of discharges and groundwater levels as a function of the proportion of drying statuses observed at ONDE sites per HER2–HR combination. LLR and LR models show similar performance and perform well between 2011 and 2017. The accuracy of predictions is dependent on the number of gauging stations, ONDE sites and piezometers available to calibrate the regressions. Regions with the highest performance are located in the sedimentary plains, where the monitoring network is dense and where the RPoD is the highest. Conversely, the worst performances are obtained in the mountainous regions. Finally, both models have been used to reconstruct historical RPoD between 1989 and 2016 and suggest the highest values of mean RPoD (> 35 %) in 1989–1991, 2003 and 2005. This is consistent with other published studies, but the high density of ONDE sites makes it possible to improve the detection of drying events and lead to better capturing of the spatial distribution of IRES located at the upstream extent of the hydrographic network. Moreover, the duration of drying is of importance for ecologists

and the prediction of a daily RPoD provides one key driver for the composition and persistence of aquatic species.

From a methodological point of view, our method relating discrete drying observation obtained by citizen science networks to continuous daily gauging data seems robust across the highly diverse (climate and topography) regions of France, and provides good predictions in an independent region excluded from the calibration process (PoC). These two results suggest a potential application of our approach in other countries. Citizen science creates opportunities to overcome the lack of hydrological data, contributes to densifying the flow-state observation network (Turner and Richter, 2011; Buytaert et al., 2014) and remains less expensive than the installation of additional gauging stations to survey flow intermittence. The next step will be to use this regional approach to simulate the RPoD in future periods by taking into account effects of climate change through predicted discharge and groundwater-level data. This would allow quantification of the evolution of the probability of drying between the current period and the different climate projections provided by the latest IPCC Report (IPCC 2014) and would assist decision makers in defining protocols for restoring flows with appropriate measures to preserve aquatic ecosystems (Woelfle-Erskine, 2017).

Secondly, further work is needed to develop an approach capable of reconstructing the drying dynamics locally by differentiating each stream. Our approach remains spatially valid for estimating RPoDs at the scale of HER2–HR combinations, but does not allow characterisation of the variability of drying occurrence between nearby streams within these regions. From a methodological point of view, statistical tools such as neural networks (Breiman, 2001) have shown good ability to assess both the occurrence and extent of perennial and temporary segments (González-Ferreras and Barquín, 2017) and could be investigated as an alternative method to reconstruct locally the temporal variability of drying.

Data availability. Data used in this study are freely available on the Eaufrance data portal (http://www.eaufrance.fr; AFB, 2018). Time series of daily regional probability of drying are available upon request from the corresponding author.

Author contributions. AB, NL and ES developed the main ideas and designed the experiments. AB implemented the algorithms and analysed the results. AB prepared the manuscript with contributions from all co-authors.

Competing interests. The authors declare that they have no conflict of interest.

Acknowledgements. The authors wish to thank Anne van Loon and Catherine Sefton for their valuable comments, suggestions and positive feedback on the manuscript. The research project was partly funded by the French Agency for Biodiversity (AFB, formerly ONEMA). This study is based upon works from COST Action CA15113 (SMIRES, Science and Management of Intermittent Rivers and Ephemeral Streams, www.smires.eu), supported by COST (European Cooperation in Science and Technology).

Edited by: Laurent Pfister
Reviewed by: Catherine Sefton and Anne Van Loon

References

Acuña, V., Datry, T., Marshall, J., Barceló, D., Dahm, C. N., Ginebreda, A., McGregor, G., Sabater, S., Tockner, K., and Palmer, M. A.: Why should we care about temporary waterways?, Science, 343, 1080–1081, 2014.

Acuña, V., Hunter, M., and Ruhí, A.: Managing temporary streams and rivers as unique rather than second-class ecosystems, Biol. Conserv., 211, 12–19, https://doi.org/10.1016/j.biocon.2016.12.025, 2017.

AFB (French Agency for Biodiversity): Observatoire National des Etiages (ONDE), available at: https://onde.eaufrance.fr (last access: 23 May 2018), 2012–2018.

Benda, L., Hassan, M. A., Church, M., and May, C. L.: Geomorphology Of Steepland Headwaters: The Transition From Hillslopes To Channels1, J. Am. Water Resour. As., 41, 835–851, 2005.

Benstead, J. P. and Leigh, D. S.: An expanded role for river networks, Nat. Geosci., 5, 678–679, 2012.

Boulton, A. J.: Conservation of ephemeral streams and their ecosystem services: what are we missing?: Editorial, Aquat. Conserv., 24, 733–738, https://doi.org/10.1002/aqc.2537, 2014.

Breiman, L.: Random forests, Mach. Learn., 45, 5–32, 2001.

Brugeron, A., Allier, D., and Klinka, T.: Approche exploratoire des liens entre référentiels hydrogéologique et hydrographique: Premières identifications des piézomètres potentiellement représentatifs d'une relation nappe/rivière et contribution à leur valorisation, Rapport final BRGM/RP-61047-FR, 241 pp., 2012.

Buytaert, W., Zulkafli, Z., Grainger, S., Acosta, L., Alemie, T. C., Bastiaensen, J., De Bièvre, B., Bhusal, J., Clark, J., Dewulf, A., Foggin, M., Hannah, D. M., Hergarten, C., Isaeva, A., Karpouzoglou, T., Pandeya, B., Paudel, D., Sharma, K., Steenhuis, T., Tilahun, S., Van Hecken, G., and Zhumanova, M.: Citizen science in hydrology and water resources: opportunities for knowledge generation, ecosystem service management, and sustainable development, Front. Earth Sci., 2, 1–21, https://doi.org/10.3389/feart.2014.00026, 2014.

Caillouet, L., Vidal, J.-P., Sauquet, E., Devers, A., and Graff, B.: Ensemble reconstruction of spatio-temporal extreme low-flow events in France since 1871, Hydrol. Earth Syst. Sci., 21, 2923–2951, https://doi.org/10.5194/hess-21-2923-2017, 2017.

Clarke, A., Mac Nally, R., Bond, N., and Lake, P. S.: Macroinvertebrate diversity in headwater streams: a review, Freshwater Biol., 53, 1707–1721, https://doi.org/10.1111/j.1365-2427.2008.02041.x, 2008.

Costigan, K. H., Jaeger, K. L., Goss, C. W., Fritz, K. M., and Goebel, P. C.: Understanding controls on flow permanence in intermittent rivers to aid ecological research: integrating

meteorology, geology and land cover: Integrating Science to Understand Flow Intermittence, Ecohydrology, 9, 1141–1153, https://doi.org/10.1002/eco.1712, 2016.

Datry, T.: Benthic and hyporheic invertebrate assemblages along a flow intermittence gradient: effects of duration of dry events: River drying and temporary river invertebrates, Freshwater Biol., 57, 563–574, https://doi.org/10.1111/j.1365-2427.2011.02725.x, 2012.

Datry, T., Larned, S. T., Fritz, K. M., Bogan, M. T., Wood, P. J., Meyer, E. I., and Santos, A. N.: Broad-scale patterns of invertebrate richness and community composition in temporary rivers: effects of flow intermittence, Ecography, 37, 94–104, https://doi.org/10.1111/j.1600-0587.2013.00287.x, 2014a.

Datry, T., Larned, S. T., and Tockner, K.: Intermittent Rivers: A Challenge for Freshwater Ecology, BioScience, 64, 229–235, https://doi.org/10.1093/biosci/bit027, 2014b.

Datry, T., Pella, H., Leigh, C., Bonada, N., and Hugueny, B.: A landscape approach to advance intermittent river ecology, Freshwater Biol., 61, 1200–1213, https://doi.org/10.1111/fwb.12645, 2016a.

Datry, T., Fritz, K., and Leigh, C.: Challenges, developments and perspectives in intermittent river ecology, Freshwater Biol., 61, 1171–1180, https://doi.org/10.1111/fwb.12789, 2016b.

De Girolamo, A. M., Lo Porto, A., Pappagallo, G., Tzoraki, O., and Gallart, F.: The Hydrological Status Concept: Application at a Temporary River (Candelaro, Italy): Evaluating Hydrological Status In Temporary Rivers, River Res. Appl., 31, 892–903, https://doi.org/10.1002/rra.2786, 2015.

De Girolamo, A. M., Bouraoui, F., Buffagni, A., Pappagallo, G., and Lo Porto, A.: Hydrology under climate change in a temporary river system: Potential impact on water balance and flow regime, River Res. Appl., 33, 1219–1232, https://doi.org/10.1002/rra.3165, 2017a.

De Girolamo, A. M., Barca, E., Pappagallo, G., and Lo Porto, A.: Simulating ecologically relevant hydrological indicators in a temporary river system, Agr. Water Manage., 180, 194–204, https://doi.org/10.1016/j.agwat.2016.05.034, 2017b.

Döll, P., and Schmied, H. M.: How is the impact of climate change on river flow regimes related to the impact on mean annual runoff? A global-scale analysis, Environ. Res. Lett., 7, 014037, https://doi.org/10.1088/1748-9326/7/1/014037, 2012.

Eng, K., Wolock, D. M., and Dettinger, M. D.: Sensitivity of Intermittent Streams to Climate Variations in the USA: Sensitivity of Intermittent Streams, River Res. Appl., 32, 885–895, https://doi.org/10.1002/rra.2939, 2016.

Finn, D. S., Bonada, N., Múrria, C., and Hughes, J. M.: Small but mighty: headwaters are vital to stream network biodiversity at two levels of organization, J. N. Am. Benthol. Soc., 30, 963–980, https://doi.org/10.1899/11-012.1, 2011.

Fritz, K. M., Hagenbuch, E., D'Amico, E., Reif, M., Wigington, P. J., Leibowitz, S. G., Comeleo, R. L., Ebersole, J. L., and Nadeau, T.-L.: Comparing the Extent and Permanence of Headwater Streams From Two Field Surveys to Values From Hydrographic Databases and Maps, J. Am. Water Resour. As., 49, 867–882, https://doi.org/10.1111/jawr.12040, 2013.

Gallart, F., Prat, N., García-Roger, E. M., Latron, J., Rieradevall, M., Llorens, P., Barberá, G. G., Brito, D., De Girolamo, A. M., Lo Porto, A., Buffagni, A., Erba, S., Neves, R., Nikolaidis, N. P., Perrin, J. L., Querner, E. P., Quiñonero, J. M., Tournoud, M. G., Tzoraki, O., Skoulikidis, N., Gómez, R., Sánchez-Montoya, M. M., and Froebrich, J.: A novel approach to analysing the regimes of temporary streams in relation to their controls on the composition and structure of aquatic biota, Hydrol. Earth Syst. Sci., 16, 3165–3182, https://doi.org/10.5194/hess-16-3165-2012, 2012.

Gallart, F., Llorens, P., Latron, J., Cid, N., Rieradevall, M., and Prat, N.: Validating alternative methodologies to estimate the regime of temporary rivers when flow data are unavailable, Sci. Total Environ., 565, 1001–1010, https://doi.org/10.1016/j.scitotenv.2016.05.116, 2016.

Garcia, C., Gibbins, C. N., Pardo, I., and Batalla, R. J.: Long term flow change threatens invertebrate diversity in temporary streams: Evidence from an island, Sci. Total Environ., 580, 1453–1459, https://doi.org/10.1016/j.scitotenv.2016.12.119, 2017a.

Garcia, C., Amengual, A., Homar, V., and Zamora, A.: Losing water in temporary streams on a Mediterranean island: Effects of climate and land-cover changes, Global Planet. Change, 148, 139–152, https://doi.org/10.1016/j.gloplacha.2016.11.010, 2017b.

Gómez, R., Hurtado, I., Suárez, M. L., and Vidal-Abarca, M. R.: Ramblas in south-east Spain: threatened and valuable ecosystems, Aquat. Conserv., 15, 387–402, https://doi.org/10.1002/aqc.680, 2005.

González-Ferreras, A. M. and Barquín, J.: Mapping the temporary and perennial character of whole river networks: Mapping Flow Permanence In River Network, Water Resour. Res., 53, 6709–6724, https://doi.org/10.1002/2017WR020390, 2017.

Huxter, E. H. H. and van Meerveld, H. J.: Intermittent and Perennial Streamflow Regime Characteristics in the Okanagan, Can. Water Resour. J., 37, 391–414, https://doi.org/10.4296/cwrj2012-910, 2012.

IPCC.: Climate Change 2014: Synthesis Report. Contribution of Working Groups I, II and III to the Fifth Assessment Report of the Intergovernmental Panel on Climate Change, edited by: Core Writing Team, Pachauri, R. K., and Meyer, L. A., IPCC, Geneva, Switzerland, 151 pp., 2014.

Jaeger, K. L., Olden, J. D., and Pelland, N. A.: Climate change poised to threaten hydrologic connectivity and endemic fishes in dryland streams, P. Natl. Acad. Sci. USA, 111, 13894–13899, https://doi.org/10.1073/pnas.1320890111, 2014.

Kelso, J. E. and Entrekin, S. A.: Intermittent and perennial macroinvertebrate communities had similar richness but differed in species trait composition depending on flow duration, Hydrobiologia, 807, 189–206, https://doi.org/10.1007/s10750-017-3393-y, 2018.

Larned, S. T., Datry, T., Arscott, D. B., and Tockner, K.: Emerging concepts in temporary-river ecology, Freshwater Biol., 55, 717–738, https://doi.org/10.1111/j.1365-2427.2009.02322.x, 2010.

Larue, J. P. and Giret A.: The drying up of streams in the Maine basin from 1989 to 1992, Norois, 192, 117–133, https://doi.org/10.4000/norois.944, 2004.

Lee, S.: Application of logistic regression model and its validation for landslide susceptibility mapping using GIS and remote sensing data, Int. J. Remote Sens., 26, 1477–1491, https://doi.org/10.1080/01431160412331331012, 2005.

Leigh, C. and Datry, T.: Drying as a primary hydrological determinant of biodiversity in river systems: a broad-scale analysis, Ecography, 40, 487–499, https://doi.org/10.1111/ecog.02230, 2017.

Leigh, C., Boulton, A. J., Courtwright, J. L., Fritz, K., May, C. L., Walker, R. H., and Datry, T.: Ecological research and management of intermittent rivers: an historical review and future directions, Freshwater Biol., 61, 1181–1199, https://doi.org/10.1111/fwb.12646, 2016.

Leopold, L. B.: A View of the River, Harvard University Press, Cambridge, Massachusetts, USA, 1994.

Leopold, L. B., Wolman, M. G., and Miller, J. P.: Fluvial Processes in Geomorphology, Dover Publications, New York, USA, 1964.

Mérillon, Y.: Sécheresse, gestion de l'eau et pratiques agricoles, L'Information agricole, 649, 25–26, 1992.

Mérillon, Y. and Chaperon, P.: Drought in France in 1989, Houille Blanche, 325–340, https://doi.org/10.1051/lhb/1990025, 1990.

Meyer, J. L., Strayer, D. L., Wallace, J. B., Eggert, S. L., Helfman, G. S., and Leonard, N. E.: The Contribution of Headwater Streams to Biodiversity in River Networks1: The Contribution of Headwater Streams to Biodiversity in River Networks, J. Am. Water Resour. As., 43, 86–103, https://doi.org/10.1111/j.1752-1688.2007.00008.x, 2007.

Moreau, F.: Drought crisis management: Loire basin example, Houille Blanche, 4, 70–76, https://doi.org/10.1051/lhb:200404010, 2004.

Nadeau, T.-L. and Rains, M. C.: Hydrological Connectivity Between Headwater Streams and Downstream Waters: How Science Can Inform Policy1: Hydrological Connectivity Between Headwater Streams and Downstream Waters: How Science Can Inform Policy, J. Am. Water Resour. As., 43, 118–133, https://doi.org/10.1111/j.1752-1688.2007.00010.x, 2007.

Nash, J. E. and Sutcliffe, J. V.: River flow forecasting through conceptual models part I – A discussion of principles, J. Hydrol., 10, 282–290, https://doi.org/10.1016/0022-1694(70)90255-6, 1970.

Nowak, C. and Durozoi, B.: Observatoire National Des Etiages, Note technique, ONEMA, 2012.

Pella, H., Lejot, J., Lamouroux, N., and Snelder, T.: Le réseau hydrographique théorique (RHT) français et ses attributs environnementaux, Géomorphologie: relief, processus, environnement, 18, 317–336, 2012.

Pumo, D., Caracciolo, D., Viola, F., and Noto, L. V.: Climate change effects on the hydrological regime of small non-perennial river basins, Sci. Total Environ., 542, 76–92, https://doi.org/10.1016/j.scitotenv.2015.10.109, 2016.

Reynolds, L. V., Shafroth, P. B., and LeRoy Poff, N.: Modeled intermittency risk for small streams in the Upper Colorado River Basin under climate change, J. Hydrol., 523, 768–780, https://doi.org/10.1016/j.jhydrol.2015.02.025, 2015.

Sarremejane, R., Cañedo-Argüelles, M., Prat, N., Mykrä, H., Muotka, T., and Bonada, N.: Do metacommunities vary through time? Intermittent rivers as model systems, J. Biogeogr., 44, 2752–2763, https://doi.org/10.1111/jbi.13077, 2017.

Sauquet, E., Gottschalk, L., and Krasovskaia, I.: Estimating mean monthly runoff at ungauged locations: an application to France, Hydrol. Res., 39, 403, https://doi.org/10.2166/nh.2008.331, 2008.

Skoulikidis, N. T.: The environmental state of rivers in the Balkans—A review within the DPSIR framework, Sci. Total Environ., 407, 2501–2516, https://doi.org/10.1016/j.scitotenv.2009.01.026, 2009.

Skoulikidis, N. T., Vardakas, L., Karaouzas, I., Economou, A. N., Dimitriou, E., and Zogaris, S.: Assessing water stress in Mediterranean lotic systems: insights from an artificially intermittent river in Greece, Aquat. Sci., 73, 581–597, https://doi.org/10.1007/s00027-011-0228-1, 2011.

Skoulikidis, N. T., Vardakas, L., Amaxidis, Y., and Michalopoulos, P.: Biogeochemical processes controlling aquatic quality during drying and rewetting events in a Mediterranean non-perennial river reach, Sci. Total Environ., 575, 378–389, https://doi.org/10.1016/j.scitotenv.2016.10.015, 2017a.

Skoulikidis, N. T., Sabater, S., Datry, T., Morais, M. M., Buffagni, A., Dörflinger, G., Zogaris, S., del Mar Sánchez-Montoya, M., Bonada, N., Kalogianni, E., Rosado, J., Vardakas, L., De Girolamo, A. M., and Tockner, K.: Non-perennial Mediterranean rivers in Europe: Status, pressures, and challenges for research and management, Sci. Total Environ., 577, 1–18, https://doi.org/10.1016/j.scitotenv.2016.10.147, 2017b.

Snelder, T. H., Datry, T., Lamouroux, N., Larned, S. T., Sauquet, E., Pella, H., and Catalogne, C.: Regionalization of patterns of flow intermittence from gauging station records, Hydrol. Earth Syst. Sci., 17, 2685–2699, https://doi.org/10.5194/hess-17-2685-2013, 2013.

Storey, R. G. and Quinn, J. M.: Survival of aquatic invertebrates in dry bed sediments of intermittent streams: temperature tolerances and implications for riparian management, Freshw. Sci., 32, 250–266, https://doi.org/10.1899/12-008.1, 2013.

Stubbington, R. and Datry, T.: The macroinvertebrate seedbank promotes community persistence in temporary rivers across climate zones, Freshwater Biol., 58, 1202–1220, https://doi.org/10.1111/fwb.12121, 2013.

Turner, D. S. and Richter, H. E.: Wet/Dry Mapping: Using Citizen Scientists to Monitor the Extent of Perennial Surface Flow in Dryland Regions, Environ. Manage., 47, 497–505, https://doi.org/10.1007/s00267-010-9607-y, 2011.

Vadher, A. N., Millett, J., Stubbington, R., and Wood, P. J.: Drying duration and stream characteristics influence macroinvertebrate survivorship within the sediments of a temporary channel and exposed gravel bars of a connected perennial stream, Hydrobiologia, 814, 121–132, https://doi.org/10.1007/s10750-018-3544-9, 2018.

van Meerveld, H. J. I., Vis, M. J. P., and Seibert, J.: Information content of stream level class data for hydrological model calibration, Hydrol. Earth Syst. Sci., 21, 4895–4905, https://doi.org/10.5194/hess-21-4895-2017, 2017.

Vardakas, L., Kalogianni, E., Economou, A. N., Koutsikos, N., and Skoulikidis, N. T.: Mass mortalities and population recovery of an endemic fish assemblage in an intermittent river reach during drying and rewetting, Fund. Appl. Limnol., 190, 331–347, https://doi.org/10.1127/fal/2017/1056, 2017.

Wasson, J.-G., Chandesris, A., Pella, H., and Blanc, L.: Typology and reference conditions for surface water bodies in France: the hydro-ecoregion approach, TemaNord, 566, 37–41, 2002.

Woelfle-Erskine, C.: Collaborative Approaches to Flow Restoration in Intermittent Salmon-Bearing Streams: Salmon Creek, CA, USA, Water, 9, 217, https://doi.org/10.3390/w9030217, 2017.

8. Annexe 2 : Statistical reconstruction of local daily drying dynamics at headwater streams based on qualitative information: a case study in France (Beaufort *et al.*, soumis à Hydrological Processes)

Aurélien BEAUFORT[1], Julie CARREAU[2] and Eric SAUQUET[1]

[1]Irstea, UR RiverLy, centre de Lyon-Villeurbanne, 5 rue de la Doua CS 20244, 69625 Villeurbanne, France

[2]HydroSciences Montpellier (Univ. Montpellier, CNRS, IRD), Maison des Sciences de l'Eau, 300 av. du Prof. Emile Jeanbrau, Montpellier, France

Abstract

Headwater streams (HS) are generally naturally prone to flow intermittence. These intermittent rivers and ephemeral streams (IRES) have recently seen a marked increase in interest, especially to assess the impact of drying on aquatic ecosystems. The two objectives of this work are (i) to identify the main drivers of flow intermittence dynamics in HS and (ii) to reconstruct local daily drying dynamics. Discrete flow states - "flowing" versus "drying" - are modeled as functions of covariates that include information on climate, hydrology, groundwater, and basin descriptors. Three classifiers to estimate flow states using covariates are tested on four contrasted regions in France: (1) a linear classifier with regularization (LASSO for Least Absolute Shrinkage and Selection Operator); and two non-linear non-parametric classifiers - (2) a one-hidden-layer feedforward Artificial Neural Network (ANN) classifier and (3) a Random Forest (RF) classifier. The three classifiers are compared to a benchmark classifier (BC) which simply estimates dominant flow state for each month based on observations (without using covariates). The performance assessment over the period 2012-2016 carried out by cross validation shows that the three classifiers for flow state based on covariates outperformed the benchmark classifier. This demonstrates the predictive power of the covariates. ANN is the classifier that globally achieves the best performance to predict the daily drying dynamics while both RF and LASSO tend to underestimate the proportion of "Drying" states. The covariates are ranked in terms of relevance for each classifier. The monthly proportion of "Drying" states provided by the discrete observation network has a major importance for the three classifiers ANN, LASSO and RF. This may reflect the proclivity of a site to flow intermittence. ANN gives higher importance to climatic and hydrological covariates and its non-linearity allows a greater degree of freedom.

Keywords: Intermittent rivers, flow state, drying prediction, Artificial Neural Network, Least Absolute Shrinkage and Selection Operator, Random Forest

1. Introduction

Headwater streams (HS) are generally defined as the uppermost streams in a watershed and represent a large part of hydrographical networks (Leopold, Wolman & Miller, 1964; Nadeau & Rains, 2007). HS can be fed by groundwater, precipitation and runoff from small drainage areas. They contribute to the good functioning of rivers (sediment flux, inputs of particulate organic matter and nutrients), provide primordial ecosystem services (biogeochemical cycling, sources of aquatic organisms, aquatic habitat, thermal refuge…) (Meyer et al., 2007; Larned, Datry, Arscott, & Tockner, 2010; Finn, Bonada, Mùrria, & Hughes, 2011) and constitute reference areas to be preserved (Lowe & Likens, 2005).

Due to their upstream position in the network, their size and their high reactivity to natural or human disturbances, HS are generally naturally prone to flow intermittence (Datry, Larned, & Tockner, 2014; Fritz et al., 2013). Intermittent rivers and ephemeral streams (IRES) are defined by periodic flow cessation and may experience partial or complete dry up at some location in time and space (Larned et al., 2010; Datry, Fritz, & Leigh, 2016; Leigh et al., 2016). They range from ephemeral streams that flow a few days after rainfall to intermittent rivers that recede to isolated pools (Datry et al., 2018). IRES have seen a marked increase in interest stimulated by the challenges of water management facing the global change context (Acuña et al., 2014; Datry et al., 2016) and by the need to improve existing knowledge on aquatic ecosystems in IRES (Larned et al., 2010; Leigh & Datry, 2017; Sarremejane et al., 2017; Stubbington, England, Wood, & Sefton, 2017).

Recent studies underline the importance to better characterize the hydrological functioning of IRES (Boulton, 2014; Acuña, Hunter, & Ruhí, 2017; Leigh & Datry, 2017). To study the impact of flow intermittence on the composition and persistence of aquatic species, freshwater biologists use quantitative metrics (e.g. to characterize the drying duration, magnitude, frequency, timing, rate of

change) determined from continuous flow series (Bunn, Thoms, Hamilton, & Capon, 2006; Kennard et al., 2010; Datry et al., 2014; Vadher, Millett, Stubbington, & Wood, 2018). However, the understanding of the spatio-temporal variability of IRES and their localization within the river network is challenging. In addition, considering only continuous gauging stations could lead to an underestimation of the proportion of IRES and of their regional extent (Snelder et al., 2013; De Girolamo, Lo Porto, Pappagallo, & Gallart, 2015; Eng, Wolock, & Dettinger, 2016).

Citizen science creates opportunities to overcome the lack of hydrological data and may contribute to densify the flow-state observation network (Turner & Richter, 2011; Buytaert et al., 2014; Datry, Pella, Leigh, Bonada, & Hugueny, 2016; van Meerveld, Vis, & Seibert, 2017). In France, new sources of observational data are available thanks to the ONDE network (Observatoire National des Etiages, https: //onde.eaufrance.fr) (Nowak & Durozoi, 2012). This unique network in Europe by its coverage, the number of monitored sites and the regularity of the observations, provides frequent discrete field observations (at least five inspections per year) of flow intermittence on more than 3 300 sites throughout France that are located mostly in headwater areas.

However, discrete observations of intermittence with irregular and at most weekly frequency cannot provide information on the persistence of dry conditions at daily temporal resolution. Thus, continuous time series of flow states are needed. Beaufort, Lamouroux, Pella, Datry, & Sauquet (2018) succeeded to relate ONDE observations to continuous hydrological and groundwater level data for predicting the daily probability of drying at the regional scale and obtained robust predictions over France. However, as predictions are aggregated over large areas, this approach does not allow to differentiate the temporal variability of "Drying" state for neighboring streams. Spatial variability of flow intermittence may be high and the understanding of local drying dynamic is crucial. Hence the main objective of this work is to extend this previous study. Specifically, we aim at (i) identifying the main drivers of the flow intermittence dynamics in HS and (ii) reconstructing the daily drying dynamics of HS at the local scale. To achieve these objectives, discrete flow states - "flowing" versus "drying" - from the ONDE observations are modeled as functions of covariates having continuous time series that include information on climate, hydrology, groundwater level, and basins descriptors.

The paper is organized in six parts. Sect. 2 describes the general modeling framework developed to predict flow states. Sect. 3 introduces the study area and the data and Sect. 4 presents the performance assessment protocol. Results are presented in Sect. 5 and discussed in Sect. 6 before drawing general conclusions in Sect. 7.

2. Statistical framework for modeling daily drying dynamics

Drying dynamics can be reconstructed from a classifier that relates flow states to covariates. More specifically, the classifier is calibrated in order to, for each day, estimate the probability of the "Drying" state given a set of covariates, described in section 3.2 to 3.5 and summarized in Table 1, that are meant to introduce information on climate, groundwater level, hydrology and basin descriptors. The flow state predicted at each ONDE site at a given day relies on the information provided by local and regional covariates observed at various dates by other ONDE sites in a same region. Due to the limitation of the observation period, the predictions are restricted to the period between the 1st May and the 30th September of each year (see Sect. 3.2).

Four classifiers are considered: (1) a benchmark classifier (BC) which does not use any covariates but is entirely based on the historical proportions of observed flow state; (2) the so-called LASSO (Least Absolute Shrinkage and Selection Operator) classifier which is a linear classifier; (3) an Artificial Neural Network (ANN) classifier which is potentially non-linear but encompasses a linear classifier as a special case; (4) a Random Forest (RF) classifier which can also be non-linear but with a different strategy than ANN. Each classifier relies on a function *f* to estimate the flow state at day "d" at each location (o_x):

$$FlowState(d, o_x) = f\big(g_1(d, o_x), \dots, g_n(d, o_x)\big) \quad (1)$$

Where g_1 to g_n are the covariates depending on time including hydro-climatic covariates and "x" represents the location of the site.

Calibrating classifiers independently at each site is not possible since there are too few ONDE observations (32 observations per sites on average between 2012 and 2016). The suggested approach as well as the related assumptions for calibrating f is commonly adopted in regionalization in hydrology (e.g., the index flood method for flood frequency analysis (Dalrymple, 1960)). By transferring information from different sites located in the same hydrologically homogeneous region, the sample size is increased and more robust estimates of the parameters are obtained. This implies that all the ONDE sites share the same classifier with the same set of parameters and that the drivers of flow

intermittence are the same. Nevertheless, drying dynamics differ from site to site due to local factors. Thus a calibration at the regional scale is considered to derive the model f_R valid for all ONDE sites o_x located in the same region R:

$$FlowState(d, o_x) = f_R(g_1(d, o_x), \dots, g_n(d, o_x), e_1(o_x), \dots, e_m(o_x)) \quad (2)$$

Where e_1 to e_m are covariates that characterize the location of the site o_x.

A performance analysis, focusing on four contrasted regions in France, is carried out over the 6-year period 2012-2017 to assess their ability to simulate the daily drying dynamics at ONDE sites and to compare the accuracy of classifiers. In a second step, the influence of covariates in each classifier was examined and main environmental drivers of flow intermittence are identified.

Type	Covariate	Description	Frequency	Spatial aggregation
Climate	R0	Rainfall accumulation over the day of observation (dayObs)	Day	Aggregating values for catchment site
	R1	Rainfall accumulation over the day before dayObs	Day	Aggregating values for catchment site
	R10	Rainfall accumulation over the 10 days before dayObs	Day	Aggregating values for catchment site
	R20	Rainfall accumulation over the 20 days before dayObs	Day	Aggregating values for catchment site
	R30	Rainfall accumulation over the 30 days before dayObs	Day	Aggregating values for catchment site
	T0	Air temperature over the day of observation (dayObs)	Day	Aggregating values for catchment site
	T1	Air temperature over the day before dayObs	Day	Aggregating values for catchment site
	T10	Air temperature average over the 10 days before dayObs	Day	Aggregating values for catchment site
	T20	Air temperature average over the 20 days before dayObs	Day	Aggregating values for catchment site
	T30	Air temperature average over the 30 days before dayObs	Day	Aggregating values for catchment site
	PET0	Evapotranspiration over the day of observation (dayObs)	Day	Aggregating values for catchment site
	PET1	Evapotranspiration over the day before dayObs	Day	Aggregating values for catchment site
	PET10	Evapotranspiration accumulation over the 10 days before dayObs	Day	Aggregating values for catchment site
	PET20	Evapotranspiration accumulation over the 20 days before dayObs	Day	Aggregating values for catchment site
	PET30	Evapotranspiration accumulation over the 30 days before dayObs	Day	Aggregating values for catchment site
	AI	Aridity index	Annual	Aggregating values for catchment site
	WR	Winter rainfall accumulation (December to March)	Annual	Aggregating values for catchment site
Hydrology	FQ0	Mean non-exceedance frequency of discharge at dayObs	Day	Based on HER-HR combination
	FQ5	Mean non-exceedance frequency of discharge average over the 5 days before dayObs	Day	Based on HER-HR combination
	FQ10	Mean non-exceedance frequency of discharge average over the 10 days before dayObs	Day	Based on HER-HR combination
Groundwater level	FGw0	Mean non-exceedance frequency of groundwater level at dayObs	Day	Based on HER
	FGw5	Mean non-exceedance frequency of groundwater level average over the 5 days before dayObs	Day	Based on HER
	FGw10	Mean non-exceedance frequency of groundwater level average over the 10 days before dayObs	Day	Based on HER
ONDE sites characteristics	Alti	Mean altitude of the catchment (m)	Constant	Based on catchment
	Area	Drainage area (km²).	Constant	Based on catchment
	Slope	Mean hill slope of the catchment (m.km^{-1}).	Constant	Based on catchment
	MPD	Monthly proportion of days with dry states observed between 2012 and 2016 (%)	Month	Based on ONDE data

Table 1. *List of covariates*

Benchmark classifier (BC)

BC is a simple classifier without any covariates which predicts, at a given site, the flow state which is the most frequently observed historically for the month considered. When there is a tie, “Drying” is predicted. Cross-validation is implemented as follows. To predict the daily flow state of a ONDE site “o” at the month “M” of the year “Y”, we select all the flow states observed at this site “o” at months “M” during the reference period of observation excluding the year “Y” (2012-2016\Y).

LASSO classifier

The LASSO (Least Absolute Shrinkage and Selection Operator) (Tibshirani, 1996) classifier estimates the drying state probability as a linear function of the covariates transformed with a sigmoid function to constrain the range to [0,1]. LASSO includes a regularization mechanism that may lead to a sparse model in which the coefficients of less relevant covariates are driven to zero (Bishop, 2006). The amount of regularization is determined through cross-validation (R package "elasticnet", Zou & Hastie, 2018). To classify into either "Flowing" or "Drying" states, an optimal threshold is set after a second cross-validation procedure using the amount of regularization determined previously and leading to the best F-score (see section 4.4; Equation 9). The relevance of each covariate is inspected directly through the magnitude of the associated coefficient estimated by the LASSO classifier. The LASSO method was recently considered in a hydrological application with other linear and nonlinear regression techniques to predict synthetic design hydrographs for ungauged catchments (Brunner et al., 2018).

ANN classifier

ANNs - feed-forward neural networks with one hidden layer - estimate the drying state probability as a potentially non-linear function of covariates. This is a non-parametric approach that combines the contribution of the neurons in the hidden layer to build an approximation. The number of neurons is related to the number of coefficients and hence the complexity of the classifier. As for LASSO, a sigmoid function is applied to constrain the range of the ANN output to [0,1] (see the implementation in the R package "nnet", Venables & Ripley, 2002). We include a direct connection between inputs and outputs so that the case with zero hidden units corresponds to a linear relationship. Weight decay regularization, also known as ridge regression, is considered to control overfitting by decreasing less relevant coefficients. Both the number of hidden units and the amount of weight decay are selected with a first cross-validation procedure (Bishop, 2006). As for the LASSO classifier, an optimal threshold is set with a second cross-validation procedure using the number of hidden units and the amount of weight decay determined previously and leading to the best F-score. The LASSO classifier can be thought of as a particular case of the ANN with no hidden units although the regularization mechanisms are different.

To quantify the relevance of the different covariates, the connection weight approach (Olden & Jackson, 2002; Olden, Joy, & Death, 2004) is employed:

$$W_V = \sum_{h=1}^{nhu} A_{V,h} B_h \quad (3)$$

Where W_V (-) is the relevance of covariate V, $A_{V,h}$ (-) are the ANN coefficients connecting hidden unit h to covariate V, B_h (-) are the ANN coefficients connecting hidden unit *h* to the output, and nhu is the number of hidden units. Artificial neural network (ANN) have been widely used as black-box tools for modeling the rainfall–runoff transform (see (ASCE 2000a, 2000b) for a review and (Abdollahi, Raeisi, Khalilianpour, Ahmadi, & Kisi, 2017) for a recent application to an intermittent river).

RF classifier

A random forest combines decision trees obtained by resampling the calibration set (Breiman, 2001). Each tree is a structure made of binary nodes associated to binary rules of the type $V \leq s$ versus $V > s$ where V is one of the covariates and s is a bound. When reaching a terminal node, a majority vote is taken among the observations belonging to the node. A single decision tree tends to yield non-robust estimation (very dependent on the selected calibration set) and the process of combining the trees in a forest circumvents this issue. We use the implementation in the R package "randomForest" (Liaw and Wiener, 2002). The covariates relevance is given directly by the "randomForest" package which determines how much the mean square errors (MSE) in prediction increases when that covariate is randomly permuted within the tree. Random Forest models have been recently used to predict the spatial distribution of intermittent and perennial rivers at the basin scale (González-Ferreras & Barquín, 2017) and at the national scale (Snelder et al., 2013).

3. Study area and data available

Study area

France is located in a temperate zone characterized by a variety of climates due to the influences of the Atlantic Ocean, the Mediterranean Sea and mountain areas. The study area is composed of four Hydro-EcoRegions (HERs) located in continental France (Figure 1). The HERs correspond to a typology based on geology, topography, and climate and accounting for stream size. They have been developed for river management in accordance with the European Water Framework Directive (Wasson, Chandesris, Pella, & Blanc, 2002). The HERs were not specifically developed to discriminate river flow regimes. However, they have demonstrated their relevance as homogeneous regions in regionalization application (e.g., Sauquet & Catalogne, 2011; Cipriani, Toilliez & Sauquet, 2010) and are chosen as the regions over which f_R is calibrated (Equation 2).

Four HERs are selected among the partition of France into 114 HERs based on the presence of several gauging stations monitoring IRES (see section 3.3). They have contrasted characteristics (Table 2) and are representative of most HERs in France except for mountainous regions. HER1 is distinguished by its hard, impermeable and non-carbonated primary rocks, a landform of hills, and an oceanic climate. HER2 is a lowland region with an altitude of less than 200 m. The subsoil is mainly composed of carbonated sedimentary rocks. However, the upper layers of these rocks have varying surface characteristics of permeability inducing differences in the density of the drainage network. HER3 is an entity of accentuated relief, with heterogeneous basements dominated by massive limestones and carbonate rocks, and a humid continental mountain climate. HER4, with its plains and hills, is characterized by a Mediterranean climate with an extended summer drought in comparison with other regions. The geology is very heterogeneous, varying from the alluvial plain to the granite massifs and massive limestone hills.

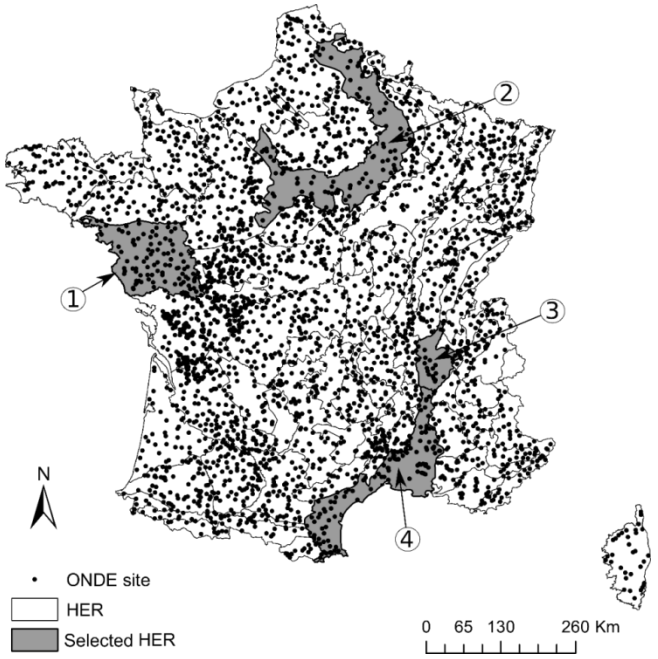

Figure 1. *Location of the 3 300 ONDE sites and partition of France into HERs.*

ONDE dataset: a discrete national flow-state observations network

The ONDE network was set up in 2012 by the French Biodiversity Agency (AFB, formerly ONEMA). Its aim is to constitute a perennial network recording summer low flow levels that can be used to anticipate and manage water crisis during severe drought events (Nowak & Durozoi, 2012).

The ONDE network remains stable over time and distributed throughout France with 3 300 sites regularly inspected (Figure 1). ONDE sites are located on HS with a Strahler order strictly less than 5 and balanced across HER to take the representativeness of the hydrological contexts into account (Nowak & Durozoi, 2012). There are two types of monitoring: an ongoing monitoring and an additional monitoring. The ongoing monitoring provides a reliable baseline of knowledge over time with at least one observation per month for each ONDE site (around the 25th) between May and September. The

additional monitoring has a frequency determined by local stakeholders (maximum weekly observations) in case of severe low-flow events for both drought preparedness and drought mitigation. The average number of ongoing and additional inspections at each ONDE site between 2012 and 2017 reaches 5 and 1.5 per year, respectively over all ONDE sites.

One of the flow states is assigned at each observation among “visible flow”, “no visible flow” and “dried out”. In this work, we pool flow states into two classes: “**Flowing**” when there is visible flow across the channel (“visible flow”) and “**Drying**” when the channel is entirely devoid of surface water (“dried out”) or when there is still water in the river bed but without visible flow (disconnected pools, lentic systems) (“no visible flow”). Beaufort et al. (2018) showed the complementary qualities of the ONDE network, more homogeneously distributed in France and the already existing French river flow monitoring network HYDRO (http://www.hydro.eaufrance.fr).

One covariate, derived from ONDE observations, is calculated to reconstruct the daily drying dynamics at each ONDE site: the Monthly Proportion of observations with “Drying” states (%) observed between 2012 and 2016 (MPD). The ONDE sites were projected on the river network RHT (Theoretical Hydrographic Network; Pella, Lejot, Lamouroux, & Snelder, 2012) and the drainage area (Area), the altitude (Alti) and the stream slope (Slope) were estimated and used as covariates to characterize ONDE sites.

Explanatory discharge dataset

ONDE sites are ungauged but gauging stations located in the same HER could potentially inform about the hydrological state of rivers at a regional scale. Time series of daily discharge were extracted from the French River discharge monitoring network (HYDRO, http://www.hydro.eaufrance.fr/). This network is composed of 1 600 gauging stations distributed across France for which flow data are available between 2011 and 2017. According to the hydrometric services in charge of the selected gauging stations, high quality of measurements is ensured and observed discharges were either not altered or only slightly altered by human actions.

Hydrological variables derived from gauging stations located in the same HER as the ONDE site, are also considered as covariates. To ensure homogeneity, only gauging stations with the same river flow regime as the ONDE site were kept. The river flow regime (HR) is taken from the classification for France suggested by Eric Sauquet, Gottschalk, & Krasovskaia, (2008) and each HER is partitioned into sub-regions defined by the river flow regimes. For the four selected HERs, a total number of three, six, one and eight HER-HR combinations are outlined in HER1, HER2, HER3 and HER4, respectively. The HER1 and HER2 are mainly composed of pluvial river flow regimes and the HER3 and HER4 are composed of a mix of pluvial river flow regimes, transition river flow regimes and Mediterranean river flow regimes. Due to scale effect, discharge time series from different gauging stations cannot be combined directly and a post-processing is required. The first step consists in selecting all gauging stations located in a given HER-HR combination. The total number of gauging stations per HER-HR combination is at least 5. In a second step, the flow duration curve is determined for each selected gauging station and 3 covariates are computed: the average non-exceedance frequency of the observed discharge at gauging stations (i) at the dayObs (FQ0); (ii) over the 5 days before dayObs (FQ5); and (iii) over the 10 days before dayObs (FQ10). The pre-processing methodology is illustrated in the appendix (Figure A1).

Each stream where a HYDRO gauging station is located is defined as IRES or perennial streams. The identification of intermittent gauging stations was carried out with the aim of: (i) selecting the four HERs where model performance is assessed (see section 3.1) and (ii) validating against continuous time series of flow states (see section 4.3). Several definitions of IRES can be found in the literature (Huxter & van Meerveld, 2012; Reynolds, Shafroth, & LeRoy Poff, 2015; Eng et al., 2016). In this study, we consider stations as intermittent when five consecutive days with discharge less than 1 l/s is observed during the observation period.

Explanatory groundwater level dataset

Daily groundwater levels are provided by the ADES database (http://www.ades.eaufrance.fr) at sites involved in groundwater/surface water exchanges (Brugeron, Allier & Klinka, 2012). This dataset is composed by 750 piezometers with daily groundwater level data available from 2011 to 2017 with less than 5% of missing data (continuous or not). The level of alteration of groundwater levels by water withdrawal is unknown because no information is available at this scale.

Groundwater level data are used as covariates. A post-processing similar to the one applied to daily discharge is applied to groundwater levels (Figure A1 in Appendix) except for the first step which consists in selecting all piezometers located in a same HER instead of HER-HR combination. In a second step, in each HER, three covariates are computed: the average non-exceedance frequency of the observed groundwater level (i) at the dayObs (FGw0); (ii) over the 5 days before dayObs (FGw5); and (iii) over the 10 days before dayObs (FGw10).

3.1. Explanatory meteorological dataset

Daily meteorological covariates are taken from the SAFRAN dataset (Quintana-Seguí et al., 2008; Vidal, Martin, Franchistéguy, Baillon, & Soubeyroux, 2010) that has an 8-km resolution grid and is available from August 1st 1958 to July 31st 2017. The SAFRAN dataset provides precipitation and air temperature. The daily reference evapotranspiration is computed with the Penman–Monteith formulation (Allen et al., 1998). Daily catchment-scale data are computed for each gauging station and ONDE site using weighted mean (for temperature) or sum (for precipitation and evapotranspiration) of each contributive cell of the 8 km grid to the catchment surface (Sauquet & Catalogne, 2011).

The daily catchment-scale air temperature (T), rainfall (R) and potential evapotranspiration (PET) data are used as covariates in order to reconstruct the daily drying dynamics at ONDE sites. For each covariate, we consider daily values observed on the current day (R0, PET0, T0) and on the previous day (R1, PET1, T1) along with values accumulated or averaged over 10, 20 or 30 days preceding the current day (Rp, PETp, Tp) with p = 10, 20 or 30.

We derive two additional annual climate descriptors, namely the aridity index (AI) and the winter rainfall accumulation (WR). AI is given by the ratio between the mean annual precipitation and the mean annual PET. The catchment is considered as “hyper-arid” if AI < 0.03, “arid” if 0.03 ≤ AI ≤ 0.2, “semi-arid” if 0.2 ≤ AI ≤ 0.5, “dry sub-humid” if 0.5 ≤ AI ≤ 0.65 and “humid” if AI ≥ 0.65. WR is determined each year as the rainfall accumulation between December of the precedent year and March of the current year (4 months).

HER	1	2	3	4
ONDE site	98	93	25	111
Intermittent ONDE site	79	42	14	79
Gauging station	26	13	4	22
Intermittent gauging station	11	2	1	9
Number of piezometers	15	119	36	130
Number of observations (ONDE)	3906	2223	785	3381
Number of “Drying” states (ONDE)	710 (18.2%)	213 (9.6%)	113 (14.4%)	892 (26.4%)
Mean altitude (m)	67	105	324	132
Area (km²)	17800	27300	5000	17600
Precipitation (mm)	895	765	1137	676
PET (mm)	715	616	711	1051
AI (-)	1.25	1.24	1.60	0.64
Air temperature (°C)	12.2	11.0	11.5	14.5

Table 2. Characteristics of each selected HER to assess and compare the classifiers performance calculated between 2012 and 2016.

4. Performance assessment and comparison

The performance of the classifiers is evaluated on the four selected HERs (Figure 1). The calibration and validation methods are described in the next sections.

Cross-validation over 2012-2016

A cross-validation procedure is carried out for each classifier in each HER. The calibration set is

constituted by selecting randomly 80% of the observations. The test set consists of the remaining 20%. Once the classifiers are trained on the calibration set, the evaluation criteria are calculated (see section 4.4) based on the prediction on the test set. This step is repeated 20 times in order to evaluate the uncertainty associated to the selection of the calibration set.

Extrapolation ability over 2017

In order to assess the extrapolation ability of the classifiers, they were calibrated over the period 2012-2016 and their performance is evaluated over the first three months of 2017 (due to SAFRAN data availability), namely May, June and July. In each HER, all the covariates associated with the ONDE observations between 2012 and 2016 are used to calibrate classifiers. Then, the covariates of the year 2017 are used as input to predict the daily flow states at the ONDE sites. For BC, benchmark values are computed excluding the year 2017.

Spatio-temporal extrapolation ability

In order to evaluate their spatio-temporal extrapolation ability over the period 2012-2016, the classifiers calibrated on the ONDE sites are applied to 65 gauging stations - 38 and 27 located on perennial and intermittent streams, respectively. Based on the continuous observations from the gauging stations, an independent test set of daily flow states is constituted and serves to evaluate the classifiers at the daily time step between May and September. The classifiers remain calibrated against observations available at the ONDE sites located in the same HER and used the covariates (Table 1) computed for 65 gauged basins to predict the flow state. Gauging stations covariates used for prediction are calculated as for the ONDE sites except for the Monthly Proportion of observations with “Drying” states (MPD). MPD is calculated by taking into account the flow observed at the gauging station on the 25th of each month corresponding approximately to the ONDE observation dates. A day in the discharge time series is classified in a “Drying” state if the observed daily flow is less than 1 l.s^{-1}. This way, potential false-positive detection of zero flows associated with measurement resolution constraints and uncertainty in discharge observations are accounted for. For BC, to predict the flow state of a gauging station “i” during the month “M” of the year “Y”, we select the most frequent flow states observed on the 25th at this station “i” on months “M” during the reference period excluding the year “Y” (2012-2016\Y). The flow state predicted is assigned to the 15 days preceding and following the 25th of month “M” and year “Y” considered in order to obtain continuous daily flow states comparable to predictions of the other classifiers.

Evaluation criteria

Several validation criteria are calculated to compare the performance of the classifiers. First, criteria based on a 2x2 contingency table, see Table 3, are used to evaluate the ability of classifiers to accurately predict flow states for a stream at a given day.

Derived from the contingency table, 5 criteria (see Equations 5 to 9), are calculated to assess classifiers performance: the Probability Of Detection (POD) (Best value is 100%), the False Alarm Ratio (FAR) (Best value is 0%), the Precision (Best value is 1), the Recall (Best value is 1) and the F-score (Best value is 1).

$$\mathrm{POD} = \frac{\mathrm{a}}{\mathrm{a+c}} \times 100 \tag{5}$$

$$\mathrm{FAR} = \frac{\mathrm{b}}{\mathrm{a+b}} \times 100 \tag{6}$$

$$Precision = \frac{\mathrm{a}}{\mathrm{a+b}} \tag{7}$$

$$Recall = \frac{\mathrm{a}}{\mathrm{a+c}} \tag{8}$$

$$\mathrm{F-score} = 2 \times \frac{\mathrm{Precision \times Recall}}{\mathrm{Precision+Recall}} \tag{9}$$

In addition, the proportions of observed and predicted days with a “Drying” state - named P_{obs} and P_{pred}, respectively - at gauging station i are compared to measure the spatio-temporal ability (section 4.3):

$$\mathrm{P(i)} = \frac{(\mathrm{N_{dr}})_\mathrm{i}}{(\mathrm{N_{fl}+N_{dr}})_\mathrm{i}} \times 100 \tag{10}$$

with N_{dr}: the number of observed or predicted daily “Drying” states between the beginning of May to the

end of September; N_{fl}: the number of observed or predicted daily "flowing" states between the beginning of May to the end of September. N_{dr} and N_{fl} can be calculated annually or over the period between 2012 and 2016. The bias and the root mean square error are calculated for a performance assessment at the HER scale:

$$\mathrm{Bias(HER)} = \frac{1}{G}\sum_{i=1}^{G}\left(P_{pred}(i) - P_{obs}(i)\right) \quad (11)$$

$$\mathrm{RMSE(HER)} = \sqrt{\frac{1}{G}\sum_{i=1}^{G}\left(P_{pred}(i) - P_{obs}(i)\right)^2} \quad (12)$$

Where "i" is a gauging station located inside a given selected HER and G is the total number of gauging stations located in each HER.

		Observations	
		Drying	Flowing
Predictions	Drying	a	b
	Flowing	c	d

Table 3. *Contingency table: a (b) represents the number of correctly (incorrectly) predicted "Drying" states; c (d) represents the number of incorrectly (correctly) predicted "Flowing" states*

Evaluation of covariate contribution

In this evaluation, the covariates are grouped according to their type defined in Table 1 except for MPD because this covariate is directly related to local observations. The methods for estimating the contribution of covariates to the prediction are different for each classifier (see Sect. 2.2 to 2.4) and the magnitude of the contribution of each covariate cannot be directly compared across classifiers. Cumulative or averaged percentages representing the relative contribution of the covariates in each classifier are used to rank the groups of covariates.

5. Results

Classifier assessment over 4 contrasted HER

Cross-validation results between May and September over the period 2012-2016

The three classifiers ANN, RF and LASSO outperforms BC in all HERs. This can be seen from the POD, FAR and F-scores in Figure 2. The LASSO classifier, although linear, performed only slightly worse than the ANN classifier, its non-linear counterpart (see the POD and FAR scores in Figure 2). Among the two non-linear classifiers, RF achieved the overall best performance in the four HERs (see the three scores in Figure 2).

The performance obtained by the two non-linear classifiers is very close and the best POD is obtained by ANN in all selected HERs (Figure 2a). However, RF minimizes the FAR and obtains a better F-score than ANN on average over the four HERs. Performance of classifiers in extrapolation over 2017

The results of the classifier predictions in extrapolation in 2017 show that BC obtains the best POD which is greater than 60% in the four HERs (Figure 3a). However, the FAR are very high and exceed 50% so BC tends to strongly overestimate "Drying" states in 2017 especially in HER1 and HER3 (Figure 3b).

ANN obtains a POD higher than 50% and a FAR significantly lower than BC whatever the HER. The ANN classifier obtains the best F-score for each selected HER (F-score > 0.5).

The performance of the LASSO and RF are rather moderate. They obtain very low POD lower than 30% on the HER1, HER2 and HER3 but also a very low FAR reaching zero for the HER3. We deduce that these two classifiers tend to underestimate the number of "Drying" states extrapolated in 2017. Their F-score is lower than BC in the HER2 but remains very close to the F-score of ANN in the HER4 which corresponds to the HER where the most "Drying" state is observed.

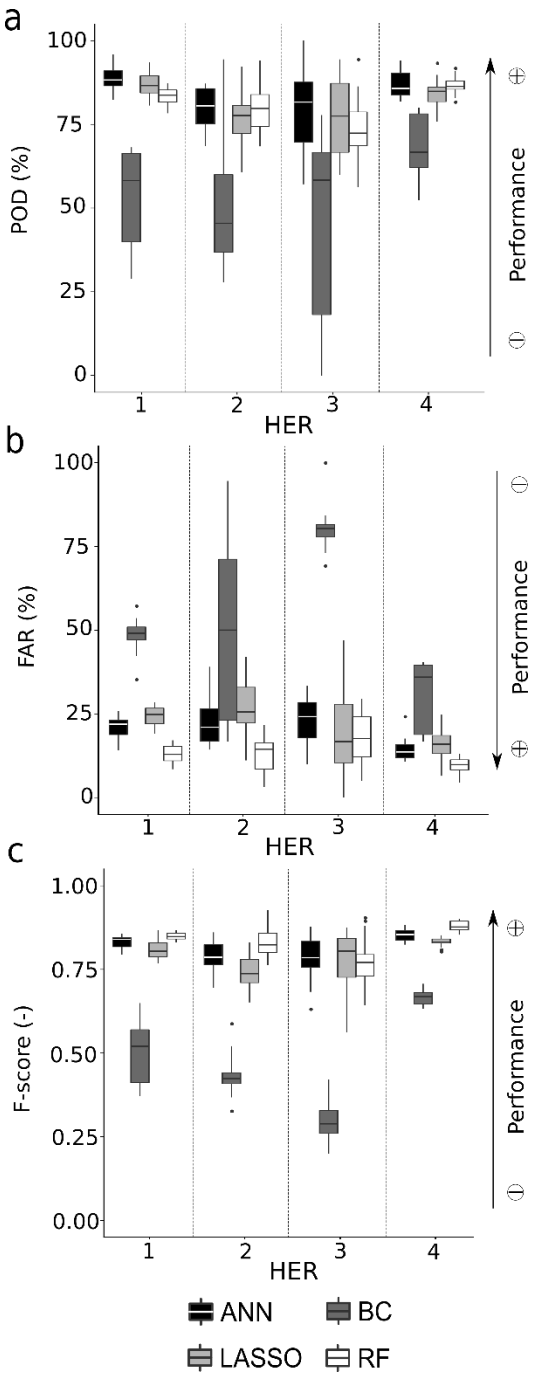

Figure 2. *Evaluation criteria calculated with the cross-validation process over the period 2012-2016 with the four classifiers: (a) POD; (b) FAR; (c) F-score.*

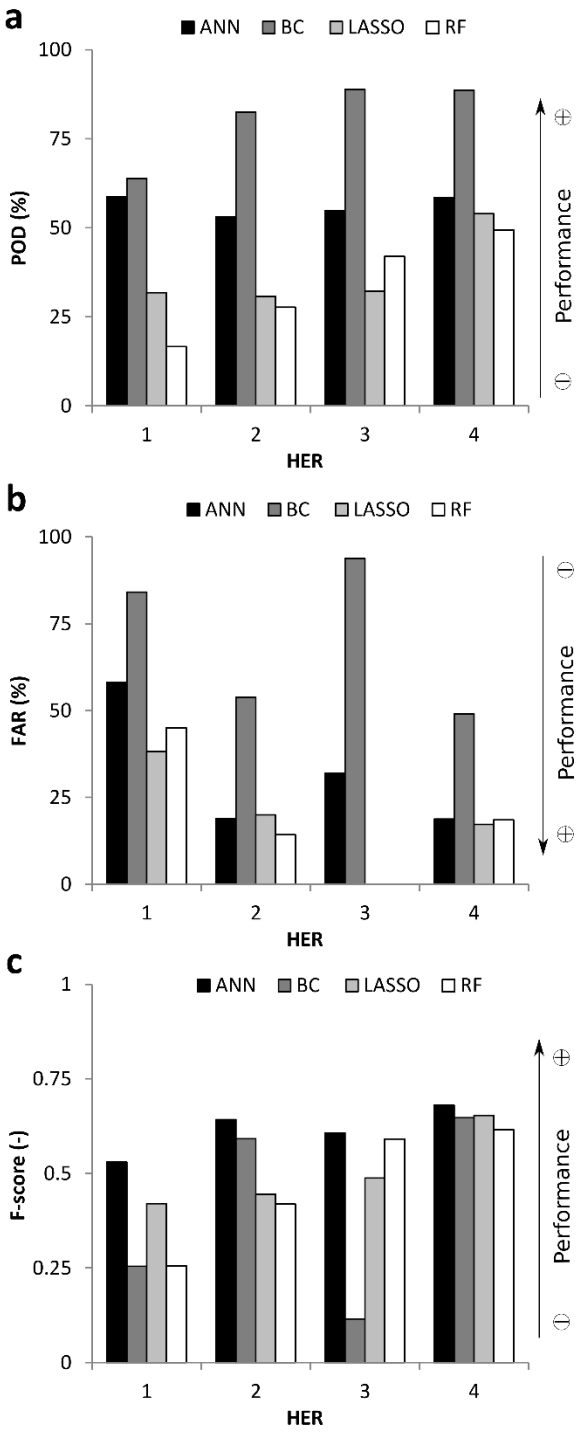

Figure 3. *Evaluation criteria calculated in extrapolation over 2017 with the four classifiers: (a) POD; (b) FAR; (c) F-score.*

Performance of the spatio-temporal extrapolation over the period 2012-2016

For the three classifiers ANN, LASSO and RF, P_{pred} are close to P_{obs} especially for gauging stations whose proportions of "Drying" states are greater than 20% (Figure 4). For stations where the proportion of "Drying" states is lower than 20%, the accuracy of the classifiers is more contrasted.

Overall, ANN achieves the best performance with an average RMSE of 3.3% over the four HERs (Table 4). The RMSE is similar and close to 3% for each HER. ANN tends to slightly overestimate the proportion of observed "Drying" states illustrated by positive biases and a FAR close to 40% on the four HERs (Table 4). RF underestimates the proportions of "Drying" states especially in the HER1, HER3 and HER4 where the biases are below -1.5%. The predictions of LASSO are more contrasted with an overestimation of the "Drying" state proportions in the HER1, an underestimation of the drying proportions in the HER3 and biases close to zero in the HER2 and HER4.

For the 27 gauging stations with at least one observed "Drying" state between 2012 and 2016, the ANN

classifier can detect “Drying” states on 23 gauging stations but failed to detect “Drying” states on 4 of them. These 4 gauging stations are located in the HER 1 and showed a proportion of “Drying” states less than 5%. In comparison RF and LASSO failed to detect “Drying” states for 7 and 9 gauging stations respectively.

On the other hand, ANN tends to predict very short “Drying” states, persisting less than 2 days, on perennial stations leading to a prediction of “Drying” states of less than 1% (Figure 4a). These incorrectly predicted “Drying” states correspond to periods of severe low flows, i.e. when most of the daily flows stay below the 90th quantile of the flow duration curve. Thus, although not strictly speaking in a “drying” state, they are consistent with the ANN classifier predictions.

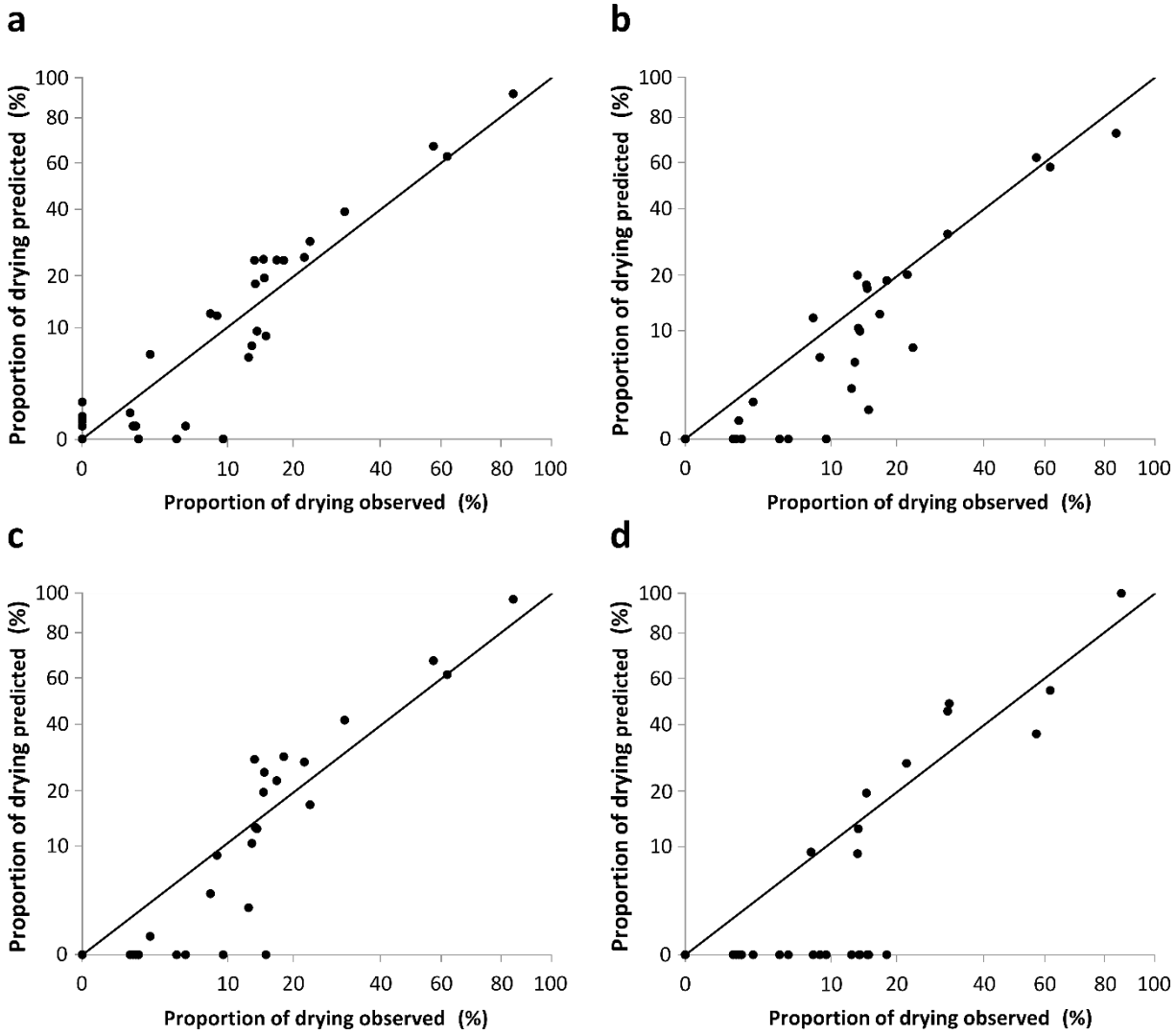

Figure 4. *Predicted and observed proportions of “drying” states over the period 2012-2016 at gauging stations located in the four selected HERs. “Drying” states predictions are obtained respectively with: (a) ANN; (b) RF; (c) LASSO and (d) BC. Each dot is a gauging station and the y-axis displays a square root scale.*

The non-exceedance frequency of discharge observed at four gauging stations, representing each selected HER and having a proportion of “Drying” states less than 20% is compared to the flow states predicted by the four classifiers (Figure 5).

During the warmest year in 2012, ANN, RF and LASSO give consistent results and suggest dry periods relatively close to observations for three of the four HERs (HER1, HER2 and HER3). Conversely, all the classifiers predict “Drying” states in HER4 whereas no event is observed but these predicted “Drying” states remain concomitant with a period of severe low flow beginning in June (most of the daily flows stay below the 80th quantile of the flow duration curve).

On the other hand, during wet years (in 2013 for HER2 and HER3 and in 2014 for HER1 and HER2, Figure 6) ANN, RF and LASSO tend to overestimate “Drying” states but the periods with “Drying” states are very short.

Globally, BC failed to detect “Drying” states in HER1 and falsely detect “Drying” states in HER2 and HER4. “Drying” states incorrectly detected by BC are not always concomitant with a period with low

flows and BC is unable to reproduce the hydrological dynamics of gauging stations.

		HER1	HER2	HER3	HER4
ANN	**Bias**	**0.3**	1.2	1.7	0.6
	RMSE	3.6	**3**	3.2	3.2
	POD	80	**96**	72	79
	FAR	39	41	44	**36**
	F-score	0.71	**0.73**	0.63	0.69
RF	**Bias**	-1.5	**0.5**	-4.3	-1.8
	RMSE	3.9	**1.4**	8.6	4.8
	POD	**73**	60	38	63
	FAR	36	**32**	48	42
	F-score	**0.62**	0.58	0.44	0.61
LASSO	**Bias**	1	**0.1**	-1.6	-0.2
	RMSE	5.9	**1.9**	3.1	4.7
	POD	58	**92**	18	59
	FAR	32	**31**	35	35
	F-score	0.60	**0.79**	0.28	0.62
BC	**Bias**	**-1.6**	-2.7	4.2	-1.8
	RMSE	**4.3**	7.2	8.4	6.3
	POD	**73**	60	38	63
	FAR	36	**32**	48	42
	F-score	**0.62**	0.58	0.44	0.61

Table 4. *Biases, RMSE, POD, FAR and F-score calculated at the gauging stations located in the four HERs over the period 2012-2016.*

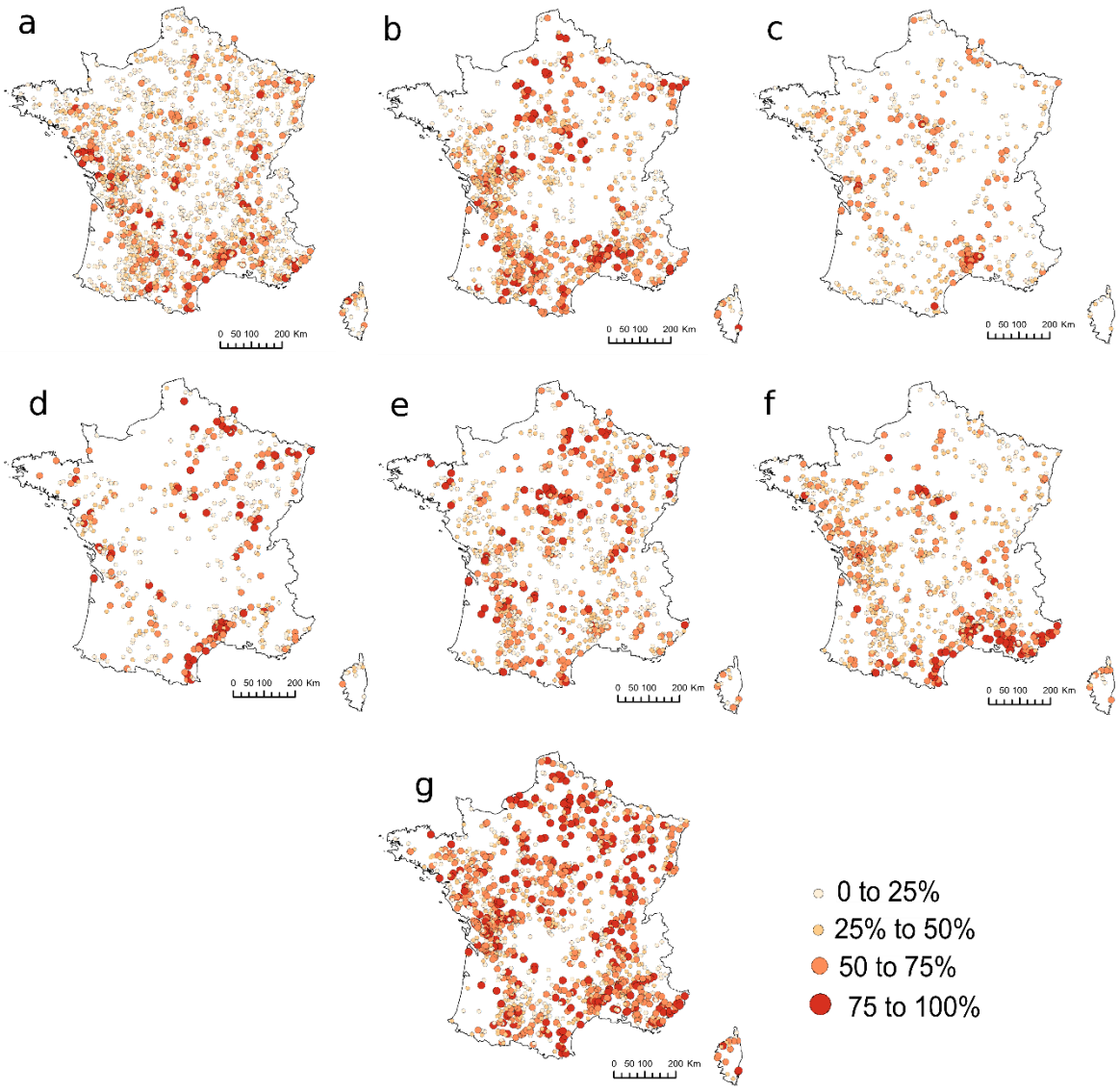

Figure 6. *Distribution of the percentages of drying observed at ONDE sites for the years: (a) 2012-2017, (b) 2012, (c) 2013, (d) 2014, (e) 2015, (f) 2016 and (g) 2017*

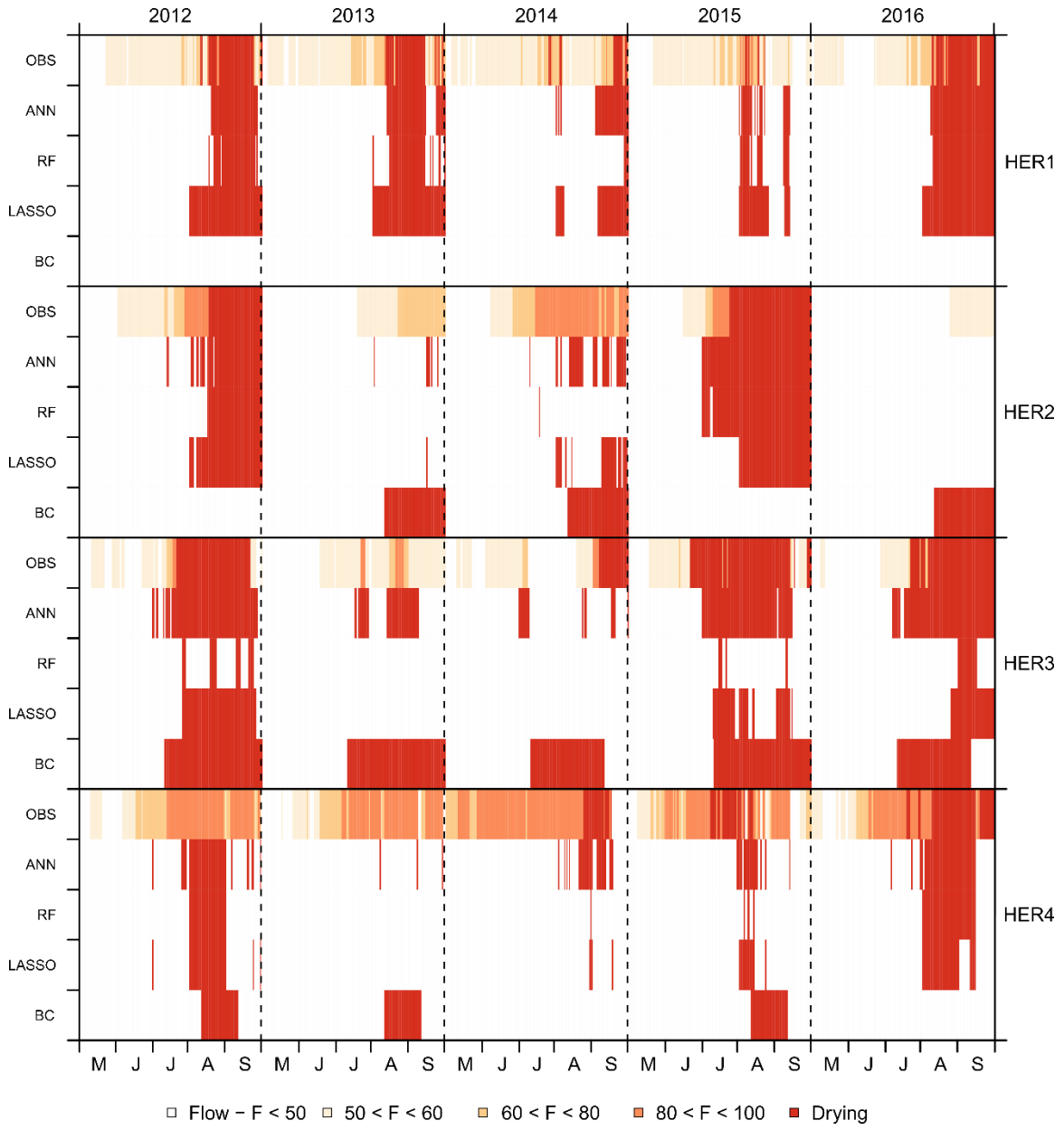

Figure 5. *Observed and predicted flow states for four gauging stations located in the four HERs. Observed daily flows are categorized in four classes based on their associated quantile of the flow duration curve (F).*

RF and LASSO can perform better than ANN in some years, especially in the HER1 and HER3. However, their accuracy is less regular and in some instances, they largely underestimate the duration of “Drying” states during some years, e.g. in 2015 and 2016 for HER3 with RF and in 2014 and 2015 for HER4 with LASSO (Figure 5).

Identification of covariate contributions to “Drying” state predictions

The analysis of the contributions of the covariates is summarized in Table 5. Results are displayed by type of covariate. The preeminence of the type of covariate differs depending on the classifier.

For the ANN classifier, climatic covariates are identified as the main drivers in cumulative value for the prediction of daily “Drying” states. The percentage of the contributions of climatic covariates reaches as much as 67.5% in the HER3. The second most relevant covariates for predicting “Drying” states are related to river flow for HER1 and HER3 or to groundwater level for HER2 and HER4. The MPD is the third most significant covariate. However, it is worthy to note that there is a balance between the relative weight of MPD and the climatic covariates: MPD has a high value while climatic covariates are found less important, and conversely. Despite a large number of climatic covariates (17, Table 1), ANN uses all of them but assigns them less weight than MPD.

For the LASSO classifier, the climatic covariates and the MPD seem to be the most relevant in

cumulative values for predicting “Drying” states. In HER1, hydrology is the third most important driver and small predictive power is given to covariates describing groundwater whereas in HER4, the results bring forward groundwater instead of river hydrology. In HER2 and HER3, groundwater and hydrology are less differentiated with covariates importance above 10%. The preeminence of hydrology against groundwater level covariates is not linked to their respective sites number located in each HER (Table 2).

In the RF classifier, the most important covariate, in cumulated or averaged value, is MPD which obtains a percentage higher than 40% for the four HERs. In HER2, HER and HER4, climate is the second main driver followed by hydrology and groundwater. The importance of hydrological covariates is, however, more important in terms of averaged values than climate covariates in all HERs.

The ONDE site characteristics, constant in time at a given site, have a minor importance for predicting daily “Drying” state for the three classifiers.

	HER	Climate	Hydrology	Groundwater level	ONDE sites characteristics	MPD
ANN	1	**38.5** (2.3)	22.4 (7.5)	13.9 (4.6)	6.5 (2.2)	18.7 **(18.7)**
	2	**66.4** (3.9)	5.5 (1.8)	14.0 (4.7)	6.7 (2.2)	7.4 **(7.4)**
	3	**67.5** (4.2)	10.8 (3.6)	6.1 (2.0)	5.7 (1.9)	9.9 **(9.9)**
	4	**49.8** (3.1)	8.7 (2.9)	25.6 (8.5)	1.6 (0.5)	14.3 **(14.3)**
LASSO	1	**37.6** (9.4)	24.7 (8.2)	0.1 (0.0)	0.1 (0.0)	37.5 **(37.5)**
	2	22.4 (2.3)	11.1 (3.7)	18.2 (6.1)	1.8 (0.6)	**46.4 (46.4)**
	3	15.5 (4.2)	16.8 (5.6)	22.2 (7.4)	0.1 (0.0)	**45.5 (45.5)**
	4	**46.2** (2.6)	1.8 (0.6)	12.7 (4.2)	0.0 (0.0)	39.3 **(39.3)**
RF	1	18.0 (1.4)	20.2 (6.7)	4.1 (1.4)	6.4 (2.1)	**51.3 (51.3)**
	2	37.9 (1.4)	7.7 (2.6)	6.8 (2.3)	6.2 (2.1)	**41.3 (41.3)**
	3	22.4 (1.3)	15.3 (5.1)	11.8 (3.9)	7.5 (2.5)	**42.9 (42.9)**
	4	27.5 (1.8)	11.2 (3.7)	6.6 (2.2)	5.9 (2.0)	**48.8 (48.8)**

Table 5. *Covariates importance (%) determined for each classifier and for each selected HER aggregated as a function of their type defined in Table 1. The first value is the cumulative importance of each covariate in a given type and the value in brackets represents the average importance of covariates.*

6. Discussion

Global comparison of the classifiers

This first conclusion is that the covariates bring valuable information in “Drying” state predictions as can be deduced from the fact that the three classifiers, ANN, LASSO and RF, perform better than BC which does not use any covariates. The cross-validation procedure between 2012 and 2016 shows similar performance between the classifiers and suggests that the non-linearity taken into account by both ANN and RF is one possible cause of improved POD and FAR scores in comparison with LASSO (Figure 2). The performance of classifiers assessed in extrapolation over the period May-July 2017 (F-score ~ 0.5) is lower than their performance obtained in cross-validation (F-score > 0.75). It can be partly explained by the particularity of the year 2017 (Figure 6) when an early drought beginning in May is observed over a large part of France. Between 2012 and 2016, the south-east of France is the only region that was affected by droughts and dryings in spring while dryings started from July in the other regions. This unusual situation was never encountered in the calibration dataset and the estimates of flow states are less accurate except in HER4 where the F-score is higher than 0.6 for the four classifiers. Nevertheless, there is a clear gain in performance with the ANN classifier in comparison to RF and LASSO. This added value is even more important when classifiers are tested against

continuous time series of daily discharges. The ANN classifier seems to better predict the year-to-year variability (dry year vs wet year) at a given station. The conclusions of this comparison are drawn only on analyses based on the 2012-2017 observation period (Figure 6). The ONDE network is still functional and we could expect that the additional flow states observations in contrasted years would contribute to improve the calibration of classifiers and this could lead to improved performances in extrapolation ability.

The main difficulty encountered by the three classifiers comes from the complexity of predicting rare events. In cross-validation over the period 2012-2016 and in extrapolation in year 2017, the best F-scores among the three classifiers are obtained in HER4 where the “Drying” state frequency is the most important (Table 2). ANN is the classifier that achieves the best performance for weakly intermittent HS. Classifiers tend to underestimate “Drying” states with an observed frequency smaller than 20% (Figure 4). It may occur that no “Drying” state is observed due to the rarity of zero-flow events and the value of MPD is zero whatever the month of the year. The high importance of this covariate in classifiers leads to an underestimation of predicted “Drying” states or to consider the HS as perennial. This underlines the importance of taking into account a calibration dataset composed of years with contrasted climate thus allowing a better representation of the extreme events. Future observations of the ONDE network will make it possible to sample more contrasted situations and to better identify sites impacted by flow intermittence leading to an updated ranking of the three classifiers.

Drivers of flow intermittence

MPD is considered as very important for the three classifiers. This covariate reflects the level of flow intermittence of each ONDE site and the classifiers aims at reproducing the variability around this average value.

ONDE site characteristics are not identified as drivers by the three classifiers. This is surprising because several studies have shown that the catchment area (Area) is a very important explanatory variable in hydrology and specifically for classifying streams as temporary or perennial (Snelder et al., 2013; González-Ferreras & Barquín, 2017). The catchment altitude (Alti) and streams slope (Slope) were also identified as relevant variable to detect intermittent streams (Snelder et al., 2013; D’Ambrosio et al., 2017). One possible reason is that the HERs are homogeneous. We may expect also that other covariates related for example, to exchanges between open channels and groundwater systems operating at small scale, riverbed permeability, aquifer structure… would be relevant to capture the variability between sites. Datry et al. (2016) showed that river network could be very fragmented at the local scale (< 100 meters) and two nearby sites can experience a very different drying dynamics albeit sharing a similar climate. Despite our effort to select unaltered ONDE sites, unexpected water withdrawal or release may govern the drying dynamics.

Classifiers use climatic, groundwater and hydrological information to capture and predict the daily variability of “Drying” state. Both RF and LASSO seem to put too much weight on MPD which leads them to underestimate “Drying” states when a new situation is encountered in extrapolation as in 2017. ANN gives more importance to climatic covariates in comparison to RF and LASSO. Some studies underlined the importance of meteorological features in drying variability. Abdollahi et al., (2017) shown the importance to combine precipitation and flow patterns for predicting daily mean streamflow of an IRES. De Girolamo et al., (2017) identified that errors in meteorological inputs are responsible of the limited performance of the model in predicting stream flow and hydrological indicators in an IRES. The regional climate patterns (Snelder et al., 2013) and the minimum monthly precipitation values in August (González- Ferreras & Barquín, 2017) were relevant variables to both detect and map IRES at the regional scale. Furthermore, the non-linear structure of ANN might enable it to better exploit the day-to-day variability of climate, groundwater and hydrological data in order to reproduce drying dynamics. Both RF and LASSO may not be flexible enough to take benefit from covariates other than MPD. ANN makes it possible to predict “Drying” states on sites where no “Drying” state was observed when the drought conditions become severe and seems to be more suitable in extrapolation. LASSO and RF seem to require a longer observation period of the flow states provided by the ONDE observations in order to more accurately estimate the MPD and thus hope to improve the drying predictions in extrapolation.

7. Conclusion

The main scientific contribution concerns the exploitation of ONDE observations, discontinuous in time and space, to improve our knowledge about the headwater catchment functioning. Despite the low

frequency of the observations, they provide essential information to be combined with statistical methods adapted to discontinuous data in time for reconstructing the dynamics of the local “Drying” states at a daily resolution.

The main conclusion of this study is that statistical classifiers predicting at-site drying states from covariates are better than using the dominant observed flow states. In this context, taking into account of the non-linearity in classification model is of importance to ensure the best predictive performance. The non-linearity of the ANN classifier gives it a greater degree of freedom and, according to our results, made it possible to improve flow state predictions, especially in extrapolation. Moreover, our results underline the importance to consider calibration datasets that span a full range of expected hydrological conditions leading to a better representation of extreme events. Another major conclusion concerns the importance of the predictive information provided by the Monthly Proportion of observations with “Drying” states (MPD). This covariate reflects the level of flow intermittence of each ONDE site and the classifiers aim at reproducing the variability around this average value. Meteorological variables as covariates appear as important drivers of the flow intermittence while the site characteristics have unexpectedly low relevance.

One of the perspectives to this work would be to explore how this non-linearity is used to predict daily drying dynamics. Studying the statistical decision boundary of ANN especially for weakly intermittent stations constitute a first step toward this goal. Another perspective concerns the determination of additional covariates more locally defined that could be tested to analyze their added value in local drying predictions. All these approaches will have to be studied in contrasted climatic and environmental situations in order to accurately assess the performance of each classifier.

Thanks to this first application, the next step will be to extend this approach in all HERs in France. It is therefore conceivable to use the results of our models, i.e. the reconstructed drying dynamics, in the context of ecological studies that focus on the distribution and persistence of aquatic communities in response to flow alterations. In addition, this work could be relevant for watershed management. The knowledge of the duration and the variability of the drying phase is very important for assessing the ecological status of IRES (Mazor, Stein, Ode, & Schiff, 2014; Prat et al., 2014). It also could help to identify which metrics are the most relevant for detecting human impacts (Datry, Bonada, & Boulton, 2017). Many IRES occur in the headwater of perennial systems and their conservation is widely recognized especially for the supply of good quality water (Lowe & Likens, 2005). The reconstruction of local drying dynamics could guide stakeholders to improve the ecological restoration and protection of IRES.

8. Acknowledgment

The authors wish to thank the two reviewers for their valuable comments, suggestions and positive feedback on the manuscript. The research project was partly funded by the French Agency for Biodiversity (AFB, formerly ONEMA). This study is based upon works from COST Action CA15113 (SMIRES, Science and Management of Intermittent Rivers and Ephemeral Streams, www.smires.eu), supported by COST (European Cooperation in Science and Technology).

9. References

Abdollahi, S., Raeisi, J., Khalilianpour, M., Ahmadi, F., & Kisi, O. (2017). Daily Mean Streamflow Prediction in Perennial and Non-Perennial Rivers Using Four Data Driven Techniques. *Water Resources Management*, *31*(15), 4855‑4874. https://doi.org/10.1007/s11269-017-1782-7

Acuña, V., Datry, T., Marshall, J., Barceló, D., Dahm, C. N., Ginebreda, A., … Palmer, M. A. (2014). Why should we care about temporary waterways? *Science*, *343*(6175), 1080–1081.

Acuña, V., Hunter, M., & Ruhí, A. (2017). Managing temporary streams and rivers as unique rather than second-class ecosystems. *Biological Conservation*, *211*, 12‑19. https://doi.org/10.1016/j.biocon.2016.12.025

Allen, R. G., Pereira, L. S., Raes, D., & Smith, M. (1998) Crop evapotranspiration-Guidelines for computing crop water requirements. *FAO Irrigation and drainage paper*, (56). Fao, Rome, 300(9), D05109.

ASCE. (2000a). Artificial neural networks in hydrology – I: preliminary concepts, *Journal of Hydrologic Engineering*, 5(2), 115–123.

ASCE. (2000b). Artificial neural networks in hydrology – II: hydrologic applications, *Journal of*

Hydrologic Engineering, 5(2), 124–137.

Beaufort, A., Lamouroux, N., Pella, H., Datry, T., & Sauquet, E. (2018). Extrapolating regional probability of drying of headwater streams using discrete observations and gauging networks. *Hydrology and Earth System Sciences*, *22*(5), 3033‑3051. https://doi.org/10.5194/hess-22-3033-2018

Bishop, C. M. (2006). *Pattern recognition and machine learning*, page 229. Springer-Verlag New York.

Boulton, A. J. (2014). Conservation of ephemeral streams and their ecosystem services: what are we missing?: Editorial. *Aquatic Conservation: Marine and Freshwater Ecosystems*, *24*(6), 733‑738. https://doi.org/10.1002/aqc.2537

Breiman, L. (2001). Random forests. *Machine learning*, *45*(1), 5–32.

Brugeron, A., Allier, D., & Klinka, T. (2012). Approche exploratoire des liens entre référentiels hydrogéologique et hydrographique: Premières identifications des piézomètres potentiellement représentatifs d'une relation nappe/rivière et contribution à leur valorisation, *Rapport final BRGM/RP-61047-FR*, 241 pp.

Brunner, M. I., Furrer, R., Sikorska, A. E., Viviroli, D., Seibert, J., & Favre, A.-C. (2018). Synthetic design hydrographs for ungauged catchments: a comparison of regionalization methods. *Stochastic Environmental Research and Risk Assessment*, *32*(7), 1993‑2023. https://doi.org/10.1007/s00477-018-1523-3

Bunn, S. E., Thoms, M. C., Hamilton, S. K., & Capon, S. J. (2006). Flow variability in dryland rivers: boom, bust and the bits in between. *River Research and Applications*, *22*(2), 179‑186. https://doi.org/10.1002/rra.904

Buytaert, W., Zulkafli, Z., Grainger, S., Acosta, L., Alemie, T. C., Bastiaensen, J., … Zhumanova, M. (2014). Citizen science in hydrology and water resources: opportunities for knowledge generation, ecosystem service management, and sustainable development. *Frontiers in Earth Science*, *2*. https://doi.org/10.3389/feart.2014.00026

D'Ambrosio, E., De Girolamo, A. M., Barca, E., Ielpo, P., & Rulli, M. C. (2017). Characterising the hydrological regime of an ungauged temporary river system: a case study. *Environmental Science and Pollution Research*, *24* (16): 13950–13966 DOI: 10.1007/s11356-016-7169-0

Dalrymple, T. (1960). Flood frequency analysis, *U.S. Geol. Surv. Water Supply Pap*., 1543-A.

Datry, T., Larned, S. T., & Tockner, K. (2014). Intermittent Rivers: A Challenge for Freshwater Ecology. *BioScience*, *64*(3), 229‑235. https://doi.org/10.1093/biosci/bit027

Datry, T., Bonada, N., & Boulton, A. J. (2017). Chapter 1 - General Introduction. In T. Datry, N. Bonada, & A. Boulton (Éd.), Intermittent Rivers and Ephemeral Streams (p. 1‑20). Academic Press. https://doi.org/10.1016/B978-0-12-803835-2.00001-2

Datry, T., Boulton, A. J., Bonada, N., Fritz, K., Leigh, C., Sauquet, E., … Dahm, C. N. (2018). Flow intermittence and ecosystem services in rivers of the Anthropocene. *Journal of Applied Ecology*, *55*(1), 353‑364. https://doi.org/10.1111/1365-2664.12941

Datry, T., Fritz, K., & Leigh, C. (2016). Challenges, developments and perspectives in intermittent river ecology. *Freshwater Biology*, *61*(8), 1171‑1180. https://doi.org/10.1111/fwb.12789

Datry, T., Pella, H., Leigh, C., Bonada, N., & Hugueny, B. (2016). A landscape approach to advance intermittent river ecology. *Freshwater Biology*, *61*(8), 1200‑1213. https://doi.org/10.1111/fwb.12645

De Girolamo, A. M., Lo Porto, A., Pappagallo, G., & Gallart, F. (2015). Assessing flow regime alterations in a temporary river – the River Celone case study. *Journal of Hydrology and Hydromechanics*, *63*(3). https://doi.org/10.1515/johh-2015-0027

De Girolamo, A. M., Barca, E., Pappagallo, G., & Lo Porto, A. (2017). Simulating ecologically relevant hydrological indicators in a temporary river system. *Agricultural Water Management 180*: 194–204 DOI: 10.1016/j.agwat.2016.05.034

Eng, K., Wolock, D. M., & Dettinger, M. D. (2016). Sensitivity of Intermittent Streams to Climate Variations in the USA: Sensitivity of Intermittent Streams. *River Research and Applications*, *32*(5), 885‑895. https://doi.org/10.1002/rra.2939

Finn, D. S., Bonada, N., Mùrria, C., & Hughes, J. M. (2011). Small but mighty: headwaters are vital to stream network biodiversity at two levels of organization. *Journal of the North American Benthological Society*, *30*(4), 963‑980. https://doi.org/10.1899/11-012.1

Fritz, K. M., Hagenbuch, E., D'Amico, E., Reif, M., Wigington, P. J., Leibowitz, S. G., … Nadeau, T.-L. (2013). Comparing the Extent and Permanence of Headwater Streams From Two Field Surveys to Values From Hydrographic Databases and Maps. *JAWRA Journal of the American Water Resources Association*, *49*(4), 867‐882. https://doi.org/10.1111/jawr.12040

González-Ferreras, A. M., & Barquín, J. (2017). Mapping the temporary and perennial character of whole river networks: MAPPING FLOW PERMANENCE IN RIVER NETWORK. *Water Resources Research*. https://doi.org/10.1002/2017WR020390

Huxter, E. H. H., & (Ilja) van Meerveld, H. J. (2012). Intermittent and Perennial Streamflow Regime Characteristics in the Okanagan. *Canadian Water Resources Journal / Revue canadienne des ressources hydriques*, *37*(4), 391‐414. https://doi.org/10.4296/cwrj2012-910

Kennard, M. J., Pusey, B. J., Olden, J. D., Mackay, S. J., Stein, J. L., & Marsh, N. (2010). Classification of natural flow regimes in Australia to support environmental flow management: Classification of natural flow regimes in Australia. *Freshwater Biology*, *55*(1), 171‐193. https://doi.org/10.1111/j.1365-2427.2009.02307.x

Larned, S. T., Datry, T., Arscott, D. B., & Tockner, K. (2010). Emerging concepts in temporary-river ecology. *Freshwater Biology*, *55*(4), 717‐738. https://doi.org/10.1111/j.1365-2427.2009.02322.x

Leigh, C., Boulton, A. J., Courtwright, J. L., Fritz, K., May, C. L., Walker, R. H., & Datry, T. (2016). Ecological research and management of intermittent rivers: an historical review and future directions. *Freshwater Biology*, *61*(8), 1181‐1199. https://doi.org/10.1111/fwb.12646

Leigh, C., & Datry, T. (2017). Drying as a primary hydrological determinant of biodiversity in river systems: a broad-scale analysis. *Ecography*, *40*(4), 487‐499. https://doi.org/10.1111/ecog.02230

Leopold, L. B., Wolman, M. G., and Miller, J. P. (1964). *Fluvial Processes in Geomorphology*, Dover Publications, New York, USA.

Liaw, A., & Wiener, M. (2002). Classification and Regression by randomForest. R News 2(3), 18-22.

Lowe, W. H., & Likens, G. E. (2005). Moving headwater streams to the head of the class. *BioScience*, *55*(3), 196–197.

Mazor, R. D., Stein, E. D., Ode, P. R., & Schiff, K. (2014). Integrating intermittent streams into watershed assessments: applicability of an index of biotic integrity. Freshwater Science, 33(2), 459‐474. https://doi.org/10.1086/675683

Meyer, J. L., Strayer, D. L., Wallace, J. B., Eggert, S. L., Helfman, G. S., & Leonard, N. E. (2007). The Contribution of Headwater Streams to Biodiversity in River Networks1: The Contribution of Headwater Streams to Biodiversity in River Networks. *JAWRA Journal of the American Water Resources Association*, *43*(1), 86‐103. https://doi.org/10.1111/j.1752-1688.2007.00008.x

Nadeau, T.-L., & Rains, M. C. (2007). Hydrological Connectivity Between Headwater Streams and Downstream Waters: How Science Can Inform Policy1: Hydrological Connectivity Between Headwater Streams and Downstream Waters: How Science Can Inform Policy. *JAWRA Journal of the American Water Resources Association*, *43*(1), 118‐133. https://doi.org/10.1111/j.1752-1688.2007.00010.x

Nowak, C., & Durozoi, B. (2012). Observatoire National Des Etiages, *Note technique*, ONEMA.

Olden, J. D., & Jackson, D. A. (2002). Illuminating the "black box": a randomization approach for understanding variable contributions in artificial neural networks. *Ecological modelling*, *154*(1‐2), 135–150.

Olden, J. D., Joy, M. K., & Death, R. G. (2004). An accurate comparison of methods for quantifying variable importance in artificial neural networks using simulated data. *Ecological Modelling*, *178*(3‐4), 389‐397. https://doi.org/10.1016/j.ecolmodel.2004.03.013

Pella, H., Lejot, J., Lamouroux, N., & Snelder, T. (2012). Le réseau hydrographique théorique (RHT) français et ses attributs environnementaux. *Géomorphologie: relief, processus, environnement*, *18*(3), 317–336.

Prat, N., Gallart, F., Von Schiller, D., Polesello, S., García-Roger, E. M., Latron, J., … Froebrich, J. (2014). THE MIRAGE TOOLBOX: AN INTEGRATED ASSESSMENT TOOL FOR TEMPORARY STREAMS: MIRAGE TOOLBOX. River Research and Applications, 30(10), 1318‐1334. https://doi.org/10.1002/rra.2757

Quintana-Seguí, P., Le Moigne, P., Durand, Y., Martin, E., Habets, F., Baillon, M., … Morel, S. (2008). Analysis of Near-Surface Atmospheric Variables: Validation of the SAFRAN Analysis over France.

Journal of Applied Meteorology and Climatology, *47*(1), 92‑107. https://doi.org/10.1175/2007JAMC1636.1

Reynolds, L. V., Shafroth, P. B., & LeRoy Poff, N. (2015). Modeled intermittency risk for small streams in the Upper Colorado River Basin under climate change. *Journal of Hydrology*, *523*, 768‑780. https://doi.org/10.1016/j.jhydrol.2015.02.025

Sarremejane, R., Cañedo-Argüelles, M., Prat, N., Mykrä, H., Muotka, T., & Bonada, N. (2017). Do metacommunities vary through time? Intermittent rivers as model systems. *Journal of Biogeography*, *44*(12), 2752‑2763. https://doi.org/10.1111/jbi.13077

Sauquet, E., & Catalogne, C. (2011). Comparison of catchment grouping methods for flow duration curve estimation at ungauged sites in France. *Hydrology and Earth System Sciences*, *15*(8), 2421‑2435. https://doi.org/10.5194/hess-15-2421-2011

Sauquet, Eric, Gottschalk, L., & Krasovskaia, I. (2008). Estimating mean monthly runoff at ungauged locations: an application to France. *Hydrology Research*, *39*(5–6), 403. https://doi.org/10.2166/nh.2008.331

Snelder, T. H., Datry, T., Lamouroux, N., Larned, S. T., Sauquet, E., Pella, H., & Catalogne, C. (2013). Regionalization of patterns of flow intermittence from gauging station records. *Hydrology and Earth System Sciences*, *17*(7), 2685‑2699. https://doi.org/10.5194/hess-17-2685-2013

Stubbington, R., England, J., Wood, P. J., & Sefton, C. E. M. (2017). Temporary streams in temperate zones: recognizing, monitoring and restoring transitional aquatic-terrestrial ecosystems: Temporary streams in temperate zones. *Wiley Interdisciplinary Reviews: Water*, *4*(4), e1223. https://doi.org/10.1002/wat2.1223

Tibshirani, R. (1996). Regression shrinkage and selection via the lasso. *Journal of the Royal Statistical Society*. Series B (Methodological), 267-288.

Turner, D. S., & Richter, H. E. (2011). Wet/Dry Mapping: Using Citizen Scientists to Monitor the Extent of Perennial Surface Flow in Dryland Regions. *Environmental Management*, *47*(3), 497‑505. https://doi.org/10.1007/s00267-010-9607-y

Vadher, A. N., Millett, J., Stubbington, R., & Wood, P. J. (2018). Drying duration and stream characteristics influence macroinvertebrate survivorship within the sediments of a temporary channel and exposed gravel bars of a connected perennial stream. *Hydrobiologia*. https://doi.org/10.1007/s10750-018-3544-9

van Meerveld, H. J. I., Vis, M. J. P., & Seibert, J. (2017). Information content of stream level class data for hydrological model calibration. *Hydrology and Earth System Sciences*, *21*(9), 4895‑4905. https://doi.org/10.5194/hess-21-4895-2017

Venables, W. N., & Ripley, B. D. (2002). *Modern Applied Statistics with S. Fourth Edition*. Springer, New York. ISBN 0-387-95457-0.

Vidal, J.-P., Martin, E., Franchistéguy, L., Baillon, M., & Soubeyroux, J.-M. (2010). A 50-year high-resolution atmospheric reanalysis over France with the Safran system. *International Journal of Climatology*, *30*(11), 1627‑1644. https://doi.org/10.1002/joc.2003

Wasson, J.-G., Chandesris, A., Pella, H., & Blanc, L. (2002). Typology and reference conditions for surface water bodies in France: the hydro-ecoregion approach. *TemaNord*, *566*, 37–41.

10. Appendix

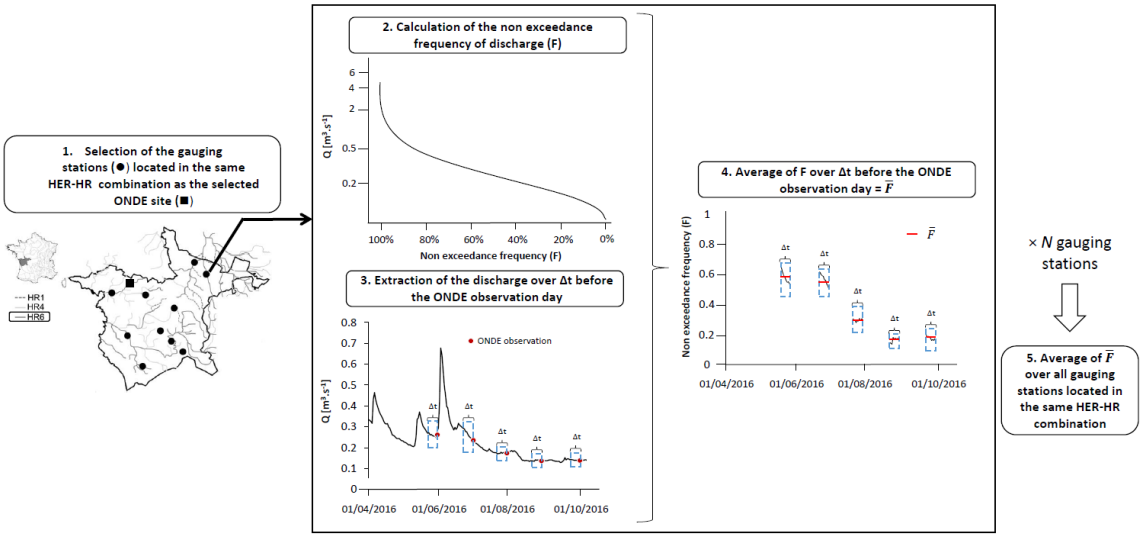

Figure A1. *Procedure to calculate the hydrological covariates FQΔt at a given ONDE site located in a sub-region HER-HR. The value of Δt is 0, 5 and 10 days to calculate FQ0, FQ5 and FQ10, respectively.*

Irstea
1, rue Pierre-Gilles de Gennes
CS 10030
92761 Antony Cedex
01 40 96 61 21
www.irstea.fr

Agence Française pour la Biodiversité
Hall C – Le Nadar
5, square Félix Nadar
94300 Vincennes
01 45 14 36 00
www.afbiodiversite.fr